From the Institute for Systems Neuroscience
at Heinrich Heine University Düsseldorf

A Comparative Neuroimaging Investigation into Great Ape Brain Aging

Dissertation

to obtain the academic title of Doctor of Philosophy (PhD) in Medical Sciences
from the faculty of Medicine at Heinrich Heine University Düsseldorf

Submitted by
Sam Vickery
(2023)

„Als Inauguraldissertation gedruckt mit Genehmigung der Medizinischen Fakultät der Heinrich-Heine-Universität Düsseldorf“

Gez.: 

Dekan: Prof. Dr. med. Nikolaj Klöcker

Gutachter/innen: Prof. Dr. Simon B. Eickhoff, Prof. Dr. Dr. Svenja Caspers

“Put another way, the chimpanzees'
closest relative is not the gorilla but humans.”
-Jared Diamond, *The Third Chimpanzee*

Parts of this work have been published:

Vickery, S., Hopkins, W.D., Sherwood, C.C, Schapiro, S.J., Latzman, R.D., Caspers, S., Gaser, C., Eickhoff, S.B., Dahnke, R., and Hoffstaedter, F. Chimpanzee brain morphometry utilizing standardized MRI preprocessing and macroanatomical annotations *eLife*, 9:e60136 (2020). https://doi.org/10.7554/eLife.60136

Friedrich, P., Forkel, S. J., Amiez, C., Balsters, J. H., Coulon, O., Fan, L., Goulas, A., Hadj-Bouziane, F., Hecht, E. E., Heuer, K., Jiang, T., Latzman, R. D., Liu, X., Loh, K. K., Patil, K. R., Lopez-Persem, A., Procyk, E., Sallet, J., Toro, R., Vickery, S., Weis, S., Wilson, C.R.E., Xu, T., Zerbi, V., Eickhoff, S.B., Margulies, D.S., Mars, R.B., and Thiebaut de Schotten, M. Imaging evolution of the primate brain: The next frontier? *NeuroImage*. 228, 117685 (2021). https://doi.org/10.1016/j.neuroimage.2020.117685

Vickery, S., Eickhoff, S.B. & Friedrich, P. Hemispheric Specialization of the Primate Inferior Parietal Lobule. *Neuroscience Bulletin*. 38, 334–336 (2022). https://doi.org/10.1007/s12264-021-00807-4

Zusammenfassung

Schimpansen sind zusammen mit Bonobos die nächsten lebenden Verwandten des Menschen und weisen Gemeinsamkeiten sowohl bei den makroanatomischen Merkmalen des Gehirns als auch bei den kognitiven Fähigkeiten und dem Genom auf. Daher bieten sie eine einzigartige Perspektive für die Untersuchung der menschlichen Gehirnentwicklung. Das Aufkommen der vergleichenden Neurowissenschaften wurde durch die wachsende Zahl offener Primatendatensätze sowie durch die Entwicklung neuartiger artspezifischer Methoden und artenübergreifender Vergleichstechniken begünstigt. In dieser Dissertation werden daher eine neuartige, Schimpansen spezifische Pipeline für die strukturelle Bildvorverarbeitung und ein datengesteuerter artenübergreifender Vergleichsrahmen vorgestellt. Die Schimpansen spezifische Verarbeitungspipeline mit arteigenen Vorlagen für die Segmentierung und Registrierung, sowie einer makroanatomischen Gehirnparzellierung ermöglicht standardisierte, exakte und reproduzierbare Ganzhirnanalysen. Der neuartige artenübergreifende Vergleichsrahmen erstellt für beide Spezies unabhängig voneinander eine anatomisch informierte Parzellierung, aus Organisationsmerkmalen der grauen Substanz (GS). Diese datengestützte vergleichende Parzellierung wird dann verwendet, um die Beziehung zwischen altersbedingtem GS-Rückgang und speziesübergreifender Expansion bei Menschen und Schimpansen zu bewerten. Darüber hinaus wird der aktuelle Stand der vergleichenden Neurowissenschaften in Bezug auf die Anatomie und Funktion des Primatengehirns zusammengefasst. Ein besonderer Schwerpunkt liegt dabei auf der Asymmetrie der Konnektivität des inferioren Parietallappens und der Frage, wie diese mit der Entwicklung von Sprache und Werkzeugeinsatz zusammenhängt. Anhand der Schimpansen spezifischen Verarbeitungspipeline wird eine signifikante altersbedingte GS-Atrophie bei Schimpansen gezeigt. Dieser eindeutig altersbedingte GS-Rückgang bei Schimpansen ist mit dem beim Menschen vergleichbar und steht im Gegensatz zu früheren Schimpansen Studien, die nur geringe oder gar keine altersbedingten Effekte zeigten. Der artenübergreifende Vergleichsrahmen zeigt beim Menschen eine positive Beziehung zwischen altersbedingter GS-Abnahme und artenübergreifender lokaler Gehirnexpansion zwischen Schimpansen und Menschen. Bei Schimpansen gibt es jedoch keinen solchen Zusammenhang, obwohl sie einen weit verbreiteten altersbedingten Rückgang von GS aufweisen. Die starke Expansion und die Alterung des Gehirns in kognitiven Bereichen höherer Ordnung, wie dem präfrontalen Kortex, sind nur beim Menschen zu beobachten. Daher könnte die starke Expansion von Bereichen höherer Ordnung im Vergleich zu unserem engsten Vorfahren zu einer Anfälligkeit für altersbedingte Atrophie geführt haben.

.

Summary

Chimpanzees, along with bonobos, are humans' closest living relative and contain commonalities in both macroanatomical brain features, cognitive abilities, and genome. Therefore, offer a unique perspective in studying human brain evolution. The emergence of comparative neuroimaging has been fostered by the growing amount of open primate datasets as well as by the development of novel species-specific methods and cross-species comparative techniques. Consequently, this dissertation presents a novel chimpanzee-specific structural image preprocessing pipeline and a data-driven cross-species comparative framework. The chimpanzee processing pipeline with associated templates for segmentation and registration along with a macroanatomical brain parcellation enables standardized, accurate, and reproducible whole-brain analyses. The novel comparative framework establishes an anatomically informed parcellation within each species independently, created from gray matter (GM) organizational features. This data-driven comparative parcellation is then used to assess the relationship between age-related GM decline and cross-species expansion in humans and chimpanzees. Additionally, the current state of comparative neuroimaging is summarized in terms of the anatomy and function of the primate brain. With a particular focus on the connectivity asymmetry of the inferior parietal lobule and how this relates to language and tool-use development. Employing the chimpanzee processing pipeline, significant age-related GM atrophy in chimpanzees is shown. Such clear chimpanzee age-mediated GM decline is comparable to that seen in humans and is contrary to previous chimpanzee studies showing little to no effect. The cross-species comparative framework shows a positive relationship in humans between age-related GM decline and cross-species local brain expansion between chimpanzees and humans. However, chimpanzees present no such relationship even though they show widespread age-mediated GM decline. The high expansion and brain aging in higher-order cognitive areas, such as the prefrontal cortex, are only present in humans. Therefore, the extensive expansion of higher-order areas compared to our closest ancestor may have led to a vulnerability to age-related atrophy.

List of Abbreviations

CAT	Computational Anatomy Toolbox
CSF	cerebrospinal fluid
DICOM	Digital Imaging and Communication in Medicine
eNKI	Enhanced Nathan Kline Institute
GM	gray matter
ICA	independent component analysis
IPL	inferior parietal lobule
IXI	Information eXtraction from Images
MRI	magnetic resonance imaging
NCBR	National Chimpanzee Brain Resource
NHP	non-human primates
NMF	non-negative matrix factorization
OPNMF	orthogonal projective non-negative matrix factorization
PCA	principal component analysis
PFC	prefrontal cortex
ROI	region of interest
SPM	Statistical Parametric Toolbox
T1w	T1- weighted
TPM	tissue probability map
VBM	voxel-based morphometry
WM	White matter
YNPRC	Yerkes National Primate Research Center

Table of Contents

1. Introduction

The organization of the modern human (*Homo sapian*) brain, entailing the shape, size, connectivity, and neurobiological composition is the result of millions of years of evolution. Understanding how the unusually large human brain with its billions of neurons, trillions of synaptic connections, and intricate network organization makes us unique is a scientific question explored for over a century. A pivotal method to understand the uniqueness of humans is through further understanding and comparing additional primate species' brains. In the humble and exciting beginning of comparative neuroscience, scientists were heavily constrained when conducting comparative investigations. This was due to the difficulty in obtaining the appropriate neuroscientific data, the specialized expertise to process and gather it, as well as sharing such data. With the advent of magnetic resonance imaging (MRI) along with improved digital technologies, the investigation and sharing of large multi-species datasets became a reality (Messinger et al., 2021; Milham et al., 2018). Enabling better storage and data standards for the sharing of neuroscientific data as well as facilitating high-throughput computing and modeling.

Chimpanzees (*Pan troglodytes*), along with bonobos (*Pan paniscus*), are the closest living relative to humans as they share a last common ancestor 6 – 8 million years ago (Langergraber et al., 2012). Moreover, chimpanzees share a substantially similar genome (Waterson et al., 2005), cognitive abilities (Hecht et al., 2017; Savage-Rumbaugh, 1986; Shumaker et al., 2011; Tomasello and Call, 1997; Waal, 1996), and cerebral anatomical features (Hopkins et al., 2017, 2014; Rilling and Insel, 1999; Zilles et al., 1989) with humans. Therefore, chimpanzees represent a unique animal model among non-human primates to understand evolutionary adaptations of the human brain and infer the origins of the human condition.

1.1 Voxel-Based Morphometry

Whole-brain structural morphometry changes can be accurately investigated using a technique called voxel-based morphometry (VBM). Brain MRI scans require several preprocessing steps for VBM investigations, namely denoising, skull-stripping, tissue type segmentation, and registration to a common template space (Ashburner, 2000). Image segmentation is conducted into gray matter (GM), white matter (WM), and cerebrospinal fluid (CSF). Segmentation is achieved by assessing the voxel intensity value, which is supplemented and enhanced by an *a priori* probability map of the tissue classes, a tissue

probability map (TPM) (Ashburner, 2000). To conduct analyses on macroanatomical changes over a large population the individual images are both linearly and non-linearly registered to a population reference template. As each brain has variations in its morphology, which are of interest and need to be conserved, following non-linear deformation the intensity of the voxel values is modulated in correspondence with the amount of deformation needed to meet the template to conserve this individual variation. Along with the mentioned registration and segmentation templates, a population reference template is needed. This template acts as a reference space for presenting and reporting findings in an understandable and reproducible fashion VBM is therefore a proficient tool to explore cerebral morphology changes during aging and age-related pathologies over a large population. Additionally, voxel-wise GM maps can be also used as inputs for machine learning algorithms such as unsupervised clustering.

1.2 Aging and Gray Matter

The widespread GM atrophy, predominantly resulting from neuronal loss during healthy aging and in neurological diseases such as Alzheimer's, dementia, and Parkinson's can be investigated *in-vivo* using VBM (Crivello et al., 2014; Good et al., 2001; Kennedy et al., 2009; Minkova et al., 2017). The robust brain aging atrophy, in particular GM, in humans have been reported to be minimal to non-existent in chimpanzees (Autrey et al., 2014; Chen et al., 2013; Herndon et al., 1999; Sherwood et al., 2011). Chimpanzees have a relatively long lifespan of approximately 40 years in the wild and over 50 in captivity. Moreover, chimpanzees have shown a decrease in performance of cognitive tasks during aging as well as the presence of Alzheimer's neuropathologies within the temporal lobe (Edler et al., 2017; Hopkins et al., 2021). The lack of findings could be due to the low number of very old (>45 y/o) chimpanzees, low sample size overall, and/or utilizing image processing tools not specialized at uncovering morphometric changes in GM. Therefore, understanding how possible structural brain changes in chimpanzees relate to those found in humans is important to comprehend the evolution of the human brain. Additionally, such information will assist in the care for elderly chimpanzees in captivity.

1.3 Primate Cross-species Comparison

Comparing brain organisation across primate species has historically been constrained to homologous regions or features. Such brain regions over species can be seen as homologous concerning their spatial location and generally in combination with cytoarchitectonic composition. Furthermore, cerebral organizational features have been compared between species, like relative brain size, gyrification, hemispheric asymmetry, sulci

location, as well as WM tract inter-connectivity and cortical termination (Bogart et al., 2012; Cheng et al., 2021; Eichert et al., 2020; Hopkins et al., 2017; Rilling and Insel, 1999; Wei et al., 2019). Such investigations provide both a deeper understanding of organizational principals within the human brain leading to our improved cognitive facilities and the neuro-evolution of these features. Studies showing that humans possess relatively larger cortical areas responsible for higher-order cognitive functions, such as the prefrontal cortex and parietal lobe (Bruner et al., 2017; Donahue et al., 2018; Hill et al., 2010; Xu et al., 2020). These regions have shown to be related to function important to human cognition, such as, self-control, executive functioning, and visuospatial processing (Cavanna and Trimble, 2006; Miller, 2000).

The homologous-centric approach has led to many important findings although it is susceptible to subjective biases (Cantalupo and Hopkins, 2001; Donahue et al., 2018; Gannon et al., 1998; Palomero-Gallagher and Zilles, 2019). The border of cross-species homologous regions can be disputed leading to possible contradicting findings. Alternatively, some comparisons are heavily restricted or cannot be conducted because of the lack of homologies. A more data-centric approach can address some of these concerns and therefore be an addition to the homologous approaches. The combination of data-driven methodologies as well as homologous structural connectivity has recently been employed to further understand the evolutionary organisation of the lateral temporal lobe and inferior parietal lobe (Cheng et al., 2021; Eichert et al., 2020). These computational techniques can leverage large samples over several species and provide findings less influenced by subjective definition of regions within different species.

1.4 Brain Parcellation

The brain can be delineated into distinct areas based on topology, cytoarchitecture, connectivity, and function (Eickhoff et al., 2018). Parcellating the brain into spatial areas based on their unique organisation has been a neuroscientific endeavour for over a century (Amunts and Zilles, 2015; Brodmann, 1909; Economo and Koskinas, 1925; Vogt and Vogt, 1926, 1919). This began with defining areas based on micro- and macro-structure, whereby, an abrupt change in an organisation feature could be witnessed from one homologous area to another. Cortical layer changes could be in the thickness or presence of specific layers, the morphology of neuronal cell types (e.g., pyramidal), or the amount of myelination. With the introduction of improved neuroscientific technologies (e.g., MRI) as well as computational power, additional in-vivo features from multiple modalities have furthered our understanding of the brain's

organisation (Glasser et al., 2016). The *in-vivo* macroanatomical features, such as gyri, sulci, and nuclei can be used to create brain parcellations using population MRI templates. Even though it is known that borders between brain areas rarely coincide with macroscopic features like the fundi of sulci (Amunts and Zilles, 2015). These maps create an *in-vivo* low dimensional space for univariate and multivariate modelling, informed by macroanatomical structures. Data-driven brain parcellations, alternatively, use statistical techniques to identify patterns in brain activity or structure to establish distinct brain regions. These techniques seek to organise the data by analysing the within brain and across subject variance in large neuroimaging samples. Clustering or factorization methods are used to create such brain parcellation maps.

Common techniques used to create data-driven parcellations using brain activity or structure, are principal component analysis (PCA), independent component analysis (ICA), and non-negative matrix factorization (NMF) (Gupta et al., 2018; Sotiras et al., 2015; Yeo et al., 2011). Utilizing structural GM maps the modelled inter-regional GM variation over a large sample, commonly known as structural covariance (Alexander-Bloch et al., 2013), is captured by these techniques. Brain regions that present structural covariance have been shown to have similar WM connectivity, functional activity, neurodevelopmental pathways, genetic underpinnings (Alexander-Bloch et al., 2013). Therefore, such regions share similar organizational features. GM maps provide a non-negative measurement of GM volume within the brain, accordingly, the positive and negative loadings in PCA and ICA can be problematic to determine anatomical meaning. NMF address this concern by enforcing a non-negativity constraint on the factorization creating an additive parts-based representation of the underlying data (Lee and Seung, 1999). The variant of NMF, called orthogonal projective NMF (OPNMF) creates spatial continuous brain parcels that further improve interpretability compared to ICA or PCA (Nassar et al., 2019; Sotiras et al., 2017, 2015; Varikuti et al., 2018).

1.5 Ethics Approval

The use of open human neuroimaging datasets IXI (Information eXtraction from Images) and eNKI (Enhanced Nathan Kline Institute) has been approved by the Ethics committee of Heinrich-Heine University Düsseldorf (2018-317-RetroDEuA). The chimpanzee data provided by the NCBR was acquired under protocols approved by the Yerkes National Primate Research Center (YNPRC) at Emory University Institutional Animal Care and Use Committee (Approval number YER2001206). The data acquired were approved by the Institutional Animal Care and Use Committees of both sites. The Data were also obtained prior to the 2015 implementation of the U.S. Fish and Wildlife Service and National Institutes of

Health regulations governing research with chimpanzees. The baboon and macaque data is from openly available T1w population templates, which were also created with the appropriate ethics approval of the associated centers.

1.6 Aims of Thesis

Human evolution has involved intricate and diverse adaptations created by a multitude of genetic, physiological, and environmental factors over hundreds of millions of years. With respect to the numerous evolutionary changes, one could argue none is as significant as that of the brain. Therefore, investigating humans' primate relatives along with cross-species comparisons gains valuable insight into understanding organization of the primate brain. Consequently, such knowledge can be employed in a general sense to understand brain organisation as well as to discern organizational facets related to human neurodevelopment, extended lifespan, and neurological disorders.

This dissertation pertains to three studies that explore primate brain organization utilizing modern MRI techniques with a focus on GM structural changes mediated by aging. Study 1 establishes a structural image preprocessing workflow for chimpanzees. Including population average, registration, and tissue segmentation templates for accurate and reproducible image processing used in group comparisons of brain morphometry. A hand-drawn macroanatomical parcellation of the chimpanzee brain is additionally provided. The newly established processing pipeline, templates, and parcellation are then used to investigate age-related changes to GM volume and hemispheric asymmetry in chimpanzees. Study 2 aims to provide a spotlight on the current state and possibilities for neuroimaging the primate brain to further our understanding of its structure, function, and evolution. Furthermore, highlighting the importance of multiple species investigations to acquire a more fine-grained understanding of neuroevolutionary changes. Particularly, the WM connectivity organization and asymmetry of the inferior parietal lobule (IPL) in humans, chimpanzees, and macaques. Study 3 conducts a multiple primate species investigation into the relationship between cross-species brain volumetric expansion and age-related changes to GM in humans and chimpanzees. To assess the expansion-aging relationship a data-driven comparison method is presented. This method creates species-specific GM macroanatomical parcellations that contain a combination of within species organizational information and cross-species similarities. The comparative parcellations are then used examine the relationship between age-mediated GM volume changes and cross-species regional brain expansion in humans and chimpanzees. Expansion was determined using recent

phylogenetic ancestors. For humans chimpanzees were used and for chimpanzees two cercopithecid monkeys, baboons and macaques, were employed. Four manuscripts, one for study 1 and study 3 and two for study 2 cover these three studies.

2. Chimpanzee brain morphometry utilizing standardized MRI preprocessing and macroanatomical annotations, Sam Vickery, William D Hopkins, Chet C Sherwood, Steven J Schapiro, Robert D Latzman, Svenja Caspers, Christian Gaser, Simon B Eickhoff, Robert Dahnke, Felix Hoffstaedter, *eLife*, 9:e60136, 2020

RESEARCH ARTICLE

Chimpanzee brain morphometry utilizing standardized MRI preprocessing and macroanatomical annotations

Sam Vickery[1,2]*, William D Hopkins[3], Chet C Sherwood[4], Steven J Schapiro[3,5], Robert D Latzman[6], Svenja Caspers[7,8,9], Christian Gaser[10,11], Simon B Eickhoff[1,2], Robert Dahnke[10,11,12†]*, Felix Hoffstaedter[1,2†]*

[1]Institute of Systems Neuroscience, Medical Faculty, Heinrich-Heine-University, Düsseldorf, Germany; [2]Institute of Neuroscience and Medicine (INM-7) Research Centre Jülich, Jülich, Germany; [3]Keeling Center for Comparative Medicine and Research, The University of Texas MD Anderson Cancer Center, Bastrop, United States; [4]Department of Anthropology and Center for the Advanced Study of Human Paleobiology, The George Washington University, Washington, United States; [5]Department of Experimental Medicine, University of Copenhagen, Copenhagen, Denmark; [6]Department of Psychology, Georgia State University, Atlanta, United States; [7]Institute of Neuroscience and Medicine (INM-1), Research Centre Jülich, Jülich, Germany; [8]Institute for Anatomy I, Medical Faculty, Heinrich-Heine-University, Düsseldorf, Germany; [9]JARA-BRAIN, Jülich-Aachen Research Alliance, Jülich, Germany; [10]Structural Brain Mapping Group, Department of Neurology, Jena University Hospital, Jena, Germany; [11]Structural Brain Mapping Group, Department of Psychiatry and Psychotherapy, Jena University Hospital, Jena, Germany; [12]Center of Functionally Integrative Neuroscience, Department of Clinical Medicine, Aarhus University, Aarhus, Denmark

***For correspondence:**
s.vickery@fz-juelich.de (SV);
robert.dahnke@uni-jena.de (RD);
f.hoffstaedter@fz-juelich.de (FH)

†These authors contributed equally to this work

Competing interests: The authors declare that no competing interests exist.

Funding: See page 15

Received: 17 June 2020
Accepted: 20 November 2020
Published: 23 November 2020

Reviewing editor: Jonathan Erik Peelle, Washington University in St. Louis, United States

Abstract Chimpanzees are among the closest living relatives to humans and, as such, provide a crucial comparative model for investigating primate brain evolution. In recent years, human brain mapping has strongly benefited from enhanced computational models and image processing pipelines that could also improve data analyses in animals by using species-specific templates. In this study, we use structural MRI data from the National Chimpanzee Brain Resource (NCBR) to develop the chimpanzee brain reference template Juna.Chimp for spatial registration and the macro-anatomical brain parcellation Davi130 for standardized whole-brain analysis. Additionally, we introduce a ready-to-use image processing pipeline built upon the CAT12 toolbox in SPM12, implementing a standard human image preprocessing framework in chimpanzees. Applying this approach to data from 194 subjects, we find strong evidence for human-like age-related gray matter atrophy in multiple regions of the chimpanzee brain, as well as, a general rightward asymmetry in brain regions.

Introduction

Chimpanzees (*Pan troglodytes*) along with bonobos (*Pan paniscus*) represent the closest extant relatives of humans sharing a common ancestor approximately 7–8 million years ago (***Langergraber et al., 2012***). Experimental and observational studies, in both the field and in captivity, have documented a range of cognitive abilities that are shared with humans such as tool use and manufacturing (***Shumaker et al., 2011***), symbolic thought (***de and Frans, 1996***), mirror self-

recognition (**Anderson and Gallup, 2015**; **Hecht et al., 2017**) and some basic elements of language (**Savage-Rumbaugh, 1986**; **Savage-Rumbaugh and Lewin, 1994**; **Tomasello and Call, 1997**) like conceptual metaphorical mapping (**Dahl and Adachi, 2013**). This cognitive complexity together with similar neuroanatomical features (**Zilles et al., 1989**; **Rilling and Insel, 1999**; **Gómez-Robles et al., 2013**; **Hopkins et al., 2014**; **Hopkins et al., 2017**) and genetic proximity (**Waterson et al., 2005**) renders these species unique among non-human primates to study the evolutional origins of the human condition. In view of evolutionary neurobiology, the relatively recent divergence between humans and chimpanzees explains the striking similarities in major gyri and sulci, despite profound differences in overall brain size. Numerous studies using magnetic resonance imaging (MRI) have compared relative brain size, shape, and gyrification in humans and chimpanzees (**Zilles et al., 1989**; **Rilling and Insel, 1999**; **Gómez-Robles et al., 2013**; **Hopkins et al., 2014**; **Hopkins et al., 2017**).

Previous studies of brain aging in chimpanzees have reported minimal indications of atrophy (**Herndon et al., 1999**; **Sherwood et al., 2011**; **Chen et al., 2013**; **Autrey et al., 2014**). Nevertheless, **Edler et al., 2017** recently found that brains of older chimpanzees' exhibit both neurofibrillary tangles and amyloid plaques, the classical features of Alzheimer's disease (AD). Neurodegeneration in the aging human brain includes marked atrophy in frontal and temporal lobes and decline in glucose metabolism even in the absence of detectable amyloid beta deposition, which increases the likelihood of cognitive decline and development of AD (**Jagust, 2018**). Given the strong association of brain atrophy and amyloid beta in humans, this phenomenon requires further investigation in chimpanzees.

Cortical asymmetry is a prominent feature of brain organization in many primate species (**Hopkins et al., 2015**) and was recently shown in humans in a large-scale ENIGMA (Enhancing Neuroimaging Genetics through Meta-Analysis) study (**Kong et al., 2018**). For chimpanzees, various studies have reported population-level asymmetries in different parts of the brain associated with higher order cognitive functions like tool-use (**Freeman et al., 2004**; **Hopkins et al., 2008**; **Hopkins et al., 2017**; **Hopkins and Nir, 2010**; **Lyn et al., 2011**; **Bogart et al., 2012**; **Gilissen and Hopkins, 2013**) but these results are difficult to compare within and across species, due to the lack of standardized registration and parcellation techniques as found for humans.

To date, there is no common reference space for the chimpanzee brain available to reliably associate and quantitatively compare neuro-anatomical evidence, nor is there a standardized image processing protocol for T1-weighted (T1w) brain images from chimpanzees that matches human imaging standards. With the introduction of voxel-based morphometry (**Ashburner and Friston, 2000**) and the ICBM (international consortium of brain mapping) standard human reference brain templates almost two decades ago (**Mazziotta et al., 2001**), MRI analyses became directly comparable and generally reproducible. In this study, we adapt state-of-the-art MRI (magnetic resonance imaging) processing methods to assess brain aging and cortical asymmetry in the chimpanzee brain. To make this possible, we rely on the largest openly available resource of chimpanzee MRI data: the *National Chimpanzee Brain Resource* (NCBR, http://www.chimpanzeebrain.org/), including in vivo MRI images of 223 subjects from 9 to 54 years of age (Mean age = 26.9 ± 10.2 years). The aim of this study is the creation of a chimpanzee template permitting automated and reproducible image registration, normalization, statistical analysis, and visualization to systematically investigate brain aging and hemispheric asymmetry in chimpanzees.

Results

Initially, we created the population-based Juna.Chimp (Forschungszentrum *Ju*elich - University Je*na*) T1-template, tissue probability maps (TPM) for tissue classification and a non-linear spatial registration 'Shooting' templates (**Figure 1**) in an iterative fashion at 1 mm spatial resolution. The preprocessing pipeline and templates creation were established using the freely available *Statistical Parametric Mapping* (SPM12 v7487, http://www.fil.ion.ucl.ac.uk/spm/) software and *Computational Anatomy Toolbox* (CAT12 r1704 http://www.neuro.uni-jena.de/cat/). Juna.Chimp templates, the Davi130 parcellation, gray matter (GM) masks utilized, as well as statistical maps from our analysis are interactively accessible and downloadable via the Juna.Chimp web viewer (http://junachimp.inm7.de/).

To enable more direct comparison to previous research, we manually created the Davi130 parcellation (by R.D. and S.V.), a whole brain macroanatomical annotation based on the Juna T1 template

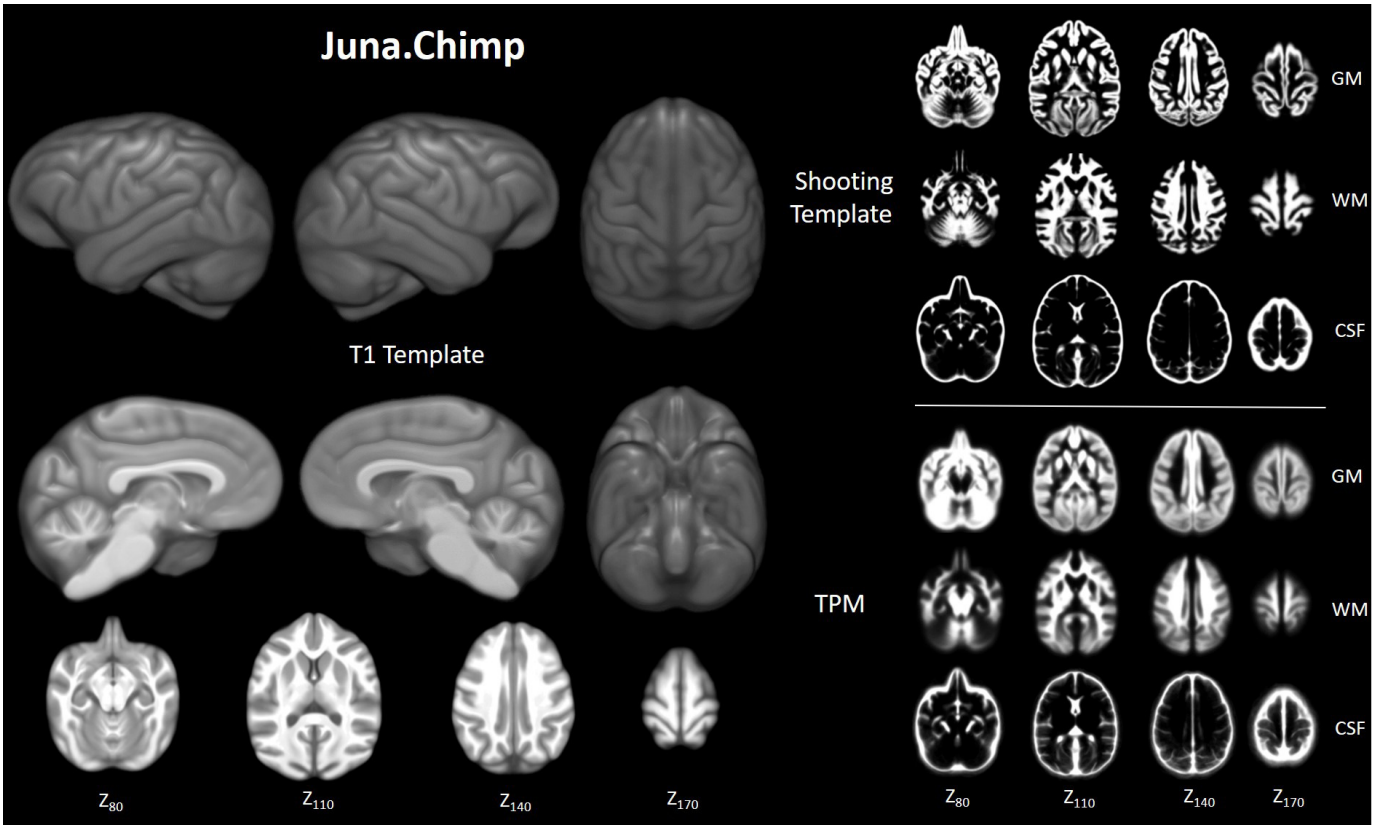

Figure 1. Juna.Chimp templates including the average. T1- template, tissue probability maps (TPM), and Geodesic Shooting template. For Shooting templates and TPM axial slices are shown of gray matter (GM), white matter (WM), and cerebrospinal fluid (CSF). All templates are presented at 0.5 mm resolution.

(***Figure 2***). The delineation of regions within the cortex was determined by following major gyri and sulci, whereby, large regions were arbitrarily split into two to three sub-regions of approximate equal size even though histological studies show that micro-anatomical borders between brain regions are rarely situated at the fundus (***Sherwood et al., 2003***; ***Schenker et al., 2010***; ***Spocter et al., 2010***; ***Amunts and Zilles, 2015***). This process yielded 65 regions per hemisphere for a total of 130 regions for the Davi130 macro-anatomical manual parcellation (***Figure 2*** and ***Figure 2—source data 1***).

Following successful CAT12 preprocessing, rigorous quality control (QC) was employed to identify individual MRI scans suitable for statistical analysis of brain aging and hemispheric asymmetry in chimpanzees. Our final sample consists of 194 chimpanzees including 130 females with an age range of 9–54 years and a mean age of 26.3 ± 9.9 years (***Figure 3A***). The linear regression model with GM fraction of total intracranial volume as the dependent variable and age, scanner field strength, sex, and rearing environment revealed a significant negative association between age and GM ($p<0.0001$) demonstrating age-related decline in overall GM density (***Figure 3B***). Both sex ($p=0.004$) and scanner field strength ($p<0.0001$) showed a significant effect on total GM volume. Therefore, the sample was split into male and female subjects and into 1.5T and 3T scanner, whereby, all subsamples showed a significant age effect on GM (male: $R^2 = 0.17$, $p=0.0004$; female $R^2 = 0.13$, $p<0.0001$, 1.5T: $R^2 = 0.19$, $p<0.0001$; 3T: $R^2 = 0.09$, $p=0.004$). There were no significant sex differences of GM decline ($p=0.3$). The same analysis was conducted on a matched human sample from the IXI dataset (***Figure 3C***; https://brain-development.org/ixi-dataset/). The human sample was matched based on age, sex, and scanner field strength (n = 194, 128 females, 20–78 y/o, mean = 39.4 ± 14.0). As life span and aging processes are different between species, the human sample was matched to chimpanzees roughly by using a factor of 1.5* for age. A significant age-

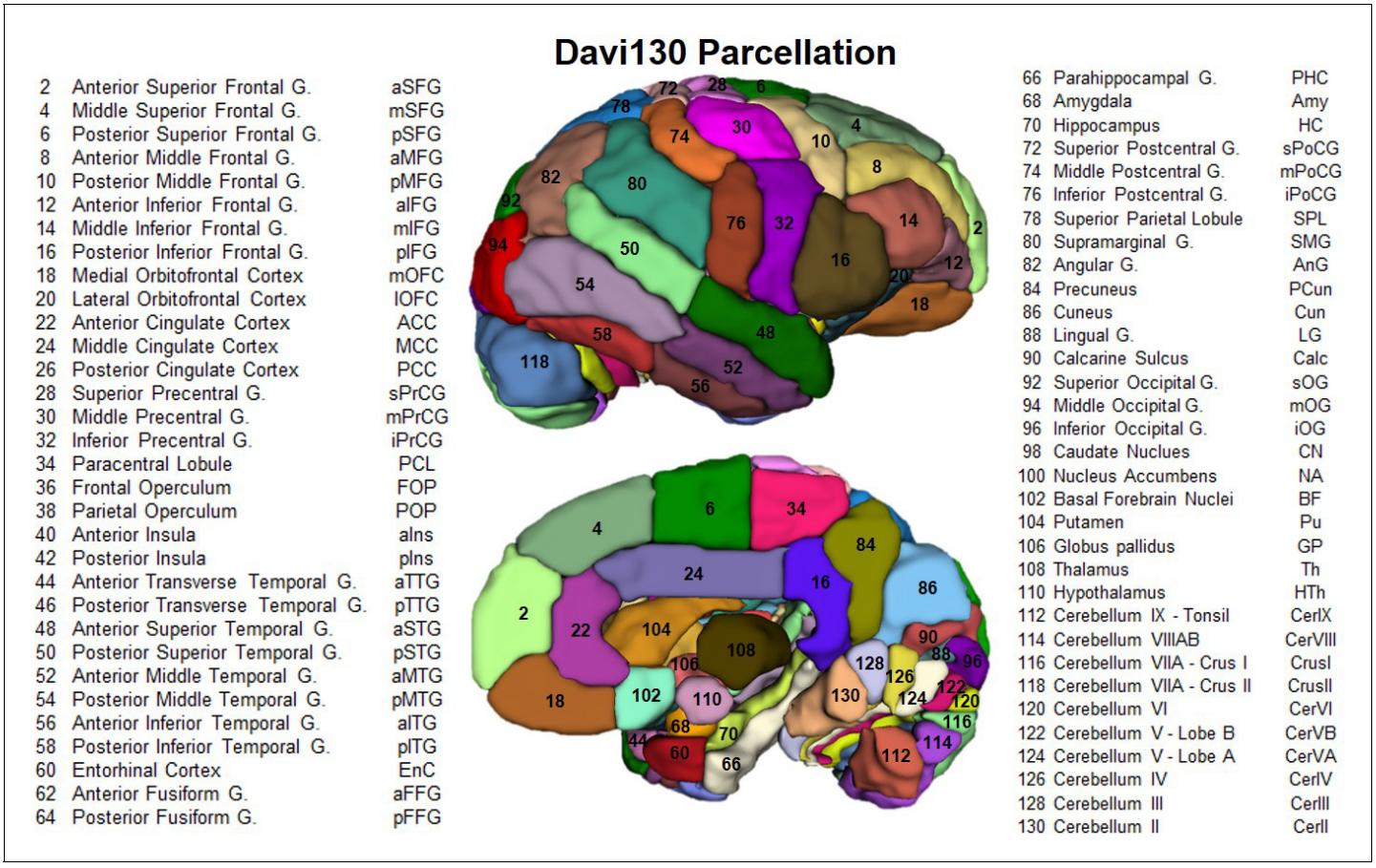

Figure 2. Lateral and medial aspect of the Davi130 parcellation right hemisphere. Visible regions are numbered with Davi130 parcellation region numbers and correspond to names in the figure. Even numbers correspond to regions in the right hemisphere (as shown in the figure), while left hemisphere regions are odd numbers. A list of all Davi130 labels can be found at ***Figure 2—source data 1***.

The online version of this article includes the following source data for figure 2:

Source data 1. Source file for Complete List of Davi130 Labels.

related decline in overall GM ($p<0.0001$) as well as a significant sex effect ($p<0.0001$) was also found in the human sample (***Figure 3D***). Similar to the chimpanzee sample, both males and female subjects show a significant age effect on total GM (male: $R^2 = 0.58$, $p<0.0001$; female: $R^2 = 0.61$, $p<0.0001$) but with no significant sex differences on GM decline ($p=0.8$). Although both species present a significant age-related GM decline, humans show a higher negative correlation between age and GM (chimpanzee: $R^2 = 0.12$; human: $R^2 = 0.55$) with less variance as compared to chimpanzees.

Region-based morphometry analysis was applied to test for local effect of age on GM. Linear regression analyses identified 55 of 130 brain regions in the Davi130 parcellation across both hemispheres that were significantly associated with age after family-wise error (FWE) correction for multiple testing (***Figure 4*** and ***Figure 4—source data 1***). Specifically, GM decline with age was found bilaterally in the superior frontal gyrus (SFG), posterior middle frontal gyrus (pMFG), posterior inferior frontal gyrus (pIFG), lateral orbitofrontal cortex (lOFC), middle and inferior precentral gyrus (PrCG), cingulate gyrus (ACC, MCC, PCC), posterior superior temporal gyrus (pSTG), anterior middle temporal gyrus (aMTG), precuneus (PCun), and lingual gyrus (LG) as well as unilaterally in the right anterior insula (aIns) and middle inferior frontal gyrus (mIFG), in addition to the left superior precentral gyrus (sPrCG), anterior transverse temporal gyrus (aTTG), posterior transverse temporal gyrus (pTTG), paracentral lobule (PCL) and the area around the calcarine sulcus (Calc) within the cerebral cortex. Subcortically, age-related GM decline was found in the bilateral putamen (Pu), caudate nucleus (CN), and the nucleus accumbens (NA), as well as in the superior cerebellum (CerVI, CerIV,

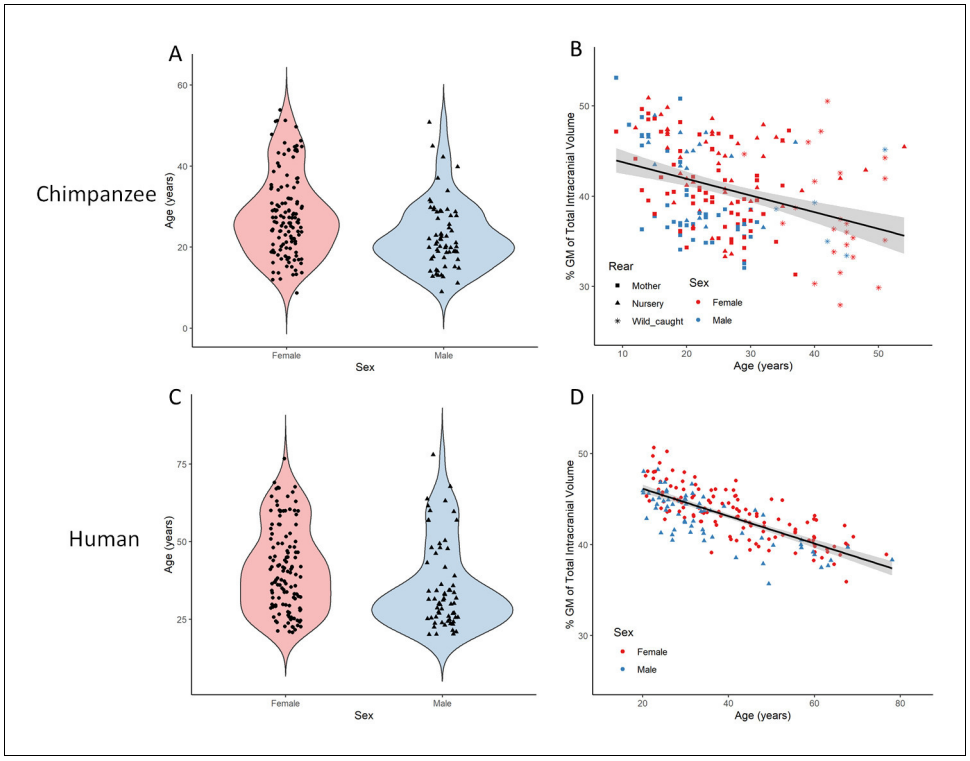

Figure 3. Total gray matter volume decline during aging in chimpanzees and matched human sample. (**A**) Distribution of age and sex in the final sample of 194 chimpanzees. (**B**) Linear relationship between GM and age with standard error for chimpanzee sample. (**C**) Distribution of age and sex in the human (IXI) matched sample of 194 humans. (**D**) Linear relationship between GM and age with standard error for human sample. ***Figure 3—figure supplement 1*** presents the age and sex distribution of the whole sample (n = 223). ***Figure 3—figure supplement 2*** presents the age and sex distribution of the whole IXI sample (n = 496).
The online version of this article includes the following figure supplement(s) for figure 3:

Figure supplement 1. Age and sex distribution of complete chimpanzee (n = 223) sample separated by scanner field strength.

Figure supplement 2. Age and sex distribution of complete IXI human sample (n = 496) separated by scanner field strength.

CerVA, Cer VB, CerIV and right CrusII). Finally, to test for more fine grained effects of aging independently of our macroanatomical parcellation, the same sample was analyzed with VBM revealing additional clusters of GM that are significantly affected by age in chimpanzees (***Figure 5***) after FWE correction using threshold-free cluster enhancement (TFCE) (***Smith and Nichols, 2009***). On top of the regions identified by region-wise morphometry, we found extensive voxel-wise effects throughout the orbitofrontal cortex (OFC), inferior temporal gyrus (ITG), transverse temporal gyrus (TTG), frontal operculum (FOP), parietal operculum (POP), postcentral gyrus (PoCG), supramarginal gyrus (SMG), angular gyrus (AnG), and in parts of the superior parietal lobule (SPL), superior occipital gyrus (sOG), and in inferior parts of the cerebellum.

Hemispheric asymmetry of the chimpanzee brain was assessed for each cortical Davi130 region with a total of 68% (44/65) exhibiting significant cortical asymmetry after FWE correction (***Figure 6*** and ***Figure 6—source data 1***). The majority of regions were found with greater GM volume in the right hemisphere (n = 32) as compared to the left (n = 12). In the left hemisphere, we found more GM in the SFG, pMFG, insula, anterior TTG, and PCun within the cortex. Rightward cortical asymmetry was located in the anterior MFG, middle and posterior IFG, medial OFC, cingulate gyrus, amygdala, STG, MTG, posterior TTG, anterior and posterior fusiform gyrus (FFG), FOP, POP, middle PrCG, middle and inferior PoCG, SMG, AnG, Calc, as well as the middle occipital gyrus. Within the basal ganglia, leftward GM asymmetry was observed in the Pu, nucleus accumbens (NA), basal forebrain nucleus (BF), and globus pallidus (GP), while, rightward asymmetry in the caudate

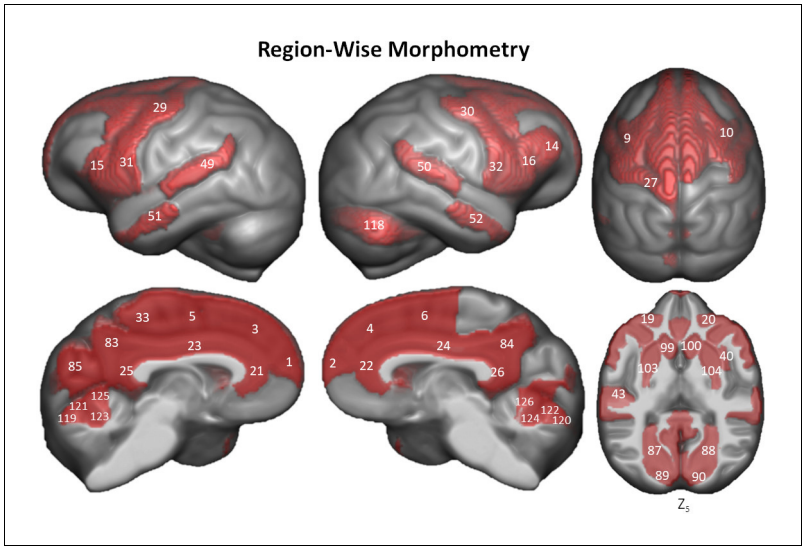

Figure 4. Region-wise morphometry in the Davi130 parcellation age regression. Red regions represent Davi130 regions that remained significant at p≤0.05 following FWE correction (Holm method). The T-statistic and p-value for all Davi130 labels can be found in ***Figure 4—source data 1***. 1 and 2 – aSFG, 3 and 4 – mSFG, 5 and 6 – pSFG, 9 and 10 – pMFG, 14 – mIFG, 15 and 16 – pIFG, 19 and 20 – lOFC, 21 and 22 – ACC, 23 and 24 – MCC, 25 and 26 – PCC, 27 – sPrCG, 29 and 30 – mPrCG, 31 and 32 – iPrCG, 33 – PCL, 40 – aIns, 43 – aTTG, 49 and 50 – pSTG, 51 and 52 – aMTG, 83 and 84 – PCun, 85 – Cun, 87 and 88 – LG, 89 and 90 – Calc, 97 and 98 – CN, 99 and 100 – NA, 103 and 104 – Pu, 118 – CrusII, 119 and 120 – CerVI, 121 and 122 – CerVB, 123 and 124 – CerVB, 125 and 126 – CerIV.

The online version of this article includes the following source data for figure 4:

Source data 1. Aging effect on gray matter in complete Davi130 Labels.

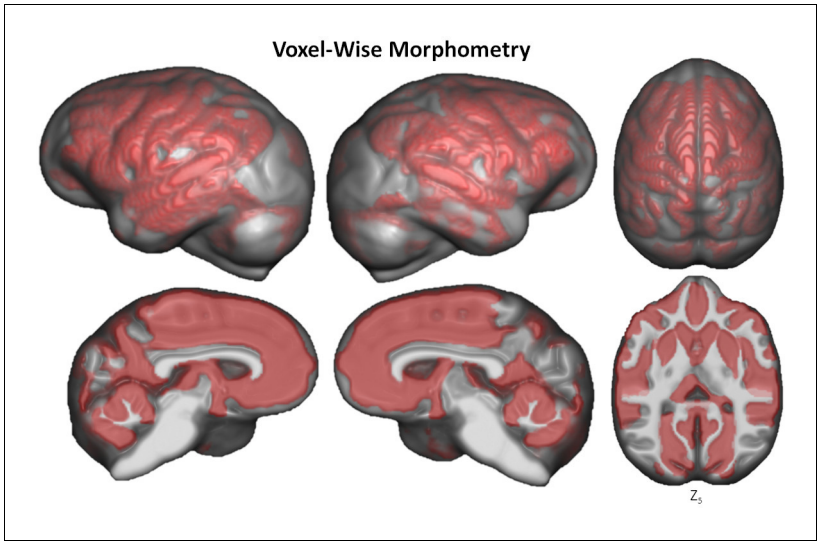

Figure 5. Voxel-based morphometry of aging on GM volume. The significant clusters are found using TFCE with FWE correction at p≤0.05.

The online version of this article includes the following figure supplement(s) for figure 5:

Figure supplement 1. Voxel-based morphometry of aging on GM volume using TFCE with FWE correction at p≤0.05 without rearing as a covariate.

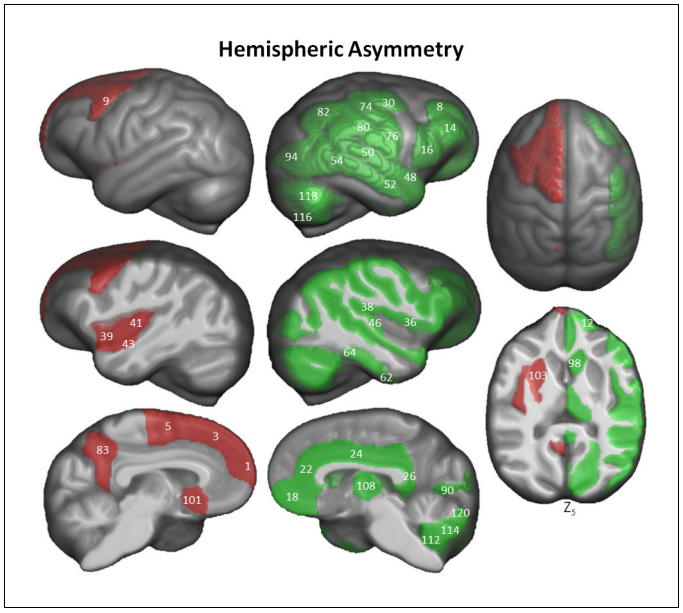

Figure 6. Hemispheric asymmetry of Davi130 regions within the chimpanzee sample. Significant leftward (red) and rightward (green) asymmetrical regions are those with a $p \leq 0.05$ after FWE correction. The T-statistic and p-value for all Davi130 labels can be found in ***Figure 6—source data 1***. 1 – aSFG, 3 – mSFG, 5 – pSFG, 8 – aMFG, 9 – pMFG, 12 – aIFG, 14 – mIFG, 16 – pIFG, 18 – mOFC, 22 – ACC, 24 – MCC, 26 – PCC, 30 – mPrCG, 36 – FOP, 38 – POP, 39 – aIns, 41 – pIns, 43 – aTTG, 46 – pTTG, 48 – aSTG, 50 – pSTG, 52 – aMTG, 54 – pMTG, 62 – aFFG, 64 – pFFG, 74 – mPoCG, 76 – iPoCG, 80 – SMG, 82, AnG, 83 – PCun, 90 – Calc, 94 – mOG, 98 – CN, 101 – BF, 103 – Pu, 108 – Th, 112 – CerIX, 114 – CerVIII, 115 –CrusI, 118 –CrusII, 120 – CerVI.
The online version of this article includes the following source data for figure 6:

Source data 1. Complete Davi130 labels hemispheric asymmetry.

nucleus (CN) and thalamus (Th). The cerebellum exclusively showed rightward GM asymmetry in the posterior cerebellar lobe (CerIX, CerVIII, CrusI, CrusII, CerVI). The hemispheric asymmetry did not show a decipherable pattern.

Discussion

As a common reference space for the analysis of chimpanzee brain data, we created the Juna.Chimp template, constructed from a large heterogeneous sample of T1w MRI's from the NCBR. The Juna.Chimp template includes a reference T1-template, along with probability maps of brain and head tissues accompanied by a Geodesic Shooting template for the publicly available SPM12/CAT12 preprocessing pipeline to efficiently segment and accurately spatially normalize individual chimpanzee T1w images. The T1-template and TPM can also be used as the target for image registration with other popular software packages, such as FSL (https://fsl.fmrib.ox.ac.uk/fsl) or ANTs (http://stnava.github.io/ANTs/). Furthermore, our processing pipeline and templates can be utilized for data-driven approaches to create connectivity-based and structural covariance parcellations of the chimpanzee brain (***Alexander-Bloch et al., 2013***; ***Eickhoff et al., 2015***).

Additionally, we provide the manually segmented, macro-anatomical Davi130 whole-brain parcellation comprising 130 cortical, sub-cortical and cerebellar brain regions, which enables systematic extraction of volumes-of-interest from chimpanzee MRI data. The image processing pipeline and Davi130 parcellation were used to investigate ageing and interhemispheric asymmetry in the chimpanzee brain. The Davi130 parcellation was realized by utilizing macroscopic gyral and sulcal features such as peaks, fundi, and bends to represent the chimpanzee brain in a reduced dimensional space based on macro-anatomical landmarks. Despite the evidence that true microanatomical borders between brain areas rarely coincide with macro-anatomical patterns (***Amunts and Zilles, 2015***), macroscopic brain parcellations like Desikan-Killany human atlas (***Desikan et al., 2006***) have successfully been utilized in many studies furthering our understanding of brain structure, function, and

disease (**Kong et al., 2020**; **van den Heuvel et al., 2020**). The Davi130 parcellation of the chimpanzee brain serves two main purposes. First, regions in Juna.Chimp template space enable increased interpretability and reproducibility of morphometric analyses and comparability between studies, even retrospectively. Second, our manual subdivision reduces the statistical problem of multiple testing for mass univariate approaches like VBM to uncover subtle brain - behavior relationships. Furthermore, our macroscopic parcellation mitigates the curse of dimensionality for multivariate machine learning methods to be applied to the relatively small samples like the NCBR.

We found clear evidence of global and local GM decline in the aging chimpanzee brain even though previous research into age-related changes in chimpanzee brain organization has shown little to no effect (**Herndon et al., 1999**; **Sherwood et al., 2011**; **Chen et al., 2013**; **Autrey et al., 2014**). (**Herndon et al., 1999**; **Sherwood et al., 2011**; **Chen et al., 2013**; **Autrey et al., 2014**). This can be attributed on the one hand to the larger number of MRI scans available via the NCBR including 30% of older subjects with 55 individuals over 30 and 12 over 45 years of age, which is crucial for modelling the effect of aging (**Chen et al., 2013**; **Autrey et al., 2014**). On the other hand, state-of-the-art image processing enabled the creation of the species-specific Juna.Chimp templates, which largely improves tissue segmentation and registration accuracy (**Ashburner and Friston, 2000**). Non-linear registration was also improved by the large heterogeneous sample utilized for the creation of the templates encompassing a representative amount of inter-individual variation. We used the well-established structural brain imaging toolbox CAT12 to build a reusable chimpanzee preprocessing pipeline catered towards analyzing local tissue-specific anatomical variations as measured with T1w MRI. The Davi130-based region-wise and the voxel-wise morphometry analysis consistently showed localized GM decline in lateral frontal cortex, lOFC, precentral gyrus, cingulate gyrus, PCun, medial parietal and occipital cortex, the basal ganglia, and superior cerebellum. The VBM approach additionally produced evidence for age effects in bilateral mOFC, PoCG, inferior temporal regions, inferior and superior lateral parietal cortex, sOG, and throughout the cerebellum. These additional effects can be expected, as VBM is more sensitive to GM changes due to aging (**Kennedy et al., 2009**). The multiple brain regions revealing GM decline reported here in both approaches have also been shown to exhibit GM atrophy during healthy aging in humans (**Good et al., 2001b**; **Kennedy et al., 2009**; **Crivello et al., 2014**; **Minkova et al., 2017**). Additionally, there was no significant difference in the age-related decline between humans and chimpanzee (**Figure 3**), even though a larger negative correlation with less variance was found in the matched human sample, which demonstrates a commonality in the healthy aging process of chimpanzees that was thought to be specific to humans. In general, GM atrophy in chimpanzees occurs across the entire cortex, sub-cortical regions, and cerebellum, however, certain local areas decline at a relative extended rate within the frontal, temporal, and parietal lobes (**Fjell et al., 2014**). Several Davi130 regions within the frontal lobe (SFG, MFG, IFG, and lOFC) have been previously reported in corresponding human loci in relation to GM volume decline due to aging (**Kennedy et al., 2009**; **Crivello et al., 2014**; **Fjell et al., 2014**; **Minkova et al., 2017**). Furthermore, aging effects in temporal (STG) and parietal (PoCG, AnG, PCun) regions in chimpanzees have additionally been revealed in analogous human areas (**Good et al., 2001b**; **Kennedy et al., 2009**; **Crivello et al., 2014**; **Fjell et al., 2014**; **Minkova et al., 2017**). The same is true for the superior occipital gyrus and caudate nucleus (**Crivello et al., 2014**). Similar age-related total GM decline along with presentation in homologous brain areas suggests common underlying neurophysiological processes in humans and chimpanzees due to shared primate evolution.

Very recently, it has been shown that stress hormone levels increase with age in chimpanzees, a process previously thought to only occur in humans, which can cause GM volume decline (**Emery Thompson et al., 2020**). This further strengthens the argument that age-related GM decline is also shared by humans closest relative, the chimpanzee. Furthermore, **Edler et al., 2017** found Alzheimer's disease-like accumulation of amyloid beta plaques and neurofibrillary tangles located predominantly in prefrontal and temporal cortices in a sample of elderly chimpanzees between 37 and 62 years of age. As the aggregation of these proteins is associated with localized neuronal loss and cortical atrophy in humans (**La Joie et al., 2012**; **Lladó et al., 2018**), the age-related decline in GM volume shown here is well in line with the findings by **Jagust, 2016** associating GM atrophy with amyloid beta. These findings provide a biological mechanism for accelerated GM decrease in prefrontal, limbic, and temporal cortices found in chimpanzees. In contrast, elderly rhesus monkeys show GM volume decline without the presence of neurofibrillary tangles (**Alexander et al., 2008**;

Shamy et al., 2011). Taken together, regionally specific GM atrophy seems to be a common aspect of the primate brain aging pattern observed in macaque monkeys, chimpanzees, and humans. To make a case for the existence of Alzheimer's disease in chimpanzees, validated cognitive tests for Alzheimer's-like cognitive decline in non-human primates are needed, to test for direct associations between cognitive decline with tau pathology and brain atrophy.

To further analyze the possible moderator effects on aging, we considered the historical composition of the NCBR sample, with respect to the rearing environment. The majority of elderly chimpanzees over 40 years old (23/26) were born in the wild and captured at a young age, whereas only very few chimpanzees under 40 were wild born (5/168). The capture, separation from their mothers, and subsequent transport to the research centers can be considered a traumatic event with possible lasting effects on brain development and morphology (*Bremner, 2006*). In captivity, different chimpanzee-rearing experiences, either by their mother or in a nursery, has been shown to affect brain morphology (*Bogart et al., 2014*; *Bard and Hopkins, 2018*). The same should be expected in comparison of captive and wild-born chimpanzees. The disproportionate distribution of rearing and early life experiences likely influences our cross-sectional analyses of the effect of aging on GM volume. However, we have some reason to be confident that the aging effect shown here is not solely driven by these factors as rearing environment was added as a covariate to all age regression models and the VBM age regression model with and without rearing as a covariate are almost identical (*Figure 5* and *Figure 5—figure supplement 1* respectively). Moreover, the GM decline we found is extensive, widespread, and also present in chimpanzees under 30 years of age ($p<0.0001$), where 99% are captive born (143/144).

Hemispheric asymmetry was found in 68% (44/65) of all regions of the Davi130 parcellation, reproducing several regional findings reported in previous studies using diverse image processing methods as well as uncovering numerous novel population-level asymmetries. Previous studies utilizing a region-wise approach based on hand-drawn or atlas derived regions to analyze asymmetry in cortical thickness also reported leftward asymmetry of the insula (*Hopkins et al., 2017*) and rightward lateralization of cortical thickness of the PCC (*Hopkins et al., 2017*) as well as STG, MTG, and SMG (*Hopkins and Avants, 2013*). Previous VBM findings also revealed leftward asymmetry in the anterior SFG (*Hopkins et al., 2008*) along with rightward lateralization of the MFG, PrCG, PoCG, mOG, and CrusII (*Hopkins et al., 2008*; *Hopkins and Avants, 2013*). In the current study, new regions of larger GM volume in the left hemisphere were found in frontal (pMFG, mSFG, pSFG), temporal (aTTG), and parietal (PCun) cortices as well as in the basal ganglia (BF,GP, Pu). Novel rightward asymmetries could also be seen in the frontal (IFG, mOFC, FrOP), limbic (CC, Amy), temporal (pTTG, FFG), parietal (POP, AnG), and occipital (Calc) cortices besides the basal ganglia (Th, CN) and the cerebellum (CrusI, CerIX, CerVI, CerVIII).

The Davi130s' region pTTG which contains the planum temporale (PT), presented significant rightward lateralization, while previous studies of the PT have shown leftward asymmetry in chimpanzee GM volume, surface area (*Hopkins and Nir, 2010*), and cytoarchitecture (*Zilles et al., 1996*; *Gannon et al., 1998*; *Spocter et al., 2010*). A possible reason for the divergence in this finding is that the anterior border of PT (*Hopkins and Nir, 2010*) lies several millimeters posterior from the anterior posterior split of the Davi130 TTG. Additionally, the left lateral sulcus in the Juna.Chimp template appears to proceed further posteriorly and superiorly compared to the right, which is consistent with previous findings in asymmetrical length of the POP in chimpanzees (*Gilissen and Hopkins, 2013*) and Sylvian fissure length in old world monkeys (*Lyn et al., 2011*; *Marie et al., 2018*). Population-level asymmetries in the pIFG in chimpanzees were documented almost two decades ago by *Cantalupo and Hopkins, 2001*, who reported a leftward asymmetry in pIFG volume in a small sample of great apes. In subsequent studies, this result could not be replicated when considering GM volume (*Hopkins et al., 2008*; *Keller et al., 2009*) or cytoarchitecture (*Schenker et al., 2010*). We also failed to find a leftward asymmetry in GM volume for the pIFG, in contrary to asymmetries found in humans (*Amunts et al., 1999*; *Uylings et al., 2006*; *Keller et al., 2009*).

A substantial amount of regions presenting significant inter-hemispheric differences of local morphology in chimpanzees has also been shown in humans (*Good et al., 2001a*; *Plessen et al., 2014*; *Kong et al., 2018*). Specifically, leftward lateralization has been found in human analogous regions of the SFG and insula utilizing GM thickness and volume in voxel-wise and atlas derived region-wise approaches (*Good et al., 2001a*; *Takao et al., 2011*; *Plessen et al., 2014*; *Kong et al., 2018*). Rightward asymmetry in the Davi130 regions IFG, STG, MTG, AnG, mOG, Calc, in addition to the

thalamus and lateral cerebellum is documented in the human brain also using both VBM and surface measures (*Good et al., 2001a*; *Takao et al., 2011*; *Plessen et al., 2014*; *Kong et al., 2018*). Gross hemispheric asymmetry in humans follows a general structure of frontal rightward and occipital leftward asymmetry known as the 'Yakovlevian torque' (*Toga and Thompson, 2003*). This general organizational pattern of asymmetry was not apparent in the chimpanzee (*Li et al., 2018*).

The NCBR offers the largest and richest openly available dataset of chimpanzee brain MRI scans acquired over a decade with 1.5T and 3T MRI at two locations, capturing valuable inter-individual variation in one large heterogeneous sample. To account for the scanner effect on GM estimation, field strength was modeled as a covariate of no interest for analyzing the age effect on GM volume. The focus of this study was the analysis of GM volume, even though the CAT12 image processing pipeline enables surface projection and analysis. Consequently, the next step will be the application of CAT12 to analyze cortical surface area, curvature, gyrification, and thickness of the chimpanzee brain, to include behavioral data and the quantitative comparison to humans and other species, as cortical surface projection permits a direct inter-species comparison due to cross-species registration.

Conclusion

In conclusion, we present the new chimpanzee reference template Juna.Chimp, TPM's, the Davi130 whole-brain parcellation, and the CAT12 preprocessing pipeline which is ready-to-use by the wider neuroimaging community. Investigations of age-related GM changes in chimpanzees using both region-wise and voxel-based morphometry showed substantial atrophy with age, which was also apparent in a matched human sample providing further evidence for human-like physiological aging processes in the chimpanzee brain. Examining population-based hemispheric asymmetry in chimpanzees showed a general rightward lateralization of higher GM volume without the presence of a distinct pattern like the 'Yakovlevian torgue' seen in humans.

Materials and methods

Key resources table

Reagent type (species) or resource	Designation	Source or reference	Identifiers	Additional information
Software, algorithm	CAT12	http://www.neuro.uni-jena.de/cat/	RRID:SCR_019184	
Software, algorithm	NCBR	http://www.chimpanzeebrain.org/	RRID:SCR_019183	
Software, algorithm	MATLAB	http://www.mathworks.com/products/matlab/	RRID:SCR_001622	
Software, algorithm	SPM	http://www.fil.ion.ucl.ac.uk/spm/	RRID:SCR_007037	
Software, algorithm	RStudio	http://www.rstudio.com/	RRID:SCR_000432	
Software, algorithm	3D Slicer	http://slicer.org/	RRID:SCR_005619	

Subject information and image collection procedure

This study analyzed structural T1w MRI scans of 223 chimpanzees (137 females; 9–54 y/o, mean age 26.9 ± 10.2 years, *Figure 3—figure supplement 1*) from the NCBR (http://www.chimpanzeebrain.org/). The chimpanzees were housed at two locations including, the *National Center for Chimpanzee Care* of *The University of Texas MD Anderson Cancer Center* (UTMDACC) and the *Yerkes National Primate Research Center* (YNPRC) of Emory University. The standard MR imaging procedures for chimpanzees at the YNPRC and UTMDACC are designed to minimize stress for the subjects. For an

in-depth explanation of the imaging procedure please refer to **Autrey et al., 2014**. Seventy-six chimpanzees were scanned with a Siemens Trio 3 Tesla scanner (Siemens Medical Solutions USA, Inc, Malvern, Pennsylvania, USA). Most T1w images were collected using a three-dimensional gradient echo sequence with 0.6 × 0.6 × 0.6 resolution (pulse repetition = 2300 ms, echo time = 4.4 ms, number of signals averaged = 3). The remaining 147 chimpanzees were scanned using a 1.5T GE echo-speed Horizon LX MR scanner (GE Medical Systems, Milwaukee, WI), predominantly applying gradient echo sequence with 0.7 × 0.7 × 1.2 resolution (pulse repetition = 19.0 ms, echo time = 8.5 ms, number of signals averaged = 8).

DICOM conversion and de-noising

The structural T1w images were provided by the NCBR in their original DICOM format and converted into Nifti using MRIcron (**Rorden and Brett, 2000**). If multiple scans were available, the average was computed. Following DICOM conversion, each image was cleaned of noise (**Manjón et al., 2010**) and signal inhomogeneity and resliced to 0.6 mm isotropic resolution. Finally, the anterior commissure was manually set as the center (0,0,0) of all Nifti's to aid in affine preprocessing.

CAT12 preprocessing segmentation

Structural image segmentation in CAT12 builds on the TPM-based approach employed by SPM12, whereby, the gray/white image intensity is aided with a priori tissue probabilities in initial segmentation and affine registration as it is in common template space. Another advantage of a TPM is that one has a template for initial affine registration, which then enables the segment maps to be non-linearly registered and spatially normalized to corresponding segment maps of the chimpanzee shooting templates. Lowering the possibility for registration errors improves the quality of the final normalized image. Improving upon SPM's segmentation (**Ashburner and Friston, 2005**), CAT12 employs Local Adaptive Segmentation (LAS) (**Dahnke et al., 2012**), Adaptive Maximum A Posterior segmentation(AMAP) (**Dahnke and Gaser, 2017**; **Gaser et al., 2020**), and Partial Volume Estimation (PVE) (**Tohka et al., 2004**). LAS creates local intensity transformations for all tissue types to limit GM misclassification due to varying GM intensity in regions such as the occipital, basal ganglia, and motor cortex because of anatomical properties (e.g. high myelination and iron content). AMAP segmentation takes the initially segmented, aligned, and skull stripped image created utilizing the TPM and disregards the a priori information of the TPM, to conduct an adaptive AMAP estimation where local variations are modeled by slowly varying spatial functions (**Rajapakse et al., 1997**). Along with the classical three tissue types for segmentation (GM, WM, and CSF) based on the AMAP estimation, an additional two PVE classes (GM-WM and GM-CSF) are created resulting in an estimate of the fraction of each tissue type contained in each voxel. These features outlined above of our pipeline allow for more accurate tissue segmentation and therefore a better representation of macroanatomical GM levels for analysis.

Creation of chimpanzee templates

An iterative process as by **Franke et al., 2017** was employed to create the Juna.Chimp template, with T1 average, Shooting registration template (**Ashburner and Friston, 2011**), as well as the TPM (**Figure 7**). Initially, a first-generation template was produced using the 'greater_ape' template delivered by CAT (**Franke et al., 2017**; **Gaser et al., 2020**) that utilizes data provided in **Rilling and Insel, 1999**. The final segmentation takes the bias-corrected, intensity-normalized, and skull-stripped image together with the initial SPM-segmentation to conduct an AMAP estimation (**Rajapakse et al., 1997**) with a partial volume model for sub-voxel accuracy (**Tohka et al., 2004**). The affine normalized tissue segments of GM, white matter (WM), and cerebrospinal fluid (CSF) were used to create a new Shooting template that consists of four major non-linear normalization steps allowing to normalize new scans. To create a chimpanzee-specific TPM, we average the different Shooting template steps to benefit from the high spatial resolution of the final Shooting steps but also include the general affine aspects to avoid over-optimization. Besides the brain tissues the TPM also included two head tissues (bones and muscles) and a background class for standard SPM12 (**Ashburner and Friston, 2005**) and CAT12 preprocessing. An internal CAT atlas was written for each subject and mapped to the new chimpanzee template using the information from the Shooting registration. The CAT atlas maps were averaged by a median filter and finally manually

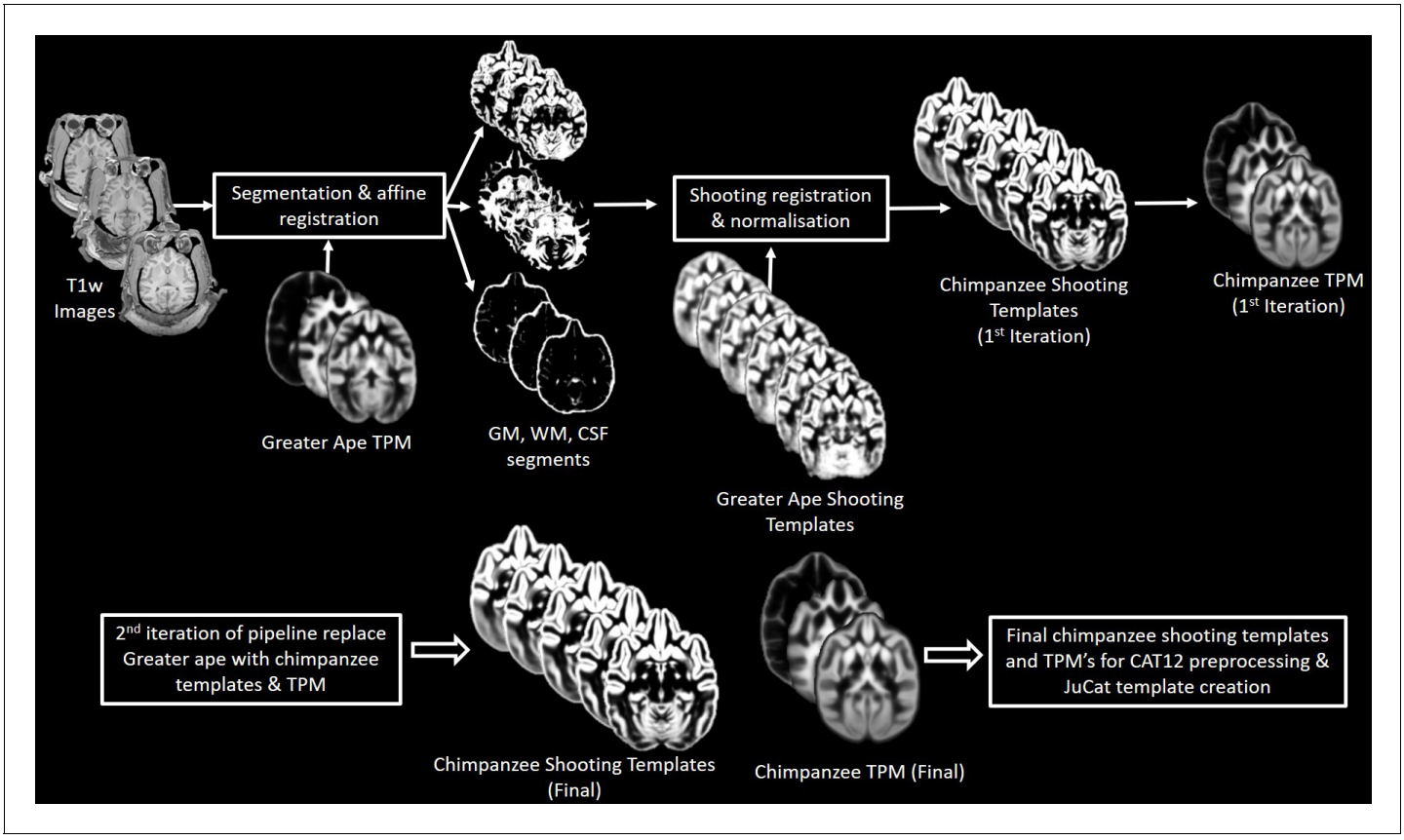

Figure 7. Workflow for creation of chimpanzee-specific shooting template and TPM, which can then be used in CAT12 structural preprocessing pipeline to create the Juna.Chimp template. The resulting chimpanzee-shooting template, TPM and CAT atlas establishes the robust and reliable base to segment and spatially normalize the T1w images utilizing CAT12's processing pipeline (***Dahnke and Gaser, 2017***; ***Gaser et al., 2020***).

corrected. This initial template was then used in the second iteration of CAT segmentation to establish the final chimpanzee-specific Juna.Chimp template, which was imported into the standard CAT12 preprocessing pipeline to create the final data used for the aging and asymmetry analyses.

Davi130 parcellation

The average T1 and final Shooting template were used for a manual delineation of macro-anatomical GM structures. Identification and annotation of major brain regions were performed manually using the program, 3D Slicer 4.10.1 (https://www.slicer.org). The labeling enables automated, region-based analysis of the entire chimpanzee brain and allows for robust statistical analysis. Nomenclature and location of regions were ascertained by consulting both chimpanzee and human brain atlases (***Bailey and Bonin GV, 1950***; ***Mai et al., 2015***). The labeling was completed by two authors (S.V. and R.D.) and reviewed by two experts of chimpanzee brain anatomy (C.C.S. and W.D.H.). A total of 65 GM structures within the cerebrum and cerebellum of the left hemisphere were annotated and then flipped to the right hemisphere. The flipped annotations were then manually adapted to the morphology of the right hemisphere to have complete coverage of the chimpanzee brain with 130 labels.

The location of macroscopic brain regions was determined based on major gyri of the cerebral cortex, as well as distinct anatomical landmarks of the cerebellar cortex, and basal ganglia. Of note, the border between two adjacent gyri was set as the mid-point of the connecting sulcus, generally at the fundus. Large gyri were further subdivided into two or three parts based on their size and structural features to enable greater spatial resolution and better inter-regional comparison. Naming of regional subdivisions were based on spatial location, for example, anterior, middle, posterior, as

these splits are based on macroanatomical features and do not necessarily correspond to functional parcellations.

Considering the limitations of macroscopic features present in T1w, we utilized distinct morphological representations to split large gyri, such as gyral/sulcal folds and continuation of sulci. If a distinguishable feature could not be determined, rough distance and regional size was employed as border defining criteria. The splits of the lateral temporal lobe, including the TTG, followed a continuation of the inferior portion of the postcentral sulcus that angles slightly posteriorly to better account for the increase in length of the gyri as it proceeds inferiorly. The central sulcus as well as the adjacent pre- and postcentral gyri contain a knob or U-shaped bend proceeding posteriorly. The superior beginning and inferior end of this bend were employed for the two splits of these gyri. Additionally, the central sulcus is the border between the frontal and parietal lobes, therefore, the FOP – POP split occurs at the termination of the central sulcus at the lateral fissure. Within the frontal cortex, the anterior posterior split of the MFG is at the meeting point of the middle frontal sulcus and the superior precentral sulcus, which translates to the inferior bend of the MFG. The tip of the fronto-orbito sulcus was used as an anchor point for the split of the pIFG and mIFG. The middle anterior split of the IFG was then determined by distance, whereby the remaining gyrus was separated into equally sized parts. The cingulate cortex anterior, middle, and posterior subdivisions were delineated by splits following the anterior and posterior bends of the gyrus around the corpus callosum. The cerebellum was divided into its major lobes which are quite similar across primates (***Apps and Hawkes, 2009***). Finally, splits within the OFC, SFG, and insula were based on equal size and/or distance.

Quality control

CAT12 provides quality measures pertaining to noise, bias inhomogeneities, resolution and an overall compounded score of the original input image. Using these ratings, poor images were flagged for visual inspection when they were two standard deviations (std) away from the sample mean of each rating. The preprocessed modulated GM maps were then tested for sample inhomogeneity separately for each scanner (3T and 1.5T) and those that have a mean correlation below two std were flagged for visual inspection. Once the original image was flagged, affine GM, and modulated GM maps were inspected for poor quality, tissue misclassification, artefacts, irregular deformations, and very high intensities. For the second and third iteration, the passed modulated GM maps were tested again for mean correlation as a complete sample, flagging the images below two std for visual inspection, looking for the same features as in the initial QC iteration. Following the three iterations of QC a total of 194 of 223 chimpanzee MRI's (130 females, 9–54 y/o, mean = 26.2 ± 9.9) qualified for statistical analysis.

Age-related changes in total gray matter

A linear regression model was used to determine the effect of aging on total GM volume. Firstly, total GM volume for each subject was converted into a percentage of total intracranial volume (TIV) to account for the variation in head size. This was then entered into a linear regression model as the dependent variable with age, sex, scanner field strength, and rearing as the independents. Sex-specific models were conducted with males and females separately using age as the only dependent variable. The slope of each regression line was determined using R^2 and a p-value of $p \leq 0.05$ was used to determine the significant effect of age and sex on total GM volume. The IXI brain development dataset (http://brain-development.org/ixi-dataset/) was utilized to compare the age effect on total GM volume between chimpanzees and humans, as it includes subjects with a wide age range and T1w images from MRI scanners of both 1.5T and 3T field strength. Prior to matching the IXI sample to the QC passed chimpanzee sample, all images collected from the Institute of Psychiatry (IOP) were removed to keep similarity to the chimpanzee sample of a single 1.5T scanner. After removing subjects without meta data, a total of 496 subjects (***Figure 3—figure supplement 2***) were used for matching to the chimpanzee sample regarding age, sex, and scanner field strength. To enable age matching between species, a factor of 1.5 of chimpanzee age was used to roughly calculate the comparable human age. This factor was chosen based on the comparable life span of the two species, because a chimpanzee 40+ years is considered elderly and so is a 60+ year old human, also a 60+ year old chimpanzee is very old and uncommon similarly to a human 90+ years old.

Furthermore, the age of sexual maturity in humans is 19.5 years, while in chimps it is 13.5 years which is also approximately a difference of 1.5 (**Robson and Wood, 2008**). The sample matching was conducted using the 'MatchIt' (**Ho et al., 2007**) R package (https://cran.r-project.org/package=MatchIt) and utilizing the 'optimal' (**Hansen and Klopfer, 2006**) algorithm. The matched human sample contained 194 subjects (128 females, 20–78 y/o, mean = 39.4 ± 14.0) for statistical analysis.

Age-related changes in gray matter using Davi130 parcellation

The Davi130 parcellation was applied to the modulated GM maps to conduct region-wise morphometry analysis. First, the Davi130 regions were masked with a 0.1 GM mask to remove all non-GM portions of the regions. Subsequently, the average GM intensity of each region for all QC-passed chimpanzees was calculated. A multiple regression model was conducted for the labels from both hemispheres, whereby, the dependent variable was GM volume and the predictor variables were age, sex, TIV, scanner strength, and rearing. Significant age-related GM decline was established for a Davi130 label with a $p \leq 0.05$, after correcting for multiple comparisons using FWE (**Holm, 1979**).

Voxel-based morphometry

VBM analysis was conducted using CAT12 to determine the effect of aging on local GM volume. The modulated and spatially normalized GM segments from each subject were spatially smoothed with a 4 mm FWHM (full width half maximum) kernel prior to analyses. To restrict the overall volume of interest, an implicit 0.4 GM mask was employed. As MRI field strength is known to influence image quality, and consequently, tissue classification, we included scanner strength in our VBM model as a covariate. The dependent variable in the model was age, with covariates of TIV, sex, scanner strength, and rearing. The VBM model was corrected for multiple comparisons using TFCE with 5000 permutations (**Smith and Nichols, 2009**). Significant clusters were determined at $p \leq 0.05$, after correcting for multiple comparisons using FWE.

Hemispheric asymmetry

As for the age regression analysis, all Davi130 parcels were masked with a 0.1 GM mask to remove non-GM portions within regions. Cortical hemispheric asymmetry of Davi130 labels was determined using the formula $Asym = (L - R) / (L + R) * 0.5$ (**Kurth et al., 2015**; **Hopkins et al., 2017**), whereby L and R represent the average GM volume for each region in the left and right hemisphere, respectively. Therefore, the bi-hemispheric Davi130 regions were converted into single *Asym* labels (n = 65) with positive *Asym* values indicating a leftward asymmetry, and negative values, a rightward bias. One-sample *t*-tests were conducted for each region under the null hypothesis of $Asym = 0$, and significant leftward or rightward asymmetry was determined with a $p \leq 0.05$, after correcting for multiple comparisons using FWE (**Holm, 1979**).

Exemplar pipeline workflow

To illustrate the structural processing pipeline, we have created exemplar MATLAB SPM batch scripts that utilizes the Juna.Chimp templates in CAT12's preprocessing workflow to conduct segmentation, spatial registration, and finally some basic age analysis on an openly available direct-to-download chimpanzee sample (http://www.chimpanzeebrain.org/). These scripts require the appropriate templates which can be downloaded from the Juna.Chimp web viewer (SPM/CAT_templates.zip) and then place the templates_animals/folder into the latest version CAT12 Toolbox directory (CAT12.7 r1609). The processing parameters are similar to those conducted in this study, although different DICOM conversions and denoising were conducted. Further information regarding each parameter can be viewed when opening the script in the SPM batch as well as the provided comments and README file. The code for the workflow in addition to the code used to conduct the aging effect and asymmetry analyses can be found here (https://github.com/viko18/JunaChimp; **Vickery, 2020**; copy archived at swh:1:rev:411f0610269416d4ee04eaf9670a9dc84e829ea0).

Acknowledgements

We thank Jona Fischer for the creation of the interactive Juna.Chimp web viewer adapted from nehuba (github).

Additional information

Funding

Funder	Grant reference number	Author
Helmholtz Association	Helmholtz Portfolio Theme 'Supercomputing and Modelling for the Human Brain	Sam Vickery Simon B Eickhoff Felix Hoffstaedter
Horizon 2020	945539 (HBP SGA 3)	Sam Vickery Simon B Eickhoff Felix Hoffstaedter
Helmholtz Association	Initiative and Networking Fund	Svenja Caspers
Horizon 2020	785907 (HBP SGA 2)	Svenja Caspers
National Institutes of Health	NS-42867	William D Hopkins
National Institutes of Health	NS092988	Chet C Sherwood
James S. McDonnell Foundation	220020293	Chet C Sherwood
Inspire Foundation	SMA-1542848	Chet C Sherwood
National Institutes of Health	U42-OD011197	Steven J Schapiro
Deutsche Forschungsgemeinschaft	417649423	Robert Dahnke
National Institutes of Health	NS-73134	William D Hopkins
National Institutes of Health	NS-92988	William D Hopkins

The funders had no role in study design, data collection and interpretation, or the decision to submit the work for publication.

Author contributions

Sam Vickery, Conceptualization, Data curation, Software, Formal analysis, Investigation, Visualization, Methodology, Writing - original draft, Project administration, Writing - review and editing; William D Hopkins, Conceptualization, Resources, Data curation, Funding acquisition, Validation, Methodology, Writing - original draft, Writing - review and editing; Chet C Sherwood, Resources, Data curation, Funding acquisition, Validation, Methodology, Writing - original draft, Writing - review and editing; Steven J Schapiro, Resources, Data curation, Funding acquisition, Writing - original draft, Writing - review and editing; Robert D Latzman, Conceptualization, Data curation, Writing - original draft, Writing - review and editing; Svenja Caspers, Conceptualization, Supervision, Writing - original draft, Writing - review and editing; Christian Gaser, Resources, Software, Methodology, Writing - original draft, Writing - review and editing; Simon B Eickhoff, Conceptualization, Resources, Supervision, Funding acquisition, Writing - original draft, Project administration, Writing - review and editing; Robert Dahnke, Conceptualization, Resources, Data curation, Software, Supervision, Validation, Investigation, Methodology, Writing - original draft, Project administration, Writing - review and editing; Felix Hoffstaedter, Conceptualization, Software, Supervision, Validation, Methodology, Writing - original draft, Project administration, Writing - review and editing

Author ORCIDs

Sam Vickery https://orcid.org/0000-0001-6732-7014
Chet C Sherwood http://orcid.org/0000-0001-6711-449X
Robert D Latzman http://orcid.org/0000-0002-1175-8090

Simon B Eickhoff http://orcid.org/0000-0001-6363-2759
Felix Hoffstaedter https://orcid.org/0000-0001-7163-3110

Ethics

Animal experimentation: the chimpanzee imaging data were acquired under protocols approved by the Yerkes National Primate Research Center (YNPRC) at Emory University Institutional Animal Care and Use Committee (Approval number YER2001206).

Decision letter and Author response

Decision letter https://doi.org/10.7554/eLife.60136.sa1
Author response https://doi.org/10.7554/eLife.60136.sa2

Additional files

Supplementary files

- Transparent reporting form

Data availability

The T1-weighted MRI's are available at the National Chimpanzee Brain Resource website as well as the direct-to-download dataset we used for our example workflow. The code used in the manuscript can be found at this GitHub repo https://github.com/viko18/JunaChimp (copy archived at https://archive.softwareheritage.org/swh:1:rev:411f0610269416d4ee04eaf9670a9dc84e829ea0/).

References

Alexander GE, Chen K, Aschenbrenner M, Merkley TL, Santerre-Lemmon LE, Shamy JL, Skaggs WE, Buonocore MH, Rapp PR, Barnes CA. 2008. Age-related regional network of magnetic resonance imaging gray matter in the rhesus macaque. *Journal of Neuroscience* **28**:2710–2718. DOI: https://doi.org/10.1523/JNEUROSCI.1852-07.2008, PMID: 18337400

Alexander-Bloch A, Giedd JN, Bullmore E. 2013. Imaging structural co-variance between human brain regions. *Nature Reviews Neuroscience* **14**:322–336. DOI: https://doi.org/10.1038/nrn3465, PMID: 23531697

Amunts K, Schleicher A, Bürgel U, Mohlberg H, Uylings HB, Zilles K. 1999. Broca's region revisited: cytoarchitecture and intersubject variability. *The Journal of Comparative Neurology* **412**:319–341. DOI: https://doi.org/10.1002/(SICI)1096-9861(19990920)412:2<319::AID-CNE10>3.0.CO;2-7, PMID: 10441759

Amunts K, Zilles K. 2015. Architectonic mapping of the human brain beyond brodmann. *Neuron* **88**:1086–1107. DOI: https://doi.org/10.1016/j.neuron.2015.12.001, PMID: 26687219

Anderson JR, Gallup GG. 2015. Mirror self-recognition: a review and critique of attempts to promote and engineer self-recognition in primates. *Primates* **56**:317–326. DOI: https://doi.org/10.1007/s10329-015-0488-9, PMID: 26341947

Apps R, Hawkes R. 2009. Cerebellar cortical organization: a one-map hypothesis. *Nature Reviews Neuroscience* **10**:670–681. DOI: https://doi.org/10.1038/nrn2698, PMID: 19693030

Ashburner J, Friston KJ. 2000. Voxel-based morphometry–the methods. *NeuroImage* **11**:805–821. DOI: https://doi.org/10.1006/nimg.2000.0582, PMID: 10860804

Ashburner J, Friston KJ. 2005. Unified segmentation. *NeuroImage* **26**:839–851. DOI: https://doi.org/10.1016/j.neuroimage.2005.02.018, PMID: 15955494

Ashburner J, Friston KJ. 2011. Diffeomorphic registration using geodesic shooting and Gauss-Newton optimisation. *NeuroImage* **55**:954–967. DOI: https://doi.org/10.1016/j.neuroimage.2010.12.049, PMID: 21216294

Autrey MM, Reamer LA, Mareno MC, Sherwood CC, Herndon JG, Preuss T, Schapiro SJ, Hopkins WD. 2014. Age-related effects in the neocortical organization of chimpanzees: gray and white matter volume, cortical thickness, and gyrification. *NeuroImage* **101**:59–67. DOI: https://doi.org/10.1016/j.neuroimage.2014.06.053, PMID: 24983715

Bailey P, Bonin GV MW. 1950. *The Isocortex of the Chimpanzee*. Urbana: Univ of Illinois Press.

Bard KA, Hopkins WD. 2018. Early socioemotional intervention mediates Long-Term effects of atypical rearing on structural covariation in gray matter in adult chimpanzees. *Psychological Science* **29**:594–603. DOI: https://doi.org/10.1177/0956797617740685, PMID: 29381427

Bogart SL, Mangin J-F, Schapiro SJ, Reamer L, Bennett AJ, Pierre PJ, Hopkins WD. 2012. Cortical sulci asymmetries in chimpanzees and macaques: a new look at an old Idea. *NeuroImage* **61**:533–541. DOI: https://doi.org/10.1016/j.neuroimage.2012.03.082

Bogart SL, Bennett AJ, Schapiro SJ, Reamer LA, Hopkins WD. 2014. Different early rearing experiences have long-term effects on cortical organization in captive chimpanzees (*Pan* Troglodytes). *Developmental Science* **17**:161–174. DOI: https://doi.org/10.1111/desc.12106, PMID: 24206013

Bremner JD. 2006. Traumatic stress: effects on the brain. *Dialogues in Clinical Neuroscience* **8**:445–461. DOI: https://doi.org/10.31887/DCNS.2006.8.4/jbremner, PMID: 17290802

Cantalupo C, Hopkins WD. 2001. Asymmetric broca's area in great apes: A region of the ape brain is uncannily similar to one linked with speech in humans. *Nature* **414**:505. DOI: https://doi.org/10.1038/35107134

Chen X, Errangi B, Li L, Glasser MF, Westlye LT, Fjell AM, Walhovd KB, Hu X, Herndon JG, Preuss TM, Rilling JK. 2013. Brain aging in humans, chimpanzees (Pan Troglodytes), and rhesus macaques (Macaca mulatta): magnetic resonance imaging studies of macro- and microstructural changes. *Neurobiology of Aging* **34**:2248–2260. DOI: https://doi.org/10.1016/j.neurobiolaging.2013.03.028, PMID: 23623601

Crivello F, Tzourio-Mazoyer N, Tzourio C, Mazoyer B. 2014. Longitudinal assessment of global and regional rate of grey matter atrophy in 1,172 healthy older adults: modulation by sex and age. *PLOS ONE* **9**:e114478. DOI: https://doi.org/10.1371/journal.pone.0114478, PMID: 25469789

Dahl CD, Adachi I. 2013. Conceptual metaphorical mapping in chimpanzees (Pan Troglodytes). *eLife* **2**:e00932. DOI: https://doi.org/10.7554/eLife.00932

Dahnke R, Ziegler G, Gaser C. 2012. Local adaptive segmentation. Hum Brain Mapp Conference.

Dahnke R, Gaser C. 2017. Voxel-based preprocessing in CAT. *Organ Hum Brain Mapp* **2**:70887. DOI: https://doi.org/10.13140/RG.2.2.11653.70887

de WFBM, Frans BM. 1996. *Good natured: the origins of right and wrong in humans and other animals*. Harvard University Press.

Desikan RS, Ségonne F, Fischl B, Quinn BT, Dickerson BC, Blacker D, Buckner RL, Dale AM, Maguire RP, Hyman BT, Albert MS, Killiany RJ. 2006. An automated labeling system for subdividing the human cerebral cortex on MRI scans into gyral based regions of interest. *NeuroImage* **31**:968–980. DOI: https://doi.org/10.1016/j.neuroimage.2006.01.021, PMID: 16530430

Edler MK, Sherwood CC, Meindl RS, Hopkins WD, Ely JJ, Erwin JM, Mufson EJ, Hof PR, Raghanti MA. 2017. Aged chimpanzees exhibit pathologic hallmarks of Alzheimer's disease. *Neurobiology of Aging* **59**:107–120. DOI: https://doi.org/10.1016/j.neurobiolaging.2017.07.006

Eickhoff SB, Thirion B, Varoquaux G, Bzdok D. 2015. Connectivity-based parcellation: critique and implications. *Human Brain Mapping* **36**:4771–4792. DOI: https://doi.org/10.1002/hbm.22933, PMID: 26409749

Emery Thompson M, Fox SA, Berghänel A, Sabbi KH, Phillips-Garcia S, Enigk DK, Otali E, Machanda ZP, Wrangham RW, Muller MN. 2020. Wild chimpanzees exhibit humanlike aging of glucocorticoid regulation. *PNAS* **117**:8424–8430. DOI: https://doi.org/10.1073/pnas.1920593117, PMID: 32229565

Fjell AM, McEvoy L, Holland D, Dale AM, Walhovd KB, Alzheimer's Disease Neuroimaging Initiative. 2014. What is normal in normal aging? effects of aging, amyloid and Alzheimer's disease on the cerebral cortex and the hippocampus. *Progress in Neurobiology* **117**:20–40. DOI: https://doi.org/10.1016/j.pneurobio.2014.02.004, PMID: 24548606

Franke K, Clarke GD, Dahnke R, Gaser C, Kuo AH, Li C, Schwab M, Nathanielsz PW. 2017. Premature brain aging in baboons resulting from moderate fetal undernutrition. *Frontiers in Aging Neuroscience* **9**:92. DOI: https://doi.org/10.3389/fnagi.2017.00092, PMID: 28443017

Freeman HD, Cantalupo C, Hopkins WD. 2004. Asymmetries in the Hippocampus and amygdala of chimpanzees (Pan Troglodytes). *Behavioral Neuroscience* **118**:1460–1465. DOI: https://doi.org/10.1037/0735-7044.118.6.1460, PMID: 15598157

Gannon PJ, Holloway RL, Broadfield DC, Braun AR. 1998. Asymmetry of chimpanzee planum temporale: humanlike pattern of Wernicke's brain language area homolog. *Science* **279**:220–222. DOI: https://doi.org/10.1126/science.279.5348.220, PMID: 9422693

Gaser C, Dahnke R, Kurth K, Luders E, Alzheimer's Disease Neuroimaging Initiative. 2020. A computational anatomy toolbox for the analysis of structural MRI data. *NeuroImage* **2**:9282. DOI: https://doi.org/10.13140/RG.2.2.19452.49282

Gilissen EP, Hopkins WD. 2013. Asymmetries of the parietal operculum in chimpanzees (Pan Troglodytes) in relation to handedness for tool use. *Cerebral Cortex* **23**:411–422. DOI: https://doi.org/10.1093/cercor/bhs029, PMID: 22368087

Gómez-Robles A, Hopkins WD, Sherwood CC. 2013. Increased morphological asymmetry, evolvability and plasticity in human brain evolution. *Proceedings of the Royal Society B: Biological Sciences* **280**:20130575. DOI: https://doi.org/10.1098/rspb.2013.0575

Good CD, Johnsrude I, Ashburner J, Henson RN, Friston KJ, Frackowiak RS. 2001a. Cerebral asymmetry and the effects of sex and handedness on brain structure: a voxel-based morphometric analysis of 465 normal adult human brains. *NeuroImage* **14**:685–700. DOI: https://doi.org/10.1006/nimg.2001.0857, PMID: 11506541

Good CD, Johnsrude IS, Ashburner J, Henson RN, Friston KJ, Frackowiak RS. 2001b. A voxel-based morphometric study of ageing in 465 normal adult human brains. *NeuroImage* **14**:21–36. DOI: https://doi.org/10.1006/nimg.2001.0786, PMID: 11525331

Hansen BB, Klopfer SO. 2006. Optimal full matching and related designs via network flows. *Journal of Computational and Graphical Statistics* **15**:609–627. DOI: https://doi.org/10.1198/106186006X137047

Hecht EE, Mahovetz LM, Preuss TM, Hopkins WD. 2017. A neuroanatomical predictor of mirror self-recognition in chimpanzees. *Social Cognitive and Affective Neuroscience* **12**:37–48. DOI: https://doi.org/10.1093/scan/nsw159, PMID: 27803287

Herndon JG, Tigges J, Anderson DC, Klumpp SA, McClure HM. 1999. Brain weight throughout the life span of the chimpanzee. *The Journal of Comparative Neurology* **409**:567–572. DOI: https://doi.org/10.1002/(SICI)1096-9861(19990712)409:4<567::AID-CNE4>3.0.CO;2-J, PMID: 10376740

Ho DE, Imai K, King G, Stuart EA. 2007. Matching as nonparametric preprocessing for reducing model dependence in parametric causal inference. *Political Analysis* **15**:199–236. DOI: https://doi.org/10.1093/pan/mpl013

Holm S. 1979. A simple sequentially rejective multiple test procedure. *Scand J Stat* **6**:65–70. DOI: https://doi.org/10.2307/4615733

Hopkins WD, Taglialatela JP, Meguerditchian A, Nir T, Schenker NM, Sherwood CC. 2008. Gray matter asymmetries in chimpanzees as revealed by voxel-based morphometry. *NeuroImage* **42**:491–497. DOI: https://doi.org/10.1016/j.neuroimage.2008.05.014, PMID: 18586523

Hopkins WD, Meguerditchian A, Coulon O, Bogart S, Mangin JF, Sherwood CC, Grabowski MW, Bennett AJ, Pierre PJ, Fears S, Woods R, Hof PR, Vauclair J. 2014. Evolution of the central sulcus morphology in primates. *Brain, Behavior and Evolution* **84**:19–30. DOI: https://doi.org/10.1159/000362431, PMID: 25139259

Hopkins WD, Misiura M, Pope SM, Latash EM. 2015. Behavioral and brain asymmetries in primates: a preliminary evaluation of two evolutionary hypotheses. *Annals of the New York Academy of Sciences* **1359**:65–83. DOI: https://doi.org/10.1111/nyas.12936, PMID: 26426409

Hopkins WD, Li X, Crow T, Roberts N. 2017. Vertex- and atlas-based comparisons in measures of cortical thickness, gyrification and white matter volume between humans and chimpanzees. *Brain Structure and Function* **222**:229–245. DOI: https://doi.org/10.1007/s00429-016-1213-1, PMID: 27100220

Hopkins WD, Avants BB. 2013. Regional and hemispheric variation in cortical thickness in chimpanzees (Pan Troglodytes). *Journal of Neuroscience* **33**:5241–5248. DOI: https://doi.org/10.1523/JNEUROSCI.2996-12.2013, PMID: 23516289

Hopkins WD, Nir TM. 2010. Planum temporale surface area and grey matter asymmetries in chimpanzees (Pan Troglodytes): the effect of handedness and comparison with findings in humans. *Behavioural Brain Research* **208**:436–443. DOI: https://doi.org/10.1016/j.bbr.2009.12.012, PMID: 20035802

Jagust W. 2016. Is amyloid-β harmful to the brain? insights from human imaging studies. *Brain* **139**:23–30. DOI: https://doi.org/10.1093/brain/awv326, PMID: 26614753

Jagust W. 2018. Imaging the evolution and pathophysiology of alzheimer disease. *Nature Reviews Neuroscience* **19**:687–700. DOI: https://doi.org/10.1038/s41583-018-0067-3, PMID: 30266970

Keller SS, Roberts N, Hopkins W. 2009. A comparative magnetic resonance imaging study of the anatomy, variability, and asymmetry of broca's area in the human and chimpanzee brain. *Journal of Neuroscience* **29**:14607–14616. DOI: https://doi.org/10.1523/JNEUROSCI.2892-09.2009, PMID: 19923293

Kennedy KM, Erickson KI, Rodrigue KM, Voss MW, Colcombe SJ, Kramer AF, Acker JD, Raz N. 2009. Age-related differences in regional brain volumes: A comparison of optimized voxel-based morphometry to manual volumetry. *Neurobiology of Aging* **30**:1657–1676. DOI: https://doi.org/10.1016/j.neurobiolaging.2007.12.020

Kong XZ, Mathias SR, Guadalupe T, Glahn DC, Franke B, Crivello F, Tzourio-Mazoyer N, Fisher SE, Thompson PM, Francks C, ENIGMA Laterality Working Group. 2018. Mapping cortical brain asymmetry in 17,141 healthy individuals worldwide via the ENIGMA consortium. *PNAS* **115**:E5154–E5163. DOI: https://doi.org/10.1073/pnas.1718418115, PMID: 29764998

Kong X-Z, Postema MC, Guadalupe T, Kovel C, Boedhoe PSW, Hoogman M, Mathias SR, Rooij D, Schijven D, Glahn DC, Medland SE, Jahanshad N, Thomopoulos SI, Turner JA, Buitelaar J, Erp TGM, Franke B, Fisher SE, Heuvel OA, Schmaal L, et al. 2020. Mapping brain asymmetry in health and disease through the ENIGMA consortium. *Human Brain Mapping* **8**:25033. DOI: https://doi.org/10.1002/hbm.25033

Kurth F, Gaser C, Luders E. 2015. A 12-step user guide for analyzing voxel-wise gray matter asymmetries in statistical parametric mapping (SPM). *Nature Protocols* **10**:293–304. DOI: https://doi.org/10.1038/nprot.2015.014

La Joie R, Perrotin A, Barré L, Hommet C, Mézenge F, Ibazizene M, Camus V, Abbas A, Landeau B, Guilloteau D, de La Sayette V, Eustache F, Desgranges B, Chételat G. 2012. Region-specific hierarchy between atrophy, hypometabolism, and β-amyloid (Aβ) load in Alzheimer's disease dementia. *Journal of Neuroscience* **32**:16265–16273. DOI: https://doi.org/10.1523/JNEUROSCI.2170-12.2012, PMID: 23152610

Langergraber KE, Prüfer K, Rowney C, Boesch C, Crockford C, Fawcett K, Inoue E, Inoue-Muruyama M, Mitani JC, Muller MN, Robbins MM, Schubert G, Stoinski TS, Viola B, Watts D, Wittig RM, Wrangham RW, Zuberbühler K, Pääbo S, Vigilant L. 2012. Generation times in wild chimpanzees and gorillas suggest earlier divergence times in great ape and human evolution. *PNAS* **109**:15716–15721. DOI: https://doi.org/10.1073/pnas.1211740109, PMID: 22891323

Li X, Crow TJ, Hopkins WD, Gong Q, Roberts N. 2018. Human torque is not present in chimpanzee brain. *NeuroImage* **165**:285–293. DOI: https://doi.org/10.1016/j.neuroimage.2017.10.017

Lladó A, Tort-Merino A, Sánchez-Valle R, Falgàs N, Balasa M, Bosch B, Castellví M, Olives J, Antonell A, Hornberger M. 2018. The hippocampal longitudinal axis-relevance for underlying tau and TDP-43 pathology. *Neurobiology of Aging* **70**:1–9. DOI: https://doi.org/10.1016/j.neurobiolaging.2018.05.035, PMID: 29935415

Lyn H, Pierre P, Bennett AJ, Fears S, Woods R, Hopkins WD. 2011. Planum temporale grey matter asymmetries in chimpanzees (Pan Troglodytes), vervet (Chlorocebus aethiops Sabaeus), rhesus (Macaca mulatta) and bonnet (Macaca radiata) monkeys. *Neuropsychologia* **49**:2004–2012. DOI: https://doi.org/10.1016/j.neuropsychologia.2011.03.030, PMID: 21447349

Mai JK, Majtanik M, Paxinos G. 2015. *Atlas of the Human Brain*. Elsevier.

Manjón JV, Coupé P, Martí-Bonmatí L, Collins DL, Robles M. 2010. Adaptive non-local means denoising of MR images with spatially varying noise levels. *Journal of Magnetic Resonance Imaging* **31**:192–203. DOI: https://doi.org/10.1002/jmri.22003, PMID: 20027588

Marie D, Roth M, Lacoste R, Nazarian B, Bertello A, Anton JL, Hopkins WD, Margiotoudi K, Love SA, Meguerditchian A. 2018. Left brain asymmetry of the planum temporale in a nonhominid primate: redefining the origin of brain specialization for language. *Cerebral Cortex* **28**:1808–1815. DOI: https://doi.org/10.1093/cercor/bhx096, PMID: 28431000

Mazziotta J, Toga A, Evans A, Fox P, Lancaster J, Zilles K, Woods R, Paus T, Simpson G, Pike B, Holmes C, Collins L, Thompson P, MacDonald D, Iacoboni M, Schormann T, Amunts K, Palomero-Gallagher N, Geyer S, Parsons L, et al. 2001. A probabilistic atlas and reference system for the human brain: international consortium for brain mapping (ICBM). *Philosophical Transactions of the Royal Society of London. Series B: Biological Sciences* **356**:1293–1322. DOI: https://doi.org/10.1098/rstb.2001.0915

Minkova L, Habich A, Peter J, Kaller CP, Eickhoff SB, Klöppel S. 2017. Gray matter asymmetries in aging and neurodegeneration: a review and meta-analysis. *Human Brain Mapping* **38**:5890–5904. DOI: https://doi.org/10.1002/hbm.23772, PMID: 28856766

Plessen KJ, Hugdahl K, Bansal R, Hao X, Peterson BS. 2014. Sex, age, and cognitive correlates of asymmetries in thickness of the cortical mantle across the life span. *Journal of Neuroscience* **34**:6294–6302. DOI: https://doi.org/10.1523/JNEUROSCI.3692-13.2014, PMID: 24790200

Rajapakse JC, Giedd JN, Rapoport JL. 1997. Statistical approach to segmentation of single-channel cerebral MR images. *IEEE Transactions on Medical Imaging* **16**:176–186. DOI: https://doi.org/10.1109/42.563663, PMID: 9101327

Rilling JK, Insel TR. 1999. The primate neocortex in comparative perspective using magnetic resonance imaging. *Journal of Human Evolution* **37**:191–223. DOI: https://doi.org/10.1006/jhev.1999.0313

Robson SL, Wood B. 2008. Hominin life history: reconstruction and evolution. *Journal of Anatomy* **212**:394–425. DOI: https://doi.org/10.1111/j.1469-7580.2008.00867.x

Rorden C, Brett M. 2000. Stereotaxic display of brain lesions. *Behavioural Neurology* **12**:191–200. DOI: https://doi.org/10.1155/2000/421719, PMID: 11568431

Savage-Rumbaugh ES. 1986. *Ape Language: From Conditioned Response to Symbol*. Oxford University Press.

Savage-Rumbaugh ES, Lewin R. 1994. *Kanzi: The Ape at the Brink of the Human Mind*. Wiley.

Schenker NM, Hopkins WD, Spocter MA, Garrison AR, Stimpson CD, Erwin JM, Hof PR, Sherwood CC. 2010. Broca's area homologue in chimpanzees (Pan troglodytes): probabilistic mapping, asymmetry, and comparison to humans. *Cerebral Cortex* **20**:730–742. DOI: https://doi.org/10.1093/cercor/bhp138, PMID: 19620620

Shamy JL, Habeck C, Hof PR, Amaral DG, Fong SG, Buonocore MH, Stern Y, Barnes CA, Rapp PR. 2011. Volumetric correlates of spatiotemporal working and recognition memory impairment in aged rhesus monkeys. *Cerebral Cortex* **21**:1559–1573. DOI: https://doi.org/10.1093/cercor/bhq210, PMID: 21127015

Sherwood CC, Broadfield DC, Holloway RL, Gannon PJ, Hof PR. 2003. Variability of broca's area homologue in African great apes: Implications for language evolution. *Anat Rec - Part a Discov Mol Cell Evol Biol* **271**:276–285. DOI: https://doi.org/10.1002/ar.a.10046

Sherwood CC, Gordon AD, Allen JS, Phillips KA, Erwin JM, Hof PR, Hopkins WD. 2011. Aging of the cerebral cortex differs between humans and chimpanzees. *PNAS* **108**:13029–13034. DOI: https://doi.org/10.1073/pnas.1016709108, PMID: 21788499

Shumaker RW, Walkup KR, Beck BB. 2011. *Animal Tool Behavior: The Use and Manufacture of Tools by Animals*. Johns Hopkins University Press.

Smith SM, Nichols TE. 2009. Threshold-free cluster enhancement: addressing problems of smoothing, threshold dependence and localisation in cluster inference. *NeuroImage* **44**:83–98. DOI: https://doi.org/10.1016/j.neuroimage.2008.03.061, PMID: 18501637

Spocter MA, Hopkins WD, Garrison AR, Bauernfeind AL, Stimpson CD, Hof PR, Sherwood CC. 2010. Wernicke's area homologue in chimpanzees (*Pan troglodytes*) and its relation to the appearance of modern human language . *Proceedings of the Royal Society B: Biological Sciences* **277**:2165–2174. DOI: https://doi.org/10.1098/rspb.2010.0011

Takao H, Abe O, Yamasue H, Aoki S, Sasaki H, Kasai K, Yoshioka N, Ohtomo K. 2011. Gray and white matter asymmetries in healthy individuals aged 21-29 years: a voxel-based morphometry and diffusion tensor imaging study. *Human Brain Mapping* **32**:1762–1773. DOI: https://doi.org/10.1002/hbm.21145, PMID: 20886579

Toga AW, Thompson PM. 2003. Mapping brain asymmetry. *Nature Reviews Neuroscience* **4**:37–48. DOI: https://doi.org/10.1038/nrn1009, PMID: 12511860

Tohka J, Zijdenbos A, Evans A. 2004. Fast and robust parameter estimation for statistical partial volume models in brain MRI. *NeuroImage* **23**:84–97. DOI: https://doi.org/10.1016/j.neuroimage.2004.05.007, PMID: 15325355

Tomasello M, Call J. 1997. *Primate Cognition*. Oxford University Press.

Uylings HB, Jacobsen AM, Zilles K, Amunts K. 2006. Left-right asymmetry in volume and number of neurons in adult broca's area. *Cortex* **42**:652–658. DOI: https://doi.org/10.1016/S0010-9452(08)70401-5, PMID: 16881273

van den Heuvel OA, Boedhoe PSW, Bertolin S, Bruin WB, Francks C, Ivanov I, Jahanshad N, Kong XZ, Kwon JS, O'Neill J, Paus T, Patel Y, Piras F, Schmaal L, Soriano-Mas C, Spalletta G, van Wingen GA, Yun JY, Vriend C, Simpson HB, et al. 2020. An overview of the first 5 years of the ENIGMA obsessive–compulsive disorder working group: The power of worldwide collaboration. *Human Brain Mapping* **10**:24972. DOI: https://doi.org/10.1002/hbm.24972

Vickery S. 2020. JunaChimp. *Software Heritage*. swh:1:rev:411f0610269416d4ee04eaf9670a9dc84e829ea0. https://archive.softwareheritage.org/swh:1:rev:411f0610269416d4ee04eaf9670a9dc84e829ea0/

Waterson RH, Lander ES, Wilson RK, Chimpanzee Sequencing and Analysis Consortium. 2005. Initial sequence of the chimpanzee genome and comparison with the human genome. *Nature* **437**:69–87. DOI: https://doi.org/10.1038/nature04072, PMID: 16136131

Zilles K, Armstrong E, Moser KH, Schleicher A, Stephan H. 1989. Gyrification in the cerebral cortex of primates. *Brain, Behavior and Evolution* **34**:143–150. DOI: https://doi.org/10.1159/000116500, PMID: 2512000

Zilles K, Dabringhaus A, Geyer S, Amunts K, Qü M, Schleicher A, Gilissen E, Schlaug G, Steinmetz H. 1996. Structural asymmetries in the human forebrain and the forebrain of Non-human primates and rats. *Neuroscience & Biobehavioral Reviews* **20**p. :593–605. DOI: https://doi.org/10.1016/0149-7634(95)00072-0

3. Imaging evolution of the primate brain: the next frontier?, Patrick Friedrich, Stephanie J. Forkel, Céline Amiez, Joshua H. Balsters, Olivier Coulon, Lingzhong Fan, Alexandros Goulas, Fadila Hadj-Bouziane, Erin E. Hecht, Katja Heuer, Tianzi Jiang, Robert D. Latzman, Xiaojin Liu, Kep Kee Loh, Kaustubh R. Patil, Alizée Lopez-Persem, Emmanuel Procyk, Jerome Sallet, Roberto Toro, Sam Vickery, Susanne Weis, Charles R. E. Wilson, Ting Xu, Valerio Zerbi, Simon B. Eickoff, Daniel S. Margulies, Rogier B. Mars, Michel Thiebaut de Schotten, *NeuroImage*, Volume 228, 2021,117685

NeuroImage 228 (2021) 117685

Contents lists available at ScienceDirect

NeuroImage

journal homepage: www.elsevier.com/locate/neuroimage

Imaging evolution of the primate brain: the next frontier?

Patrick Friedrich[a,b,e,*], Stephanie J. Forkel[a,b,c], Céline Amiez[o], Joshua H. Balsters[i], Olivier Coulon[p,q], Lingzhong Fan[s,t], Alexandros Goulas[m], Fadila Hadj-Bouziane[v], Erin E. Hecht[n], Katja Heuer[w,x], Tianzi Jiang[s,t,u], Robert D. Latzman[j], Xiaojin Liu[d,e], Kep Kee Loh[p,q], Kaustubh R. Patil[d,e], Alizée Lopez-Persem[f,r], Emmanuel Procyk[o], Jerome Sallet[o,r], Roberto Toro[w,y], Sam Vickery[d,e], Susanne Weis[d,e], Charles R. E. Wilson[o], Ting Xu[k], Valerio Zerbi[l], Simon B. Eickoff[d,e,1], Daniel S. Margulies[a,z], Rogier B. Mars[g,h,1], Michel Thiebaut de Schotten[a,b,1,*]

[a] Brain Connectivity and Behaviour Laboratory, Sorbonne Universities, Paris, France
[b] Groupe d'Imagerie Neurofonctionnelle, Institut des Maladies Neurodégénératives-UMR 5293, CNRS, CEA, University of Bordeaux, Bordeaux, France
[c] Centre for Neuroimaging Sciences, Department of Neuroimaging, Institute of Psychiatry, Psychology and Neuroscience, King's College London, London, United Kingdom
[d] Institute of Systems Neuroscience, Medical Faculty, Heinrich-Heine University Düsseldorf, Germany
[e] Institute of Neuroscience and Medicine (Brain & Behaviour, INM-7), Research Center Jülich, Germany
[f] Frontlab, Institut du Cerveau et de la Moelle épinière (ICM), UPMC UMRS 1127, Inserm U 1127, CNRS UMR 7225, Paris, France
[g] Wellcome Centre for Integrative Neuroimaging, Centre for Functional MRI of the Brain (FMRIB), Nuffield Department of Clinical Neurosciences, John Radcliffe Hospital, University of Oxford, Oxford, United Kingdom
[h] Donders Institute for Brain, Cognition and Behaviour, Radboud University Nijmegen, Nijmegen, Netherlands
[i] Department of Psychology, Royal Holloway University of London, United Kingdom
[j] Department of Psychology, Georgia State University, Atlanta, United States
[k] Child Mind Institute, New York, United States
[l] Neural Control of Movement Lab, Department of Health Sciences and Technology, ETH Zurich, Zurich, Switzerland
[m] Institute of Computational Neuroscience, University Medical Center Hamburg-Eppendorf, Hamburg University, Hamburg, Germany
[n] Department of Human Evolutionary Biology, Harvard University, Cambridge, MA, United States
[o] Univ Lyon, Université Lyon 1, Inserm, Stem Cell and Brain Research Institute, U1208 Bron, France
[p] Institut de Neurosciences de la Timone, Aix Marseille Univ, CNRS, UMR 7289, Marseille, France
[q] Institute for Language, Communication, and the Brain, Aix-Marseille University, Marseille, France
[r] Wellcome Centre for Integrative Neuroimaging, Department of Experimental Psychology, University of Oxford, Oxford, United Kingdom
[s] Brainnetome Center and National Laboratory of Pattern Recognition, Institute of Automation, Chinese Academy of Sciences, Beijing 100190, China
[t] CAS Center for Excellence in Brain Science and Intelligence Technology, Institute of Automation, Chinese Academy of Sciences, Beijing 100190, China
[u] The Queensland Brain Institute, University of Queensland, Brisbane QLD 4072, Australia
[v] Lyon Neuroscience Research Center, ImpAct Team, INSERM U1028, CNRS UMR5292, Université Lyon 1, Bron, France
[w] Center for Research and Interdisciplinarity (CRI), Université de Paris, Inserm, Paris 75004, France
[x] Max Planck Institute for Human Cognitive and Brain Sciences, Leipzig, Germany
[y] Neuroscience department, Institut Pasteur, UMR 3571, CNRS, Université de Paris, Paris 75015, France
[z] Integrative Neuroscience and Cognition Center (UMR 8002), Centre National de la Recherche Scientifique (CNRS) and Université de Paris, 75006, Paris, France

ABSTRACT

Evolution, as we currently understand it, strikes a delicate balance between animals' ancestral history and adaptations to their current niche. Similarities between species are generally considered inherited from a common ancestor whereas observed differences are considered as more recent evolution. Hence comparing species can provide insights into the evolutionary history. Comparative neuroimaging has recently emerged as a novel subdiscipline, which uses magnetic resonance imaging (MRI) to identify similarities and differences in brain structure and function across species. Whereas invasive histological and molecular techniques are superior in spatial resolution, they are laborious, post-mortem, and oftentimes limited to specific species. Neuroimaging, by comparison, has the advantages of being applicable across species and allows for fast, whole-brain, repeatable, and multi-modal measurements of the structure and function in living brains and post-mortem tissue. In this review, we summarise the current state of the art in comparative anatomy and function of the brain and gather together the main scientific questions to be explored in the future of the fascinating new field of brain evolution derived from comparative neuroimaging.

* Corresponding authors: Brain Connectivity and Behaviour Laboratory, Sorbonne Universities, Paris, France.
E-mail addresses: patrick.friedrich@rub.de (P. Friedrich), michel.thiebaut@gmail.com (M. Thiebaut de Schotten).
[1] These authors Contributed equally to this paper.

https://doi.org/10.1016/j.neuroimage.2020.117685
Received 23 June 2020; Received in revised form 14 December 2020; Accepted 16 December 2020
Available online 5 January 2021

Introduction

Our brain is the fruit of billions of years of evolution. Evolution, as we currently understand it, strikes a delicate balance between animals' ancestral history and adaptations to their current niche. Within each generation, discreet changes can occur across phenotypes mostly through genetic recombination (Hirsch 1963). If disadvantageous, these changes are more likely eliminated by natural selection (i.e. survival and reproduction). Accordingly, it is generally assumed that similarities between species are inherited from a common ancestor whereas observed differences are more recent occurrences (Darwin 1859; Fig. 1a). Hence comparing species gives us insight into evolutionary history, and has been applied in multiple fields where precise quantitative measurements are easy to access in large numbers including, for example skeletal structure (e.g. Dutel et al., 2019, see also Fig. 1b) or genetics (e.g. Boffelli et al., 2003; Clifen et al., 2003, see also Fig. 1c)

Thus far, however, large numbers of observations and precise quantitative measurements are lacking for the brain across species due to its fragile, ephemeral and complex organisation. While we know a great deal about the evolution of species, the aforementioned difficulty to work with brain data has hampered progress in our understanding of the evolution of the brain. Better understanding evolution will allow for targeted studies with animal models matching the brain mechanisms in the human to its phylogenetic counterpart. Further, it may also help discover neuroprotective mechanisms allowing for resilience to disease in animals. Recent advancements in neuroimaging, with regard to both hardware and software as well as larger cohort datasets are now opening the door to embark on this new adventure of comparative brain evolution.

Brains differ in many respects across species (Haug, 1987; Stephan, 1975; Ariëns Kappers, 1909) and MRI can compare most of these levels digitally at moderate costs (Krubitzer and Kaas, 2005; Mars et al., 2018). With the advent of better hardware and higher-resolution magnetic resonance imaging sequences that allow researchers to characterise many different aspects of the same brain's structure and function, it has become feasible to compare different species using a non-invasive repeatable multimodal method of investigation (Thiebaut de Schotten, Croxson and Mars, 2019). Another striking advantage of using magnetic resonance imaging for comparative studies is its feasibility to study large cohorts longitudinally as there is no need to sacrifice animals. Thereby, brains can be manipulated, and the effects of aging, training or lesions can be compared not only within but also between species. Finally, the non-invasive nature of the methods facilitates functional studies that better elucidate brain-behaviour interactions. Amongst the most commonly used MRI sequences to probe the structure of the brain are T1-weighted and T2-weighted scans to visualise different brain tissues (i.e. separate grey matter and white matter). Diffusion-weighted imaging (DWI) can be used to estimate microstructural properties within the white matter (Zhang et al., 2012) and to visualise the trajectory of white matter pathways (Basser, Mattiello & Le Bihan, 1994). Other sequences have been tuned to assess myelination (Glasser and Van Essen, 2011; Prasloski et al., 2012; for review see Heath et al., 2018). Using *in-vivo* recordings, the function of the brain can be assessed by measuring task-related blood oxygen level changes (BOLD; Ogawa et al., 1990; Logothetis et al., 2001) or modelling brain functional dynamics at rest (Fox and Raichle, 2007; Biswal, 2012). Compared to histology, MRI data gives access to a significantly greater number of specimens as it does not require the death (i.e. natural or sacrifice) of animals and allows to acquire complementary information on the structure and function of the brain within the same sample and can even be extended to measures of plasticity mechanisms using longitudinal designs. MRI is conveniently digital and shareable amongst researchers for easier replication of findings. MRI can also be mathematically modified (e.g. log transformation, Donahue et al., 2016) and reanalysed to address novel questions in already collected data (Balezeau et al., 2020). Finally, while acquiring and using MRI data in primates come with challenges with regards to collecting and harmonising data across species (see Milham et al., 2020 for a detailed discussion), MRI allows for the methodologically most similar cross-species comparisons (Thiebaut de Schotten and Zilles, 2019).

In this review, we summarise the emerging field of MRI-based neuroimaging of the primate brain evolution as well as gather the main scientific questions to be explored in the future.

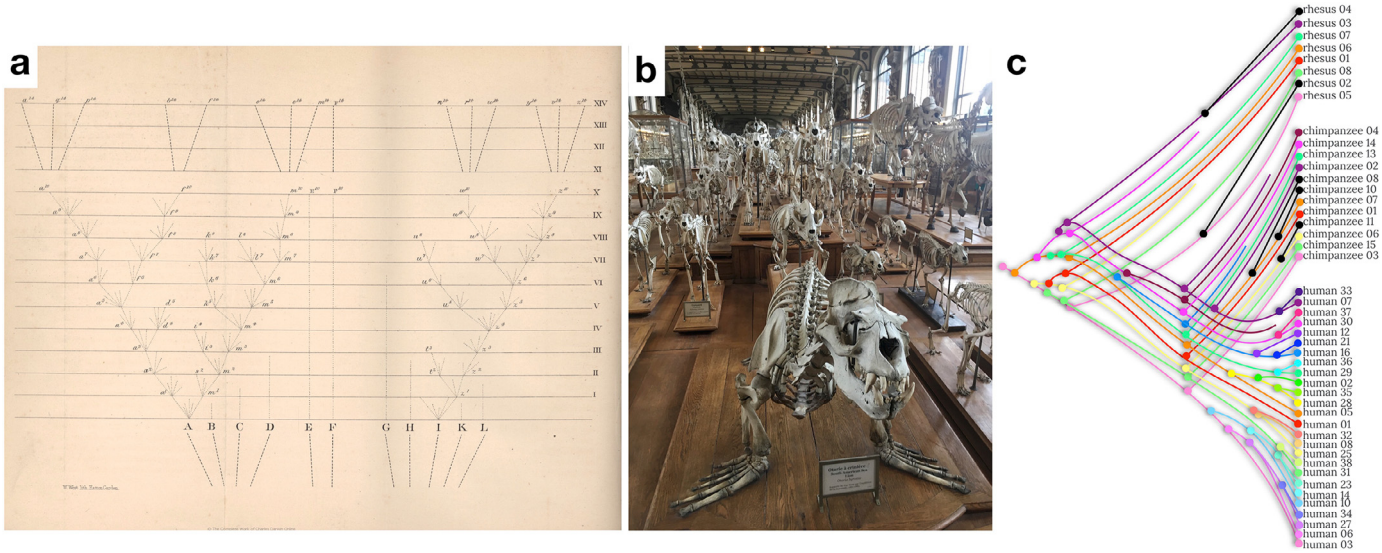

Fig. 1. Comparative anatomy as a glimpse at the evolution of species. a) First evolutionary tree (courtesy of © The Complete Work of Charles Darwin Online) as depicted in the 6th edition of the origin of species (Darwin 1859), b) Comparative anatomy of the skeletal structure whereby obvious similarities can be found between a sea lion and a cheetah, suggesting a close common ancestor (Rybczynski et al., 2009, picture taken at the Museum National D'Histoire Naturelle in Paris) c) Example of comparative genetics (limited to the Preferentially Expressed Antigen In Melanoma – PRAME – gene cluster) whereby the evolutionary tree combine within (i.e. interindividual variability in genetics) and between species (comparative genetics) differences (modified from Gibbs et al., 2007). Hue level differences have been coded so that it represents the level of difference with the original phylogenetic branch (in pink). New non-human variations have been coloured in black.

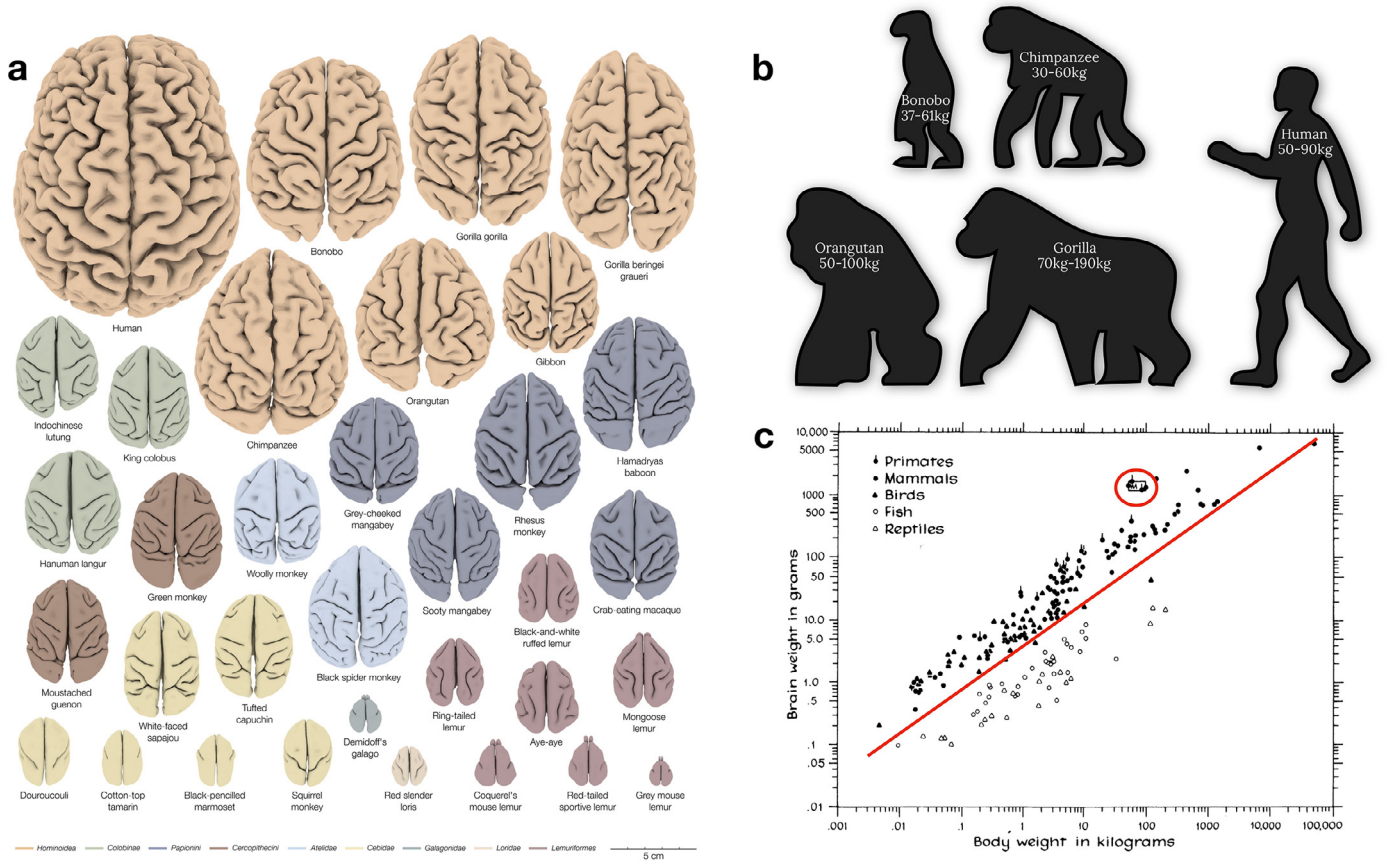

Fig. 2. Relative brain size cross-species comparison. a) 34 three-dimensional digital brain reconstructions from the brain catalogue (Heuer et al., 2019) b) Body size and weight comparison across apes c) Brain and body weight scatter plot comparison (Jerison 1975). Note that the red circle indicates human primates who deviate from the linear relationship existing between body and brain weight.

Brain structure

Brain size

The arguably most apparent and seemingly systematic change that occurred over primate brain evolution is the increase in total brain size relative to body size (Fig. 2). The effect of evolutionary expansion in relation to brain size is, however, not equally distributed across brain structures. This disproportional composition of the brain led to investigations of allometric rules of brain evolution. The size of one region can vary consistently with the size of another structure within the brain (Butler and Hodos, 2005). In this context, allometry refers to the study of the different pace of expansion of brain regions (Montgomery et al., 2016).

Allometric changes may provide a window for understanding the adaptations of specific neural systems in response to evolutionary pressure (Willemet, 2019; Finlay et al., 2001). In this regard, evolutionary psychology and neuroscience suggest that allometry arises from evolutionary developmental constraints, as a brain adjustment to optimise its functional organisation (Montgomery 2013; Willemet, 2015a, Montgomery et al., 2016). Along these lines, some authors have argued that similar patterns of allometric slopes across brain regions can be used to identify different grades of evolution. For instance, it has been argued that across different primate species, the prefrontal cortex shows allometric scaling with the visual cortex size. Importantly, this scaling factor is different in apes compared to monkeys (Passingham and Smaers, 2014). This finding suggests that the same developmental constraints happened across all primates, but that a major adaptive change separates monkeys from apes.

Due to the limited availability of tissue, comparative studies often rely on small samples and many studies still rely on antiquated datasets. These datasets often did not delineate different cortical territories with high accuracy, leading to fierce debates (e.g., Passingham and Smaers, 2014; Barton and Venditti, 2013). These limitations impede on our ability to assess within-species diversity accurately and might have biased our understanding of between-species differences. The ability of neuroimaging to acquire data from multiple individuals per species and imaging sequences might allow a more representative parcellation of the brain (Van Essen et al., 2011, 2016 Donahue et al., 2018). Such an approach will benefit allometric studies by providing better quantitative measurements and replicable findings as well as improve the granularity of investigations.

Gyrification

Typically, primates with smaller brains show a smoother, less convoluted brain surface than species with larger brains (see Fig. 2a; Hofmann, 2012; Heuer et al., 2019). The level of convolution of the cortex, also called gyrification index, is easily quantifiable with surface-derived MRI measurements. A convoluted cortex allows for more surface area to be packed into the limited volume within the skull (i.e. linear scaling between surface area and brain volume; Prothero and Sundsten, 1984) providing more space for grey matter cell bodies, white matter connections, and glial cells (Namba and Huttner 2017). The convolution of the cortex (i.e. gyrification) would occur because of an imbalance in the expansion of cortical (i.e. outer layer) and subcortical layers (i.e. inner layer) of the brain (Richman, 1975; adapted by Lui et al., 2011). Computational modelling of an imbalance between inner and outer layer growth success-

fully reproduced a folding pattern similar to the mammalian brain (i.e. buckling shell models, Toro and Burnod 2005; Toro 2012; Bayly et al., 2013; Tallinen et al., 2014, 2016; Foubet et al., 2019). Biologically, the cortico-subcortical imbalance would be due to the tangential migration (Lui et al., 2011; Reillo et al., 2011), and the radial intercalation of neurons during development (i.e. pushing of neighbouring neurons in the outer cortical plate aside, Striedter et al., 2015). With evolutionary expansion, a disproportional expression of these biological mechanisms could explain increased cortical folding (Mota and Herculano-Houzel 2015; Amiez et al., 2019). This latter hypothesis partially implies that the dynamic relationship between brain expansion and gyrification during early stages of brain development differ across species. However, investigating such relationships across the brain developmental stages is more likely achievable by means of comparative "longitudinal" imaging during brain development, which is typically be unthinkable with standard histological methods but is feasible with MRI (Rabiei et al., 2017). While models based on the ideas described above are successful in producing random folding patterns, they do not explain why folding patterns show similarities across the brains of the same or even different species (see Fig. 2a).

Hypothetically, similarities in folding patterns could be related to preferences for neurons to migrate in cortical areas (i.e. proliferation hotspots; Retzius, 1896; Kriegstein et al., 2006) and genetically coded. If this assumption is correct, combining genetic measurements with cortical folding patterns derived from neuroimaging in the future should offer some novel insights. Recent evidence already demonstrates a significant relationship between brain surface and genetics in humans in a collaborative cross-laboratory dataset of more than 50,000 participants (Grasby et al., 2020) as well as its distribution over the brain (Valk et al., 2020). Extending genetic brain imaging MRI to other primates will not only validate this work but also shed light on the main brain surface evolutionary mechanisms.

While the placement of proliferation hotspots may as well be determined genetically, other authors pointed out that the mechanical formation of folding leads to a complex stress influencing the stiffness of the cortex (e.g., Foubet et al., 2019). The resulting differences in stiffness might potentially influence the migration of neurons during brain development (Franze, 2013). Therefore, initial folding as proposed by the buckling shell models might be sufficient to create the intricate folding pattern as seen in mammalian cortices, which in turn, may lead to the observed pattern of regional cell composition and neural connections (Heuer and Toro, 2019). Reversely, another hypothesis suggests that the stereotypical pattern of folding would come from the tension applied by the axons on the cortex (i.e. axonal tension hypothesis; Van Essen, 1997). In this theory, tangential forces that are created by the tension along obliquely oriented axonal trajectories induce folds at specific locations. As genetic molecular gradients drive axonal migration during brain development (Krubitzer, 2007; Renier et al., 2017), the future combination of cortical folding estimate, white matter diffusion imaging tractography and genetic measurements across species may reveal a tripartite relationship between these factors.

Sulcal anatomy

A prominent anatomical feature on the primate brain is the presence of folds, or sulci (Fig. 2a). Even though folding patterns may appear to vary greatly, even between individuals of the same species, sulcal organisation is not at all random, and adheres strongly to a topographical organisation (Petrides, 2012). Anatomically, sulci often constitute borders between cytoarchitectonic areas (White et al., 1997). For instance, across human (Penfield and Boldrey, 1937) and non-human mammal brains (Ferrier, 1873), the central sulcus serves as the border between the motor cortex and the somatosensory cortex. Functionwise, a growing body of work has demonstrated precise relationships between an individual's local sulcal morphology and the location of functional areas including the sensorimotor cortex (e.g. Zlatkina et al., 2016; Germann et al., 2020), prefrontal cortex (e.g. Loh et al., 2020; Lopez-Persem et al., 2019; Amiez and Petrides, 2018), cingulate cortex (Amiez and Petrides, 2014) and the temporal cortex (Bodin et al., 2018). This robust correspondences with the anatomical-functional organisation of the brain allows for the sulcal organisation to guide our interpretation of neuroimaging data. Especially since brain sulci are still often used as critical anatomical landmarks for navigating the brain during human and non-human primate brain surgeries. Also, most surface-based registration methods use sulci either explicitly (Auzias et al., 2013) or implicitly via geometrical maps such as curvature that are indicators of folding (Robinson et al., 2014).

In the primate brain, some brain sulci are conserved across species. These typically include primary sulci such as the central sulcus, superior temporal sulcus, cingulate sulcus, and the calcarine sulcus. The relationship between these primary sulci and the location of anatomical/functional regions appear to be conserved across species. For instance, the somatotopic organisation along the dorsal-ventral extent of the central sulcus, as well as along the rostro-caudal extent of the cingulate sulcus appears to be highly conserved across the primate lineage (Procyk et al., 2016; Loh et al., 2018). This indicates that we can potentially anchor the brains of various primate species on the basis of homologous sulcal landmarks, to perform interspecies comparisons on brain structure. In Amiez et al., 2019, this principle has been implemented to reveal the evolutionary trajectories of the medial frontal cortex across macaques, baboons, chimpanzees, and humans (Fig. 3a, 3b). This work demonstrated that, unlike previously thought the paracingulate sulcus is not a human specific feature and could be observed in chimpanzees (Amiez et al., 2019; Fig. 3a). The lateralisation of these sulci, however, is only observed in humans, which suggests further hemispheric specialisation in humans since the last common ancestors to humans and great apes (Croxson et al., 2018). As shown in Fig. 3b, by aligning brains on the basis of common sulci landmarks, the evolutionary changes in the primate medial frontal cortex become apparent and quantifiable.

Inter-species sulcal-based brain alignment can be implemented and tested using model-driven cortical surface matching (Fig. 3c, 3d). For a given species, after building a model of relative positions, orientations, and alignment of sulci in a rectangular domain, any individual cortical surface can be registered to this rectangular model, which leads to an explicit matching of different cortical surfaces based on their sulci (Auzias et al., 2013). For two different species, two different rectangular models can be built, and inter-species sulcal correspondences can then be used to define a homology between the two models (Fig. 3c). This allows for a correspondence between inter-species cortical surfaces, which can be used to compare these species and warp information from one species to the other (Coulon et al., 2018; Fig. 3d).

A key challenge to this approach is the great inter-individual variability of sulci morphology. More work will be necessary to (1) characterise the morphological variability of the various sulci in the primate brain, (2) to determine the relationship between these variations and the localisation of anatomical and functional areas, and lastly, (3) to establish the sulcal homologies between the various species. Such work would only be achievable by means of comparative MRI and data sharing in order to gather enough data to model evolutionary trends (with a minimum of three species; e.g. Balezeau et al., 2020) and quantify variability appropriately (with a minimum of 10 sample per species; Croxson et al., 2018).

Brain connectivity

Brain areas interact in order to orchestrate cognition and behaviour. Short (local) and long (distant) connections link neighbouring and remote brain regions to facilitate these interactions. Importantly, exploring connections informs about the organisational principles of the information processing in the brain (Mars et al., 2018) and is one step closer to explaining the functioning of the brain (Takemura and Thiebaut de Schotten 2020). Therefore, studying the extent to which evolutionary

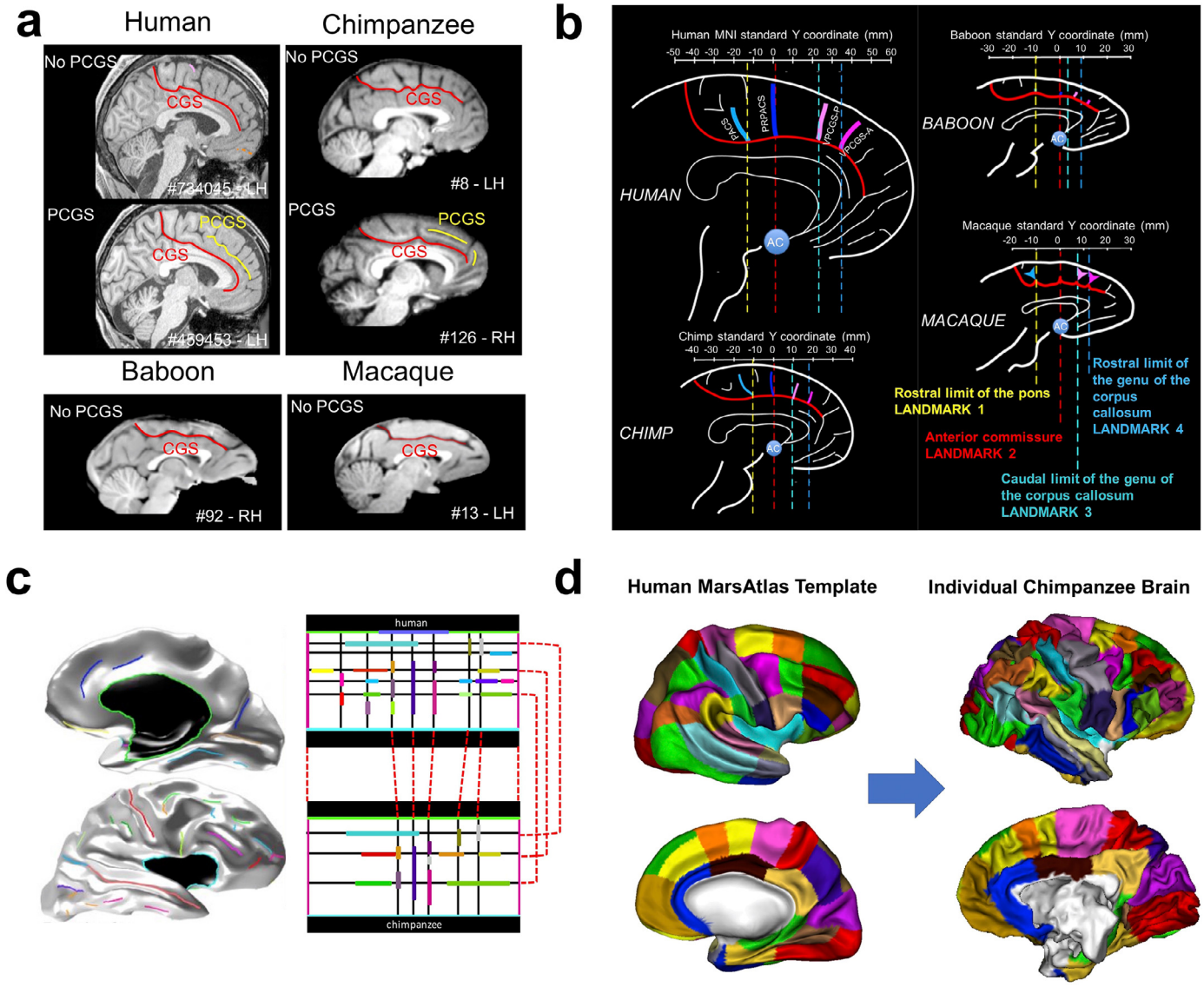

Fig. 3. Sulcal anatomy for inter-primate brain comparisons. a) Emergence of the para-cingulate sulcus (PCGS) the primate medial frontal cortex (Amiez et al., 2019: non-existing in baboons and macaques, but sometimes present for great apes and humans. b) Sulcal landmarks in the primate medial frontal cortex (Amiez et al., 2019). c) Projection of human brain sulci (left) onto a rectangular sulcal model (top right). Correspondences are defined between the human rectangular cortical sulci model and its chimpanzee equivalent (bottom right). d) Application of the model correspondences to map a human surface-based brain atlas onto an individual chimpanzee surface (Coulon et al., 2018).

changes in brain structure entail specific differences in brain connectivity is a current agenda in comparative neuroscience. Neuroimaging is ideal for this purpose, as there are many imaging techniques available to elucidate various aspects of connectivity. Hence, connectivity is one of the most developed areas of comparative neuroimaging (Goulas et al., 2014; Miranda-Dominguez et al., 2014; van den Heuvel et al. 2016).

Brain connectivity can be assessed either by reconstructing structural connections (i.e. tractography based on diffusion weighted imaging) or measuring the covariation of activity across brain regions (i.e. the synchronisation of activation derived from functional MRI).

Gross anatomy

Comparative neuroimaging has revealed gross connectivity differences between primate species (Ardesch et al., 2019; Balsters et al., 2020; Xia et al., 2019). For instance, the inferior fronto-occipital connections (Thiebaut de Schotten et al., 2012; Barrett et al., 2020) and the arcuate fasciculus (see Fig. 4a, Rilling, 2008; Thiebaut de Schotten et al., 2012; Eichert et al., 2018; Barrett et al., 2020; Balezeau et al., 2020) are more prominent in humans than in monkeys. The arcuate fasciculus has sparked interest, in particular, because of its fundamental role in human language processing (Barbeau et al., 2020; Balezeau et al., 2020). In addition, the parietal lobe has been linked to uniquely human functions and the underlying white matter has some prominent structures in humans but also some unique connections in monkeys (Catani et al., 2017). The functional interactions between the frontal and parietal lobes are also more prominent in humans than in macaques (see Fig. 4b, Patel et al., 2015; Mantini et al., 2013; Mars et al., 2011) and might reflect evolutionary trends within the attentional networks (Patel et al., 2015). However, structural connections and functional connectivity are usually examined separately. Comprehensive models of connectivity will require the combination of structural-functional methods to fully grasp the *modus operandi* of how evolutionary pressure and adaptation might have modified the wiring and the organisational principles of information processing in the brain.

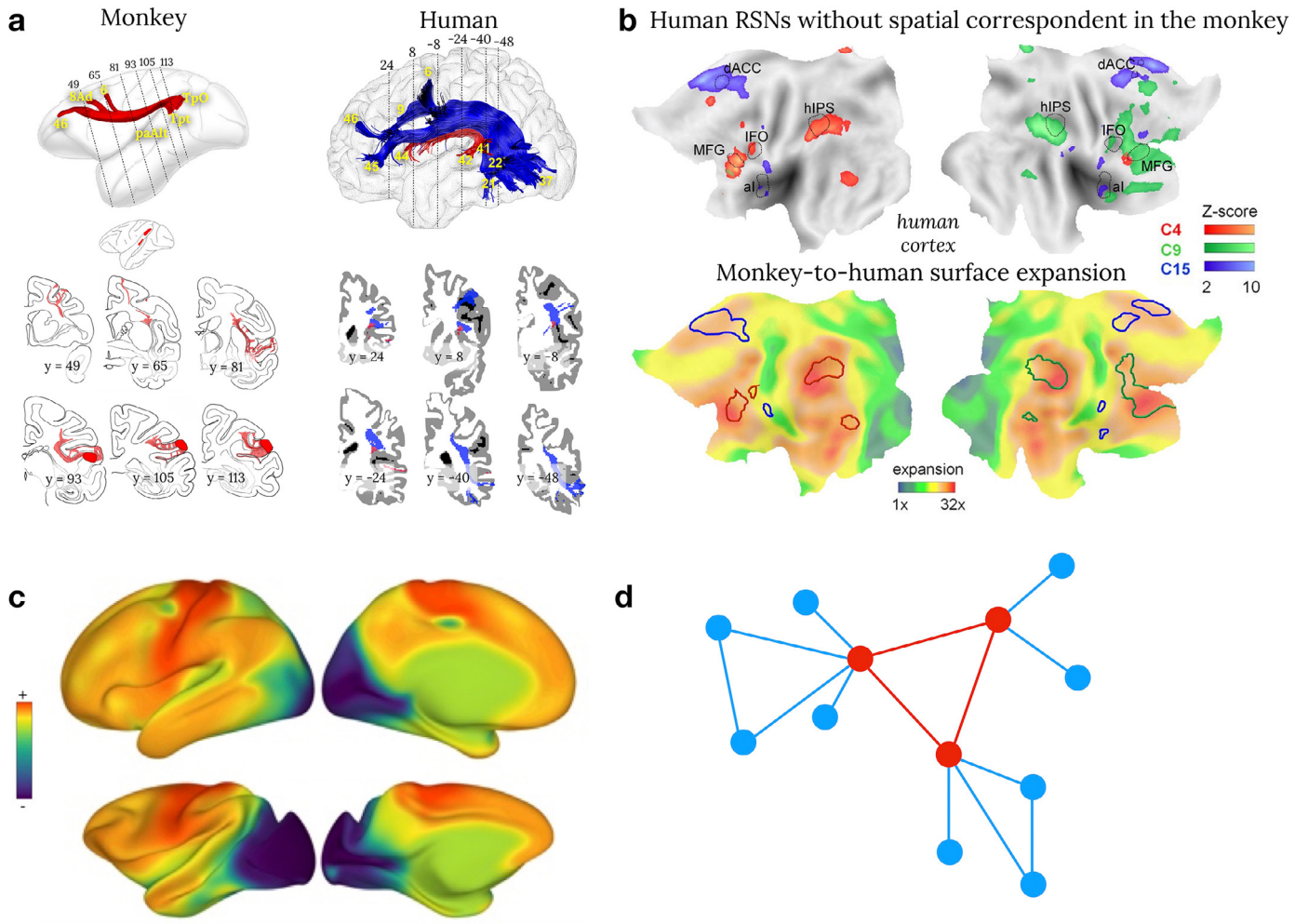

Fig. 4. Brain connectivity cross-species comparison. a) Comparison between post-mortem axonal tracing in monkeys (cases 7&9 modified from Schmahmann and Pandya, 2006) and human in vivo spherical deconvolution tractography. Common anatomical features between human and monkey are reconstructed in red whereas anatomical differences have been coloured in blue (Thiebaut de Schotten et al., 2012) b) Flat maps of the human resting state functional connectivity without correspondence with the monkey (upper row) and its correspondence to cortical expansion maps (Mantini et al., 2013) c) Preliminary comparison of the principal gradient in humans and macaques (see Brain integration section of this paper for a definition of brain gradients; Xu et al., 2019) d) The rich club organisation of the brain where regions in red are interconnected together and a hub for regions in blue (Bullmore and Sporns 2012).

Connectivity principles

Although species-specific features exist in connectivity, the tendency of two regions to be connected respects several organisational principles across (mammalian) species (Bullmore and Sporns, 2012; Ercsey-Ravasz et al., 2013, Horvat et al., 2016, Goulas et al., 2019, Vértes et al., 2012). In particular, two regions are more likely to display interconnections if they are adjacent to each other (Human: Betzel et al., 2016; Macaque: Kaiser and Hilgetag, 2006). They will also be more connected to each other if they share a similar microstructural composition (Pandya et al., 2015; Barbas, 2015) or connections with the same regions (Song et al., 2014). Recent efforts in human neuroimaging have revealed a seemingly overarching organisation principle (Huntenburg et al., 2018), providing a window of comparison into the features that underlie the spatial arrangement of cortical areas previously reported (Abbie 1940, 1942; Sanides 1962, 1970; Brockhaus 1940; Goulas et al., 2018). While classical studies have focused mainly on cross-species similarities in this overarching organisation scheme (Margulies et al., 2016; Goulas et al., 2019) preliminary evidence suggest these differences might be an evolutionary adaptation (Fig. 4c; Xu et al., 2019).

Since the neural system is costly in energy consumption, one core principle in the neural architecture has to be the minimisation of energy costs (Bullmore and Sporns, 2012). The brain wiring, therefore, can be expected to follow rules that minimise energy costs while maintaining a set of features that are indispensable for efficient brain functioning. The "rich-club organisation" (van den Heuvel and Sporns, 2011) represents a shared feature of brain architecture that fits this description (see Fig. 4d). Within the rich-club, few nodes act as hubs between otherwise segregated nodes and thus, facilitate efficient communication across the entire network (Sporns, 2013). Additionally, hubs tend to interconnect densely with each other. However, the unique properties of hubs come at a high price (van den Heuvel and Sporns, 2011). Cortical regions that represent hubs of the rich-club tend to show high metabolic demand and are vulnerable targets for pathogenic agents (Bullmore and Sporns, 2012; Griffa and Van den Heuvel, 2018). From an evolutionary perspective, the advantages of a rich-club organisation appear to outweigh its drawbacks. Rich-club topology is a common feature amongst various species, ranging from invertebrates to primates (van den Heuvel, Bullmore and Sporns, 2016; Rubinov et al., 2016). Another example includes the comparison of the macroscale organisation of human and macaque connectivity (Goulas et al., 2014; Miranda-Dominguez 2014). However, these promising analyses should be extended to other primates in order to establish their approximate phylogeny.

Brain function

Brain areas increase their activity when contributing to cognitive function, and this increase is detectable with task-related functional magnetic resonance imaging. The question about comparability between cognitive abilities is debated, for advanced functions such as communication (Mertz et al., 2019) or decision making (Tremblay et al., 2017; Fouragnan et al., 2019) as well as more primary functions such as episodic memory (Croxson et al., 2011; Pause et al., 2013) or even motor cognition (Borra and Luppino 2019). For instance, the superiority of chimpanzees over college students in a working memory task (Inoue and Matsuzawa 2007) is directly related to training (Cook and Wilson 2010) and indeed highlights the issue of comparability of functions across species. A recent alternative has been to compare functional activation related to the free viewing of video during fMRI measurements across primates (Mantini et al., 2012ab; Mantini et al., 2013; Russ and Leopold 2015; Sliwa and Freiwald 2017). However, species differences likely exist in the interpretation of the video limiting the interpretability of such interspecies differences. Therefore, more general features of brain function, such as brain lateralisation and brain integration measures, have been preferred in comparative neuroimaging paradigms.

Brain lateralisation

In order to conserve the speed of brain oscillations across species, a functional reorganisation might have occurred (Buzsaki, Logothetis & Singer, 2013) to compensate for interhemispheric delay related to brain size (Phillips et al., 2015). Accordingly, the inter-hemispheric independence theory suggests that during evolution, the increase in brain size led to increased functional lateralisation in order to avoid excessive conduction delays between the hemispheres (Ringo et al., 1994). Functional processing asymmetries have been derived from the neuroimaging-based study of the corpus callosum (Friedrich et al., 2017; Karolis et al., 2019; Horowitz et al., 2015) and hemispheric asymmetries (Hopkins 2015; Margiotoudi et al., 2019; Eichert et al., 2019; Marie, 2018; Thiebaut de Schotten, 2011; Amiez et al., 2019). Accordingly, an increase in functional lateralisation should be associated with a decrease of corpus callosum size or density as well as an increase in anatomical asymmetries. However, a comprehensive study of functional lateralisation across primate brains is still missing due to the scarcity of appropriate data. Lateralised patterns in tracing studies and cytoarchitectonic maps from macaques and marmosets, for instance, are rarely investigated for understandable ethical and financial reasons. As a consequence, both hemispheres are usually considered as equal limiting this line of research. An HCP-like multimodal neuroimaging approach would enable addressing brain lateralisations at the microarchitecture, connectomics, and functional levels as well as their interdependencies. For instance, in the orbitofrontal cortex, even when both hemispheres are similar at the cytoarchitectonic level (Mackey and Petrides, 2010), rs-fMRI analysis can reveal hemispheric differences in connectivity within the default-mode network (Lopez-Persem et al., 2020), in both humans and macaques. Studying the evolution of brain lateralisation in primate models would benefit from the reuse of MRI data progressively made available thanks to new open data initiatives (Milham et al., 2018, 2020). This will allow to compare larger numbers of species and to disentangle true species differences from individual noise.

Brain integration

The brain processes incoming sensory information (e.g. auditory and visual) along processing streams towards increasingly abstract and integrative, or *associative*, levels (Pandya and Yeterian 1990). Before comparative neuroimaging, post-mortem studies already suggested that cortical areas related to association processes are enlarged in humans compared to other primate species (Schoenemann, 2006; Van Essen and Dierker, 2007; Hrvoj-Mihic et al., 2013; Hofman, 2014). The prefrontal lobe has been specifically explored, comparatively, with regards to expansion (Sherwood et al., 2005; Semendeferi et al., 2002, 2001 Petrides et al., 2012; Hofman 2014), cytoarchitecture (Palomero-Gallagher et al., 2013; 2019) and relative scaling of white matter (Smaers et al., 2010; Barrett et al., 2020). Bryant et al. (2019) extended this work to the visual and auditory systems. They investigated the connections of the primary and secondary processing areas of the visual and auditory cortex. In humans, chimpanzees and macaques, the connectivity of the primary visual cortex showed a retinotopic organisation with its association area. However, the primary visual cortex had additional connections to the temporal pole only in humans and chimpanzees. Quite similarly, the primary auditory cortex showed a gradual increase of connection with temporal associative cortex in chimpanzee and humans, but not in the macaque. These results suggest that a gradual expansion of the associative cortex between the auditory and visual cortices must have occurred along the chimp-human phylogenetic lineage. In line with these gradual changes, the advent of advanced MRI analyses has enabled the comparison of a variety of other properties such as the “principal gradient” of connective properties (Margulies et al., 2016; Buckner and Margulies, 2019), which summarise a specific functional connectivity signature distributed across the human brain (Huntenburg et al., 2018).

While the idea of organising the brain in terms of gradients is relatively new in neuroimaging, the concept itself has been evinced across modalities and species for more than 100 years (Vogt and Vogt, 1919; Flechsig 1920; Hopf, 1954a,b, 1955, 1956, 1968a, 1969, 1970b). In a broad perspective, comparative neuroimaging could provide a systematic assessment of the structural variation between cortical areas in multiple species. This could test whether this organisational principle is the basis of functional specialisation and evolution of brain areas, as recently suggested in rodents (Fulcher et al., 2019; Lu et al., 2012) and humans (Waymel et al., 2020).

Overall, these results are encouraging in our endeavour to understand the differences in the structure of the brain and its functions across species. However, it is important to stress that the same network in different species can have different dynamic properties and potentially different functions (Mantini et al., 2013). Consequently, similarities in brain organisation across species should not be considered as entirely equivalent brain functions.

Perspectives & future directions

Imaging the primate evolutionary tree would be a new stepping-stone for neuroscience. Access to more data across species will allow us to model the brains of common ancestors by extrapolating from the wealth of information on commonalities and divergences between species, families, orders, and classes. Having access to all levels of primate entities will allow us to create reference spaces, which in turn may grant better methods for inter- and intra-species comparisons. Ultimately, these developments can help us to form a true ‘neuroecology’ of different brains (Mars and Bryant, in press). In other words, we would be able to understand how a given brain is adapted to fit its environmental niche within the constraints of its evolutionary history.

The resources and methodologies outlined above not only allow for further investigation of primate evolution but can be extended to address crucial questions about similarities and differences in other mammalian species, including humans. The mouse is currently the most commonly used mammalian model in scientific research (Dietrich et al., 2014), and the species for which the most detailed mapping of a wide range of cellular and anatomical brain properties has been obtained. Yet, there is still limited consensus on how primates and rodents differ in terms of their brain structure and connectivity. Employing the MRI-based methodologies outlined above, Balsters et al. (2020) showed an 69-80% overlap in cortico-striatal connectivity fingerprints for humans and macaques compared to a meagre 15% overlap between humans and mice and a 31% overlap between mice and macaques. Given the prevalence of animal models in biomedical research, it is of paramount impor-

tance that neuroecology understand the differences between primates, both human and nonhuman, and other species such as rodents.

Whilst primates share some cognitive abilities such as visual perception and motor functions, as well as many emotional processes, their underlying neurobiology may differ. These similarities in function are typically investigated with the assumption that shared traits between primates (i.e. homology) are inherited from a common ancestor—divergent evolution. Most comparative neuroimaging studies investigate closely related species and hence examine divergent evolution. In more distant species, however, another process may have led to the onset of a similar function— "convergent evolution". This so-called convergent evolution postulates that similar functions in distantly related species evolved independently from each other as a result of evolutionary pressure to adapt to similar environmental or ecological factors (i.e. homoplasy). As a consequence, both evolutionary principles, namely homology and homoplasy, can both lead to structural and/or functional similarities. Supporting evidence for homology and homoplasy is well documented in the field of genetics. For instance, many animal phyla share basic multifunctional regulatory genes such as Pax-6. This gene is involved in the development of light-sensitive cells and initiates eye formation in flies, but also frogs (Altmann et al., 1997; Halder et al., 1995). Despite the eyes of flies and frogs being homoplasies, the initiating gene is homologous. Hence, homology and homoplasy should be considered as complementary in our understanding of brain evolution and can be assessed using an extensive database of primate species only accessible through collaborative neuroimaging.

Another perspective would be to derive the brain of our phylogenetic ancestors (see Kaas, 2011; 2013 for discussion) by registering different species' brains into a common space Although this might sound implausible, recent preliminary evidence already indicates that it is feasible (Heuer et al., 2020; https://katjaq.github.io/brainscapes). Using this possibility across proximal and more distantly related primate species may offer new insights into brain anatomy across taxonomic families, classes, and orders. Ideally, such endeavours will require the integration of multiple modalities of magnetic resonance imaging with several specimens for each primate species.

Finally, although there is much effort to identify the neural basis of species-defining cognitive functions, less research is devoted to the evolutionary processes through which those functions and their underlying neural adaptations have arisen. Questions about the evolutionary processes imply that an event, such as a genetic mutation or external evolutionary pressure, is responsible for the occurrence of adaptations. In this regard, many species share a common environment and live through competitive or collaborative interactions or in a predator-prey relationship. Therefore, the imaging of the evolutionary tree is accompanied by the intriguing opportunity to investigate the co-evolution of brain structures across interacting species and thus, investigate brain evolution from a novel neuro-ecological perspective.

Acknowledgements

This work was inspired by the #CompMRI meeting in Dusseldorf, Germany (April 11–12 2019), which was supported by the Human Brain Project. The work of RBM is supported by the Biotechnology and Biological Sciences Research Council (BBSRC) UK [BB/N019814/1] and the Netherlands Organization for Scientific Research NWO [452-13-015]. J.S. was supported by a Sir Henry Dale Wellcome Trust Fellowship (105651/Z/14/Z) and IDEXLYON "IMPULSION 2020 grant (IDEX/IMP/2020/14). The Wellcome Centre for Integrative Neuroimaging is supported by core funding from the Wellcome Trust [203139/Z/16/Z]. MTS has received funding from the European Research Council (ERC) under the European Union's Horizon 2020 research and innovation programme (grant agreement No. 818521). EEH was supported by National Science Foundation awards IOS-1457291 and NCS-1631563.

Credit Author Statement

All the authors wrote and revised the manuscript.

Data and code availability

N/A

References

Abbie, A.A., 1940. The excitable cortex in Perameles, Sarcophilus, Dasyurus, Trichosurus and Wallabia (Macropus). J. Comp. Neurol. 72 (3), 469–487.
Abbie, A.A., 1942. Cortical lamination in a polyprotodont marsupial, Perameles nasuta. J. Comp. Neurol. 76 (3), 509–536.
Altmann, C.R., Chow, R.L., Lang, R.A., Hemmati-Brivanlou, A., 1997. Lens Induction by Pax-6 inXenopus laevis. Dev. Biol. 185 (1), 119–123.
Amiez, C., Petrides, M., 2014. Neuroimaging evidence of the anatomo-functional organization of the human cingulate motor areas. Cereb. Cortex 24 (3), 563–578. doi:10.1093/cercor/bhs329.
Amiez, C., Petrides, M, 2018. Functional rostro-caudal gradient in the human posterior lateral frontal cortex. Brain Structu. Funct. 223, 1487–1499.
Amiez, C., Sallet, J., Hopkins, W.D., Meguerditchian, A., Hadj-Bouziane, F., Hamed, S.B., Petrides, M., 2019. Sulcal organization in the medial frontal cortex provides insights into primate brain evolution. Nat. Commun. 10 (1), 1–14.
Ardesch, D.J., Scholtens, L.H., Li, L., Preuss, T.M., Rilling, J.K., van den Heuvel, M.P., 2019. Evolutionary expansion of connectivity between multimodal association areas in the human brain compared with chimpanzees. Proc. Natl. Acad. Sci. 116 (14), 7101–7106.
Ariëns Kappers, C.U., 1909. The phylogenesis of the paleocortex and archicortex compared with the evolution of the visual neocortex. Arch. Neurol. Psychiatry 4, 161–173.
Auzias, G., Lefevre, J., Le Troter, A., Fischer, C., Perrot, M., Regis, J., Coulon, O., 2013. Model-driven harmonic parameterization of the cortical surface: HIP-HOP. IEEE Trans. Med. Imaging 32 (5), 873–887. doi:10.1109/TMI.2013.2241651.
Balezeau, F., Wilson, B., Gallardo, G., Dick, F., Hopkins, W., Anwander, A., Petkov, C.I., 2020. Primate auditory prototype in the evolution of the arcuate fasciculus. Nat. Neurosci. 23 (5), 611–614.
Balsters, J.H., Zerbi, V., Sallet, J., Wenderoth, N., Mars, R.B., 2020. Primate homologs of mouse cortico-striatal circuits. Elife 9, e53680.
Barbas, H., 2015. General cortical and special prefrontal connections: principles from structure to function. Ann. Rev. Neurosci. 38, 269–289.
Barbeau, E.B., Descoteaux, M., Petrides, M., 2020. Dissociating the white matter tracts connecting the temporo-parietal cortical region with frontal cortex using diffusion tractography. Sci. Rep. 10, 8186.
Barrett, R.L., Dawson, M., Dyrby, T.B., Krug, K., Ptito, M., D'Arceuil, H., Dell'Acqua, F., 2020. Differences in frontal network anatomy across primate species. J. Neurosci. 40 (10), 2094–2107.
Basser, P.J., Mattiello, J., Le Bihan, D., 1994. MR diffusion tensor spectroscopy and imaging. Biophys. J. 66, 259–267.
Barton, R.A., Venditti, C., 2013. Reply to Smaers: Getting human frontal lobes in proportion. Proc. Natl. Acad. Sci. USA 110 (22), E3683–3684.
Bayly, P.V., Okamoto, R.J., Xu, G., Shi, Y., Taber, L.A., 2013. A cortical folding model incorporating stress-dependent growth explains gyral wavelengths and stress patterns in the developing brain. Phys. Biol. 10 (1), 016005.
Betzel, R.F., Avena-Koenigsberger, A., Goñi, J., He, Y., De Reus, M.A., Griffa, A., Van Den Heuvel, M., 2016. Generative models of the human connectome. Neuroimage 124, 1054–1064.
Biswal, B.B., 2012. Resting state fMRI: a personal history. Neuroimage 62 (2), 938–944.
Bodin, C., Takerkart, S., Belin, P., Coulon, O., 2018. Anatomo-functional correspondence in the superior temporal sulcus. Brain Struct. Funct. 223 (1), 221–232.
Boffelli, D., McAuliffe, J., Ovcharenko, D., Lewis, K.D., Ovcharenko, I., Pachter, L., Rubin, E.M., 2003. Phylogenetic shadowing of primate sequences to find functional regions of the human genome. Science 299 (5611), 1391–1394.
Borra, E., Luppino, G., 2019. Large-scale temporo–parieto–frontal networks for motor and cognitive motor functions in the primate brain. Cortex 118, 19–37.
Brockhaus, H., 1940. Cyto-and myelo-architectonics of the cortex claustralis and the claustrum in humans. Journal fur Psychologie und Neurologie 49, 249–348.
Bryant, K.L., Glasser, M.F., Li, L., Bae, J.J.C., Jacquez, N.J., Alarcón, L., Preuss, T.M, 2019. Organization of extrastriate and temporal cortex in chimpanzees compared to humans and macaques. Cortex 118, 223–243.
Buckner, R.L., Margulies, D.S., 2019. Macroscale cortical organization and a default-like apex transmodal network in the marmoset monkey. Nat. Commun. 10 (1), 1–12.
Bullmore, E., Sporns, O., 2012. The economy of brain network organization. Nat. Rev. Neurosci. 13 (5), 336–349.
Butler, A.B., Hodos, W., 2005. Comparative Vertebrate Neuroanatomy: Evolution and Adaptation. John Wiley & Sons, Inc, Hoboken, NJ, USA.
Buzsáki, G., Logothetis, N., Singer, W., 2013. Scaling brain size, keeping timing: evolutionary preservation of brain rhythms. Neuron 80 (3), 751–764.
Catani, M., Robertsson, N., Beyh, A., Huynh, V., de Santiago Requejo, F., Howells, H., Krug, K., 2017. Short parietal lobe connections of the human and monkey brain. Cortex 97, 339–357.
Cliften, P., Sudarsanam, P., Desikan, A., Fulton, L., Fulton, B., Majors, J., Johnston, M., 2003. Finding functional features in Saccharomyces genomes by phylogenetic footprinting. Science 301 (5629), 71–76.

Cook, P., Wilson, M., 2010. Do young chimpanzees have extraordinary working memory. Psychon. Bull. Rev. 17 (4), 599–600.
Coulon, O., Auzias, G., Lemercier, P., Hopkins, W., 2018. Nested cortical organization models for human and non-human primate inter-species comparisons. In: Proceedings of the 24th Annual Meeting of the Organization for Human Brain Mapping, Singapore.
Croxson, P.L., Forkel, S.J., Cerliani, L., Thiebaut de Schotten, M., 2018. Structural variability across the primate brain: a cross-species comparison. Cereb. Cortex 28 (11), 3829–3841.
Darwin, C., 1859. On the Origin of Species London. John Murray, UK, p. 62.
Dietrich, M.R., Ankeny, R.A., Chen, P.M., 2014. Publication trends in model organism research. Genetics 198 (3), 787–794.
Donahue, C.J., Glasser, M.F., Preuss, T.M., Rilling, J.K., Van Essen, D.C., 2018. Quantitative assessment of prefrontal cortex in humans relative to nonhuman primates. Proc. Natl. Acad. Sci. 115 (22), E5183–E5192.
Donahue, C.J., Sotiropoulos, S.N., Jbabdi, S., Hernandez-Fernandez, M., Behrens, T.E., Dyrby, T.B., Glasser, M.F., 2016. Using diffusion tractography to predict cortical connection strength and distance: a quantitative comparison with tracers in the monkey. J. Neurosci. 36 (25), 6758–6770.
Dutel, H., Galland, M., Tafforeau, P., Long, J.A., Fagan, M.J., Janvier, P., Herbin, M., 2019. Neurocranial development of the coelacanth and the evolution of the sarcopterygian head. Nature 569 (7757), 556–559.
Eichert, N., Verhagen, L., Folloni, D., Jbabdi, S., Khrapitchev, A.A., Sibson, N.R., Mantini, D., Sallet, J., Mars, R.B., 2018. What is special about the human arcuate fasciculus? Lateralization, projections, and expansion. Cortex.
Eichert, N., Verhagen, L., Folloni, D., Jbabdi, S., Khrapitchev, A.A., Sibson, N.R., Mars, R.B., 2019. What is special about the human arcuate fasciculus? Lateralization, projections, and expansion. Cortex 118, 107–115.
Ercsey-Ravasz, M., Markov, N.T., Lamy, C., Van Essen, D.C., Knoblauch, K., Toroczkai, Z., Kennedy, H., 2013. A predictive network model of cerebral cortical connectivity based on a distance rule. Neuron 80 (1), 184–197.
Ferrier, D., 1873. Experimental researches in cerebral physiology and pathology. West Rid Lunatic Asylum Med. Rep. 3, 30–96.
Finlay, B.L., Darlington, R.B., Nicastro, N., 2001. Author's Response: developmental structure in brain evolution. Behav. Brain Sci. 24 (2), 298–304.
Flechsig, P., 1920. Anatomie Des Menschlichen Gehirns und Ruckenmarks auf Myelogenetischer Grundlage. Thieme, Leipzig.
Fulcher, B.D., Murray, J.D., Zerbi, V., Wang, X.J., 2019. Multimodal gradients across mouse cortex. Proc. Natl. Acad. Sci. 116 (10), 4689–4695.
Foubet, O., Trejo, M., Toro, R., 2019. Mechanical morphogenesis and the development of neocortical organisation. Cortex 118, 315–326.
Fouragnan, E.F., Chau, B.K., Folloni, D., Kolling, N., Verhagen, L., Klein-Flügge, M., Rushworth, M.F., 2019. The macaque anterior cingulate cortex translates counterfactual choice value into actual behavioral change. Nat. Neurosci. 22 (5), 797–808.
Fox, M.D., Raichle, M.E., 2007. Spontaneous fluctuations in brain activity observed with functional magnetic resonance imaging. Nat. Rev. Neurosci. 8 (9), 700–711.
Franze, K., 2013. The mechanical control of nervous system development. Development 140 (15), 3069–3077.
Friedrich, P., Ocklenburg, S., Heins, N., Schlüter, C., Fraenz, C., Beste, C., Genç, E., 2017. Callosal microstructure affects the timing of electrophysiological left-right differences. Neuroimage 163, 310–318.
Goulas, A., Bastiani, M., Bezgin, G., Uylings, H.B., Roebroeck, A., Stiers, P., 2014. Comparative analysis of the macroscale structural connectivity in the macaque and human brain. PLoS Comput. Biol. 10 (3), e1003529.
Goulas, A., Betzel, R.F., Hilgetag, C.C., 2019. Spatiotemporal ontogeny of brain wiring. Sci. Adv. 5 (6), eaav9694.
Goulas, A., Zilles, K., Hilgetag, C.C., 2018. Cortical gradients and laminar projections in mammals. Trends Neurosci. 41 (11), 775–788.
Germann, J., Chakravarty, M.M., Collins, D.L., Petrides, M., 2020. Tight coupling between morphological features of the central sulcus and somatomotor body representations: a combined anatomical and functional MRI study. Cereb. Cortex 30 (3), 1843–1854 Mar 14.
Gibbs, R.A., Rogers, J., Katze, M.G., Bumgarner, R., Weinstock, G.M., Mardis, E.R., Batzer, M.A., 2007. Evolutionary and biomedical insights from the rhesus macaque genome. Science 316 (5822), 222–234.
Glasser, M.F., Van Essen, D.C., 2011. Mapping human cortical areas in vivo based on myelin content as revealed by T1-and T2-weighted MRI. J. Neurosci. 31 (32), 11597–11616.
Grasby, K.L., Jahanshad, N., Painter, J.N., Colodro-Conde, L., Bralten, J., Hibar, D.P., Shatokhina, N., 2020. The genetic architecture of the human cerebral cortex. Science 367 (6484).
Griffa, A., Van den Heuvel, M.P., 2018. Rich-club neurocircuitry: function, evolution, and vulnerability. Dialogues Clin. Neurosci. 20 (2), 121.
Halder, G., Callaerts, P., Gehring, W.J., 1995. Induction of ectopic eyes by targeted expression of the eyeless gene in Drosophila. Science 267 (5205), 1788–1792.
Haug, H., 1987. Brain sizes, surfaces, and neuronal sizes of the cortex cerebri: a stereological investigation of man and his variability and a comparison with some mammals (primates, whales, marsupials, insectivores, and one elephant). Am. J. Anat. 180 (2), 126–142.
Heath, F., Hurley, S.A., Johansen-Berg, H., Sampaio-Baptista, C., 2018. Advances in noninvasive myelin imaging. Dev. Neurobiol. 78 (2), 136–151.
Heuer, K., Gulban, O.F., Bazin, P.L., Osoianu, A., Valabregue, R., Santin, M., Toro, R., 2019. Evolution of neocortical folding: a phylogenetic comparative analysis of MRI from 34 primate species. Cortex 118, 275–291.
Heuer, K., Kleineberg, M., Dinnage, R., Sherwood, C., Schwartz, E., Langs, G., Valabregue, R., Santin, M., Herbin, M., & Toro, R. (2020). A Generative Model For Primate Brain Shapes. 10.5281/ZENODO.4291032.
Heuer, K., Toro, R., 2019. Role of mechanical morphogenesis in the development and evolution of the neocortex. Phys. Life Rev. 31, 233–239.
Hrvoj-Mihic, B., Bienvenu, T., Stefanacci, L., Muotri, A.R., Semendeferi, K., 2013. Evolution, development, and plasticity of the human brain: from molecules to bones. Front. Hum. Neurosci. 7, 707.
Huntenburg, J.M., Bazin, P.L., Margulies, D.S., 2018. Large-scale gradients in human cortical organization. Trends Cogn. Sci. (Regul. Ed.) 22 (1), 21–31.
Hirsch, J., 1963. Behavior genetics and individuality understood. Science 142 (3598), 1436–1442.
Hofman, M.A., 2012. Design principles of the human brain: an evolutionary perspective. In: Progress in Brain Research, 195. Elsevier, pp. 373–390.
Hofman, M.A., 2014. Evolution of the human brain: when bigger is better. Front. Neuroanat. 8, 15.
Hopf, A., 1954a. Die Myeloarchitektonik des Isocortex temporalis beim Menschen. J. Hirnforsch. 1, 208–279.
Hopf, A., 1954b. Die Myeloarchitektonik des Isocortex temporalis beim Menschen. J. Hirnforsch. 1, 443–496.
Hopf, A., 1955. Über die Verteilung myeloarchitektonischer Merkmale in der isokortikalen Schla¨fenlappenrinde beim Menschen. J. Hirnforsch. 2, 36–54.
Hopf, A., 1956. Über die Verteilung myeloarchitektonischer Merkmale in der Stirnhirnrinde beim Menschen. J. Hirnforsch. 2 (4), 311–333.
Hopf, A., 1968a. Photometric studies on the myeloarchitecture of the human temporal lobe. J. Hirnforsch. 10 (4), 285–297.
Hopf, A., 1969. Photometric studies on the myeloarchitecture of the human parietal lobe. I. Parietal region. J. Hirnforsch. 11 (4), 253–265.
Hopf, A., 1970b. Photometric studies on the myeloarchitecture of the human parietal lobe. II. Postcentral region. J. Hirnforsch. 12 (1), 135–141.
Hopkins, W.D., Misiura, M., Pope, S.M., Latash, E.M., 2015. Behavioral and brain asymmetries in primates: a preliminary evaluation of two evolutionary hypotheses. Ann. N. Y. Acad. Sci. 1359 (1), 65–83. doi:10.1111/nyas.12936.
Horvát, S., Gămănuț, R., Ercsey-Ravasz, M., Magrou, L., Gămănuț, B., Van Essen, D.C., Kennedy, H., 2016. Spatial embedding and wiring cost constrain the functional layout of the cortical network of rodents and primates. PLoS Biol. 14 (7), e1002512.
Inoue, S., Matsuzawa, T., 2007. Working memory of numerals in chimpanzees. Curr. Biol. 17 (23), R1004–R1005.
Jerison, H.J., 1975. Evolution of the brain and intelligence. Curr. Anthropol. 16 (3), 403–426.
Kaas, J.H., 2011. Neocortex in early mammals and its subsequent variations. Ann N Y Acad Sci. 2011.
Kaas, J.H., 2013. The Evolution of Brains from Early Mammals to Humans. Wiley Interdiscip Rev Cogn Sci 4 (1), 33–45.
Kaiser, M., Hilgetag, C.C., 2006. Nonoptimal component placement, but short processing paths, due to long-distance projections in neural systems. PLoS Comput. Biol. 2 (7), e95.
Kriegstein, A., Noctor, S., Martínez-Cerdeño, V., 2006. Patterns of neural stem and progenitor cell division may underlie evolutionary cortical expansion. Nat. Rev. Neurosci. 7 (11), 883–890.
Krubitzer, L., 2007. The magnificent compromise: cortical field evolution in mammals. Neuron 56 (2), 201–208.
Krubitzer, L., Kaas, J., 2005. The evolution of the neocortex in mammals: how is phenotypic diversity generated? Curr. Opin. Neurobiol. 15 (4), 444–453.
Logothetis, N.K., Pauls, J., Augath, M., Trinath, T., Oeltermann, A., 2001. Neurophysiological investigation of the basis of the fMRI signal. Nature 412 (6843), 150–157.
Loh, K.K., Procyk, E., Neveu, R., Lamberton, F., Hopkins, W.D., Petrides, M., Amiez, C., 2020. Cognitive control of orofacial motor and vocal responses in the ventrolateral and dorsomedial human frontal cortex. Proc. Natl. Acad. Sci. 117 (9), 4994–5005.
Loh, K.K., Hadj-Bouziane, F., Petrides, M., Procyk, E., Amiez, C., 2018. Rostro-caudal organization of connectivity between cingulate motor areas and lateral frontal regions. Front Neurosci 11, 753.
Lopez-Persem, A., Verhagen, L., Amiez, C., Petrides, M., Sallet, J., 2019. The human ventromedial prefrontal cortex: sulcal morphology and its influence on functional organization. J. Neurosci. 39 (19), 3627–3639.
Lopez-Persem, A., Roumazeilles, L., Folloni, D., Marche, K., Fouragnan, E.F., Khalighinejad, N., Rushworth, M.F.S., Sallet, J., 2020. Differential functional connectivity underlying asymmetric reward-related activity in human and nonhuman primates. Proc. Natl. Acad. Sci. 117 (45), 2845262.
Lu, H., Zou, Q., Gu, H., Raichle, M.E., Stein, E.A., Yang, Y., 2012. Rat brains also have a default mode network. Proc. Natl. Acad. Sci. 109 (10), 3979–3984.
Lui, J.H., Hansen, D.V., Kriegstein, A.R., 2011. Development and evolution of the human neocortex. Cell 146 (1), 18–36.
Mackey, S., Petrides, M., 2010. Quantitative demonstration of comparable architectonic areas within the ventromedial and lateral orbital frontal cortex in the human and the macaque monkey brains. Eur. J. Neurosci. 32, 1940–1950.
Mantini, D., Corbetta, M., Romani, G.L., Orban, G.A., Vanduffel, W., 2013. Evolutionarily novel functional networks in the human brain? J. Neurosci. 33 (8), 3259–3275.
Mantini, D., Hasson, U., Betti, V., Perrucci, M.G., Romani, G.L., Corbetta, M., Vanduffel, W., 2012. Interspecies activity correlations reveal functional correspondence between monkey and human brain areas. Nat. Methods 9 (3), 277–282.
Margiotoudi, K., Marie, D., Claidière, N., Coulon, O., Roth, M., Nazarian, B., Anton, J.L., 2019. Handedness in monkeys reflects hemispheric specialization within the central sulcus. An in vivo MRI study in right-and left-handed olive baboons. Cortex 118, 203–211.
Margulies, D.S., Ghosh, S.S., Goulas, A., Falkiewicz, M., Huntenburg, J.M., Langs, G., Jefferies, E., 2016. Situating the default-mode network along a principal gradient of macroscale cortical organization. Proc. Natl. Acad. Sci. 113 (44), 12574–12579.

Marie, D., Roth, M., Lacoste, R., Nazarian, B., Bertello, A., Anton, J.L., Meguerditchian, A., 2018. Left Brain Asymmetry of the Planum Temporale in a Nonhominid Primate: redefining the Origin of Brain Specialization for Language. Cereb. Cortex 28 (5), 1808–1815. doi:10.1093/cercor/bhx096.

Mars, R.B., Eichert, N., Jbabdi, S., Verhagen, L., Rushworth, M.F., 2018a. Connectivity and the search for specializations in the language-capable brain. Curr. Opin. Behav. Sci. 21, 19–26.

Mars, R.B., Jbabdi, S., Sallet, J., O'Reilly, J.X., Croxson, P.L., Olivier, E., Behrens, T.E., 2011. Diffusion-weighted imaging tractography-based parcellation of the human parietal cortex and comparison with human and macaque resting-state functional connectivity. J. Neurosci. 31 (11), 4087–4100.

Mertz, J., Surreault, A., van de Waal, E., Botting, J., 2019. Primates are living links to our past: the contribution of comparative studies with wild vervet monkeys to the field of social cognition. Cortex 118, 65–81.

Milham, M.P., Ai, L., Koo, B., Xu, T., Amiez, C., Balezeau, F., Croxson, P.L., 2018. An open resource for non-human primate imaging. Neuron 100 (1), 61–74.

Milham, M., Petkov, C.I., Margulies, D.S., Schroeder, C.E., Basso, M.A., Belin, P., Messinger, A., 2020. Accelerating the evolution of nonhuman primate neuroimaging. Neuron 105 (4), 600–603.

Miranda-Dominguez, O., Mills, B.D., Grayson, D., Woodall, A., Grant, K.A., Kroenke, C.D., Fair, D.A., 2014. Bridging the gap between the human and macaque connectome: a quantitative comparison of global interspecies structure-function relationships and network topology. J. Neurosci. 34 (16), 5552–5563.

Mota, B., Herculano-Houzel, S., 2015. Cortical folding scales universally with surface area and thickness, not number of neurons. Science 349 (6243), 74–77.

Montgomery, S.H., 2013. The human frontal lobes: not relatively large but still disproportionately important? A commentary on Barton and Venditti. Brain Behav. Evol. 82 (3), 147–149.

Montgomery, S.H., Mundy, N.I., Barton, R.A., 2016. Brain evolution and development: adaptation, allometry and constraint. Proc. Royal Soc. B: Biol. Sci. 283 (1838), 20160433.

Namba, T., Huttner, W.B., 2017. Neural progenitor cells and their role in the development and evolutionary expansion of the neocortex. Wiley Interdiscip. Rev.: Dev. Biol. 6 (1), e256.

Ogawa, S., Lee, T.M., Kay, A.R., Tank, D.W., 1990. Brain magnetic resonance imaging with contrast dependent on blood oxygenation. Proc. Natl. Acad. Sci. 87 (24), 9868–9872.

Palomero-Gallagher, N., Zilles, K., Schleicher, A., Vogt, B.A., 2013. Cyto-and receptor architecture of area 32 in human and macaque brains. J. Comp. Neurol. 521 (14), 3272–3286.

Pandya, D., Petrides, M., Cipolloni, P.B., 2015. Cerebral cortex: architecture, connections, and the Dual Origin Concept. Oxford University Press.

Pandya, D.N., Yeterian, E.H., 1990. Architecture and connections of cerebral cortex: implications for brain evolution and function. Neurobiology of Higher Cognitive Function. The Guiford Press, New York, NY.

Passingham, R.E., Smaers, J.B., 2014. Is the prefrontal cortex especially enlarged in the human brain? Allometric relations and remapping factors. Brain Behav. Evol. 84 (2), 156–166.

Pause, B.M., Zlomuzica, A., Kinugawa, K., Mariani, J., Pietrowsky, R., Dere, E., 2013. Perspectives on episodic-like and episodic memory. Front. Behav. Neurosci. 7, 33.

Patel, G.H., Yang, D., Jamerson, E.C., Snyder, L.H., Corbetta, M., Ferrera, V.P., 2015. Functional evolution of new and expanded attention networks in humans. Proc. Natl. Acad. Sci. 112 (30), 9454–9459.

Penfield, W., Boldrey, E., 1937. Somatic motor and sensory representation in the cerebral cortex of man as studied by electrical stimulation. Brain 60, 389–440.

Petrides, M., 2012. The Human Cerebral cortex: An MRI Atlas of the Sulci and Gyri in MNI Stereotaxic Space. Academic Press.

Petrides, M., Tomaiuolo, F., Yeterian, E.H., Pandya, D.N., 2012. The prefrontal cortex: comparative architectonic organization in the human and the macaque monkey brains. Cortex 48 (1), 46–57.

Phillips, K.A., Stimpson, C.D., Smaers, J.B., Raghanti, M.A., Jacobs, B., Popratiloff, A., Hof, P.R., Sherwood, C.C., 2015. The corpus callosum in primates: processing speed of axons and the evolution of hemispheric asymmetry. Proc. Biol. Sci. 282, 20151535.

Prasloski, T., Rauscher, A., MacKay, A.L., Hodgson, M., Vavasour, I.M., Laule, C., Mädler, B., 2012. Rapid whole cerebrum myelin water imaging using a 3D GRASE sequence. Neuroimage 63 (1), 533–539.

Procyk, E., Wilson, C.R., Stoll, F.M., Faraut, M.C., Petrides, M., Amiez, C., 2016. Midcingulate motor map and feedback detection: converging data from humans and monkeys. Cereb. Cortex 26 (2), 467–476.

Prothero, J.W., Sundsten, J.W., 1984. Folding of the cerebral cortex in mammals. Brain Behav. Evol. 24 (2–3), 152–167.

Rabiei, H., Richard, F., Coulon, O., Lefevre, J., 2016. Local spectral analysis of the cerebral cortex: new gyrification indices. IEEE Trans. Med. Imaging 36 (3), 838–848.

Reillo, I., de Juan Romero, C., García-Cabezas, M.Á., Borrell, V., 2011. A role for intermediate radial glia in the tangential expansion of the mammalian cerebral cortex. Cereb. Cortex 21 (7), 1674–1694.

Renier, N., Dominici, C., Erzurumlu, R.S., Kratochwil, C.F., Rijli, F.M., Gaspar, P., Chédotal, A., 2017. A mutant with bilateral whisker to barrel inputs unveils somatosensory mapping rules in the cerebral cortex. Elife 6, e23494.

Retzius, G., 1896. Das Menschenhirn. K. Buchdruckerei, Stockholm.

Richman, D.P., Stewart, R.M., Hutchinson, J.W., Caviness, V.S., 1975. Mechanical model of brain convolutional development. Science 189 (4196), 18–21.

Rilling, J.K., Glasser, M.F., Preuss, T.M., Ma, X., Zhao, T., Hu, X., Behrens, T.E., 2008. The evolution of the arcuate fasciculus revealed with comparative DTI. Nat. Neurosci. 11 (4), 426–428.

Ringo, J.L., Doty, R.W., Demeter, S., Simard, P.Y., 1994. Time is of the essence: a conjecture that hemispheric specialization arises from interhemispheric conduction delay. Cereb. Cortex 4 (4), 331–343.

Robinson, E.C., Jbabdi, S., Glasser, M.F., Andersson, J., Burgess, G.C., Harms, M.P., Jenkinson, M., 2014. MSM: a new flexible framework for Multimodal Surface Matching. Neuroimage 100, 414–426.

Rubinov, M., 2016. Constraints and spandrels of interareal connectomes. Nat Commun 7 (1), 1–11.

Russ, B.E., Leopold, D.A., 2015. Functional MRI mapping of dynamic visual features during natural viewing in the macaque. Neuroimage 109, 84–94.

Rybczynski, N., Dawson, M.R., Tedford, R.H., 2009. A semi-aquatic Arctic mammalian carnivore from the Miocene epoch and origin of Pinnipedia. Nature 458 (7241), 1021–1024.

Sanides, F., 1962. Architectonics of the human frontal lobe of the brain. With a demonstration of the principles of its formation as a reflection of phylogenetic differentiation of the cerebral cortex. Monographien aus dem Gesamtgebiete der Neurologie und Psychiatrie 98, 1.

Sanides, F., 1970. Evolutionary aspect of the primate neocortex. Proc. 3rd Int. Congr. Primat., Zürich 1, 92–98.

Schmahmann, J.D., Pandya, D.N., 2006. Fiber Pathways of the Brain. Oxford University Press, New York.

Schoenemann, P.T., 2006. Evolution of the size and functional areas of the human brain. Annu. Rev. Anthropol. 35, 379–406.

Semendeferi, K., Armstrong, E., Schleicher, A., Zilles, K., Van Hoesen, G.W., 2001. Prefrontal cortex in humans and apes: a comparative study of area 10. Am. J. Physical Anthropol.: Offic. Publ. Am. Assoc. Phys. Anthropol. 114 (3), 224–241.

Semendeferi, K., Lu, A., Schenker, N., Damásio, H., 2002. Humans and great apes share a large frontal cortex. Nat. Neurosci. 5 (3), 272–276.

Sherwood, C.C., Holloway, R.L., Semendeferi, K., Hof, P.R., 2005. Is prefrontal white matter enlargement a human evolutionary specialization? Nat. Neurosci. 8 (5), 537.

Sliwa, J., Freiwald, W.A., 2017. A dedicated network for social interaction processing in the primate brain. Science 356 (6339), 745–749.

Smaers, J.B., Schleicher, A., Zilles, K., Vinicius, L., 2010. Frontal white matter volume is associated with brain enlargement and higher structural connectivity in anthropoid primates. PLoS One 5 (2), e9123.

Song, H.F., Kennedy, H., Wang, X.J., 2014. Spatial embedding of structural similarity in the cerebral cortex. Proc. Natl. Acad. Sci. 111 (46), 16580–16585.

Sporns, O., 2013. Network attributes for segregation and integration in the human brain. Curr. Opin. Neurobiol. 23 (2), 162–171.

Stephan, H., 1975. Allocortex. Springer, Berlin.

Striedter, G.F., Srinivasan, S., Monuki, E.S., 2015. Cortical folding: when, where, how, and why? Ann. Rev. Neurosci. 38, 291–307.

Takemura, H., Thiebaut de Schotten, M., 2020. Perspectives given by structural connectivity bridge the gap between structure and function. Brain Struct. Funct. 225 (4), 1189–1192.

Tallinen, T., Chung, J.Y., Biggins, J.S., Mahadevan, L., 2014. Gyrification from constrained cortical expansion. Proc. Natl. Acad. Sci. 111 (35), 12667–12672.

Tallinen, T., Chung, J.Y., Rousseau, F., Girard, N., Lefèvre, J., Mahadevan, L., 2016. On the growth and form of cortical convolutions. Nat. Phys. 12 (6), 588–593.

Thiebaut de Schotten, M., Croxson, P.L., Mars, R.B., 2019. Large-scale comparative neuroimaging: where are we and what do we need? Cortex 118, 188–202.

Thiebaut de Schotten, M., Dell'Acqua, F., Valabregue, R., Catani, M., 2012. Monkey to human comparative anatomy of the frontal lobe association tracts. Cortex 48 (1), 82–96.

Thiebaut De Schotten, M., Dell'Acqua, F., Forkel, S., Simmons, A., Vergani, F., Murphy, D.G., Catani, M., 2011. A lateralized brain network for visuo-spatial attention. Nat. Proc. 14, 1245–1246.

Thiebaut de Schotten, M., Zilles, K., 2019. Evolution of the mind and the brain. Cortex 118, 1.

Toro, R., 2012. On the possible shapes of the brain. Evol. Biol. 39 (4), 600–612.

Toro, R., Burnod, Y., 2005. A morphogenetic model for the development of cortical convolutions. Cereb. Cortex 15 (12), 1900–1913.

Tremblay, S., Sharika, K.M., Platt, M.L., 2017. Social decision-making and the brain: a comparative perspective. Trends Cogn. Sci. (Regul. Ed.) 21 (4), 265–276.

Valk, S.L., Xu, T., Margulies, D.S., Masouleh, S.K., Paquola, C., Goulas, A., Eickhoff, S.B., 2020. Shaping Brain structure: Genetic and Phylogenetic Axes of Macro Scale Organization of Cortical Thickness. BioRxiv.

Van den Heuvel, M.P., Bullmore, E.T., Sporns, O., 2016. Comparative connectomics. Trends Cogn. Sci. 20 (5), 345–361.

Van Den Heuvel, M.P., Sporns, O, 2011. Rich-club organization of the human connectome. J. Neurosci. 31 (44), 15775–15786.

Van Essen, D.C., 1997. A tension-based theory of morphogenesis and compact wiring in the central nervous system. Nature 385 (6614), 313–318.

Van Essen, D.C., Dierker, D.L., 2007. Surface-based and probabilistic atlases of primate cerebral cortex. Neuron 56 (2), 209–225.

Van Essen, D.C., Donahue, C., Dierker, D.L., Glasser, M.F., 2016. Parcellations and connectivity patterns in human and macaque cerebral cortex. In: Kennedy, H., Van Essen, D.C., Christen, Y. (Eds.), Micro-, Meso- and Macro-Connectomics of the Brain. Cham (CH), pp. 89–106.

Van Essen, D.C., Glasser, M.F., Dierker, D.L., Harwell, J., Coalson, T., 2012. Parcellations and hemispheric asymmetries of human cerebral cortex analyzed on surface-based atlases. Cereb. Cortex 22, 2241–2262.

Vértes, P.E., Alexander-Bloch, A.F., Gogtay, N., Giedd, J.N., Rapoport, J.L., Bullmore, E.T., 2012. Simple models of human brain functional networks. Proc. Natl. Acad. Sci. U.S.A. 109 (15), 5868–5873.

Vogt, C., Vogt, O., 1919. Allgemeine Ergebnisse unserer Hirnforschung. J. Psychol. Neurol. 25, 279–468.

Waymel, A., Friedrich, P., Bastian, P.A., Forkel, S.J., De Schotten, M.T., 2020. Anchoring the human olfactory system to a functional gradient. Neuroimage 216, 116863.

White, L.E., Andrews, T.J., Hulette, C., Richards, A., Groelle, M., Paydarfar, J., Purves, D., 1997. Structure of the human sensorimotor system. I: morphology and cytoarchitecture of the central sulcus. Cereb. Cortex 7 (1), 18–30.
Willemet, R., 2019. Allometry unleashed: an adaptationist approach of brain scaling in mammalian evolution. PeerJ Preprints 7, e27872v1.
Willemet, R., 2015. Commentary: greater addition of neurons to the olfactory bulb than to the cerebral cortex of eulipotyphlans but not rodents, afrotherians or primates. Front. Neuroanat. 9, 84.
Xia, X., Fan, L., Cheng, C., Yao, R., Deng, H., Zhao, D., Jiang, T., 2019. Interspecies differences in the connectivity of ventral striatal components between humans and macaques. Front. Neurosci. 13, 623.
Xu, T., Nenning, K.H., Schwartz, E., Hong, S.J., Vogelstein, J.T., Fair, D.A., Langs, G., 2019. Cross-species functional alignment reveals evolutionary hierarchy within the connectome. Neuroimage 223, 117346.
Zhang, H., Schneider, T., Wheeler-Kingshott, C.A., Alexander, D.C., 2012. NODDI: practical in vivo neurite orientation dispersion and density imaging of the human brain. Neuroimage 61 (4), 1000–1016.
Zlatkina, V., Amiez, C., Petrides, M., 2016. The postcentral sulcal complex and the transverse postcentral sulcus and their relation to sensorimotor functional organization. Eur. J. Neurosci. 43 (10), 1268–1283.

4. Hemispheric Specialization of the Primate Inferior Parietal Lobule, Sam Vickery, Simon B. Eickhoff, Patrick Friedrich, *Neuroscience Bulletin.* 38, 334–336 (2022).

Neurosci. Bull. March, 2022, 38(3):334–336
https://doi.org/10.1007/s12264-021-00807-4

www.neurosci.cn
www.springer.com/12264

RESEARCH HIGHLIGHT

Hemispheric Specialization of the Primate Inferior Parietal Lobule

Sam Vickery[1,2] · Simon B Eickhoff[1,2] · Patrick Friedrich[1]

Received: 17 September 2021 / Accepted: 8 October 2021 / Published online: 29 December 2021

Hemispheric asymmetries can be seen as one of the evolutionary adaptations that allowed the human brain to muster more complex cognitive processes than other primates. In this vein, the study published by Cheng *et al.* [1] presents a pivotal investigation of both the regional and connectional asymmetries within the inferior parietal lobule (IPL) in human, chimpanzee, and macaque. By investigating 4 sub-divisions of the IPL across the three species, Cheng and colleagues showed that the macroanatomical and connectional architecture of the IPL became more asymmetric throughout the primate lineage. While macaques show little to no structural asymmetries, chimpanzees display a more asymmetric architecture but with both leftward and rightward asymmetries in various connections. In contrast, the human IPL displayed the highest number of asymmetries among the three species with a clear tendency towards more lateralization. This evolutionary trend towards a more lateralized organization of the IPL may have accompanied an improved command of tool-use, stronger forelimb asymmetries, and the increasing complexity of communicative behavior.

The IPL is a part of the primate association cortex that plays an important role in language and tool-use along with a multitude of different functions [2]. Given its functional diversity and heterogeneity, a comprehensive analysis of the IPL's macroanatomy and connectivity requires investigation on a sub-division level. However, translating a set of sub-regions from one species to another poses a central challenge for comparative research. There are various strategies to solve the issue of inter-species comparison, such as establishing a common feature space between species based on structure and/or functional measures [3], or one can investigate homologous regions and/or features in each species. To accomplish this task, Cheng et al. implemented the latter by using a connectivity-based parcellation approach, which creates sub-divisions based on diffusion-weighted probabilistic tractography. This approach can give several solutions that vary in the number of sub-divisions. The authors choose a 4-cluster solution with divisions that follow a rostral-to-caudal (anterior-posterior) organization in macaques, chimpanzees, and humans. This solution maximizes the similarity across species and is consistent with previously reported anatomical and cytoarchitecture parcellations.

Utilizing the IPL subdivisions derived by connectivity-based parcellation, Cheng *et al.* conducted a thorough exploration of the structural asymmetries within the IPL across the three species. The investigation was centered around the gray matter (GM) volume, probabilistic white matter (WM) connections, and the cortical surface vertices of the WM connections. Regarding the different structural measures, the old-world monkeys (macaques) did not present any asymmetries while the great apes (chimpanzees and humans) showed similar and divergent asymmetrical organization. In great apes, rostral subdivisions were leftward asymmetric and caudal subdivisions were rightward asymmetric. This indicates a switch from a symmetrical to an asymmetrical organization in the IPL in a common ancestor of the great apes and old-world monkeys. Asymmetric WM connection from the IPL sub-divisions

✉ Sam Vickery
s.vickery@fz-juelich.de

[1] Institute of Neuroscience and Medicine, Brain & Behaviour (INM-7), Research Centre Jülich, 52428 Jülich, Germany

[2] Institute of Systems Neuroscience, Medical Faculty, Heinrich-Heine University Düsseldorf, 40225 Düsseldorf, Germany

and the resulting cortical surface regions of said connections is where Cheng and colleagues found divergences from chimpanzees to humans. Humans presented more plentiful lateralized IPL connections, in particular those towards the left hemisphere, as well as to unique cortical areas such as the ventral frontal cortex, motor cortex, and the lateral temporal cortex as compared to chimpanzees (Fig. 1). Cheng and colleagues propose that this increase in organizational asymmetries may have contributed to the evolution of language, tool-use, and handedness in the primate lineage.

The leftward asymmetry of connectivity between the IPL and primary motor cortex (M1) appears particularly interesting, given its potential implications for manual skills as outlined by the authors. Human handedness is an unprecedented example of behavioral laterality, as it is strongly skewed towards a population-wide and task-invariant preference of the right hand, which is unparalleled in other vertebrates [5]. Comparisons of primate handedness indicate a potential evolutionary continuum of manual dexterity, given that evidence points towards a population-level handedness in chimpanzees, which is however less robustly expressed than human handedness [6]. The leftward asymmetric IPL–M1 connectivity might represent an important evolutionary adaptation that contributed to the increased left-hemispheric dominance in motor functions from chimpanzee to human. As such, this finding aligns with the idea that the sensory-motor system may have evolved to form the foundation of increased manual skills [7], including tool-use.

While this work makes an important contribution to our understanding of the potential role of connectional brain asymmetries in primate brain evolution, it also gives some important leads for future studies. For instance, one topic concerns the relationship between structure and function. It is known that brain regions can be functionally connected and thus take part in the same functional network, albeit in the absence of direct structural connections [8]. Structure and function are especially decoupled in association cortices compared to primary sensory and motor cortices [9]. Therefore, the effect of IPL connections and their asymmetry on functional networks and behavior need further investigation.

In a similar vein, Cheng and colleagues show group-level differences in IPL asymmetries between the three species. The variability and individual differences of these IPL asymmetries within a species grant another perspective that may help to unravel their functional relevance. A study by Croxson and colleagues [10] indicates that WM is more variable than GM in humans and macaque monkeys. However, the human brain is generally more variable than the macaque monkey's brain, implying a higher degree of individual differences in the human brain's architecture. Although the main findings of Cheng *et al*. did not address individual differences, such difference in IPL asymmetries is indeed important and demands further study to link to individual performance in the functional domains.

In summary, the observations made by Cheng *et al*. advance our understanding of the presence and evolution of anatomical and connectional asymmetries. In doing so, this

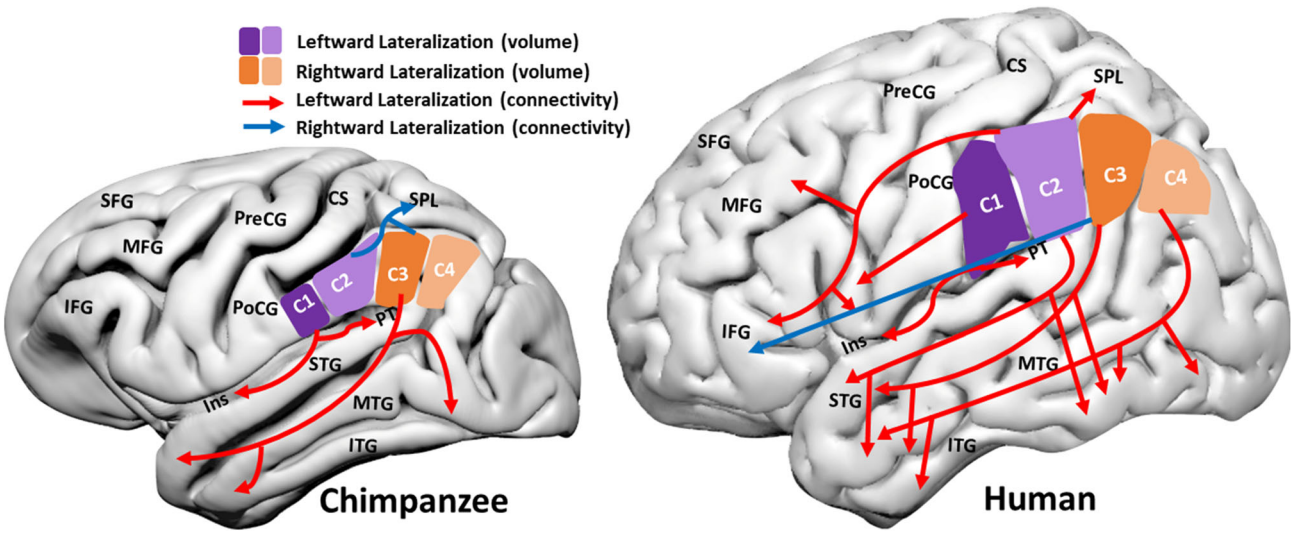

Fig. 1 An adaptation of the graphical abstract originally provided in Cheng *et al*. which represents the connectivity and volumetric asymmetries found in chimpanzees and humans. The results are presented on a surface projection of the chimpanzee reference template (JunaChimp [4]) and human (MNI). C1:C4, subdivisions of the IPL; CS, central sulcus; IFG, inferior frontal gyrus; Ins, insula; ITG, inferior temporal gyrus; MFG, middle frontal gyrus; MTG, middle temporal gyrus; PoCG, postcentral gyrus; PreCG. precentral gyrus; PT, planum temporale; SFG, superior frontal gyrus; SPL, superior parietal lobule.

study marks an important step towards a better understanding of how evolutionary changes in structural asymmetries may have contributed to the evolution of primate cognition.

References

1. Cheng LQ, Zhang YC, Li G, Wang JJ, Sherwood C, Gong GL. Connectional asymmetry of the inferior parietal lobule shapes hemispheric specialization in humans, chimpanzees, and rhesus macaques. Elife 2021, 10: e67600.
2. Bzdok D, Hartwigsen G, Reid A, Laird AR, Fox PT, Eickhoff SB. Left inferior parietal lobe engagement in social cognition and language. Neurosci Biobehav Rev 2016, 68: 319–334.
3. Friedrich P, Forkel SJ, Amiez C, Balsters JH, Coulon O, Fan LZ, *et al*. Imaging evolution of the primate brain: The next frontier? Neuroimage 2021, 228: 117685.
4. Vickery S, Hopkins WD, Sherwood CC, Schapiro SJ, Latzman RD, Caspers S, *et al*. Chimpanzee brain morphometry utilizing standardized MRI preprocessing and macroanatomical annotations. Elife 2020, 9: e60136.
5. Ströckens F, Güntürkün O, Ocklenburg S. Limb preferences in non-human vertebrates. Laterality 2013, 18: 536–575.
6. Hopkins WD. Neuroanatomical asymmetries and handedness in chimpanzees (Pan troglodytes): A case for continuity in the evolution of hemispheric specialization. Ann N Y Acad Sci 2013, 1288: 17–35.
7. Eickhoff SB, Grefkes C, Fink GR, Zilles K. Functional lateralization of face, hand, and trunk representation in anatomically defined human somatosensory areas. Cereb Cortex 2008, 18: 2820–2830.
8. Honey CJ, Sporns O, Cammoun L, Gigandet X, Thiran JP, Meuli R, *et al*. Predicting human resting-state functional connectivity from structural connectivity. Proc Natl Acad Sci U S A 2009, 106: 2035–2040.
9. Vázquez-Rodríguez B, Suárez LE, Markello RD, Shafiei G, Paquola C, Hagmann P, *et al*. Gradients of structure-function tethering across neocortex. Proc Natl Acad Sci U S A 2019, 116: 21219–21227.
10. Croxson PL, Forkel SJ, Cerliani L, Thiebaut de Schotten M. Structural variability across the primate brain: A cross-species comparison. Cereb Cortex 2018, 28: 3829–3841.

5. The Uniqueness of. Human Vulnerability to Brain Aging in Great Ape Evolution, Sam Vickery, Kaustubh R. Patil, Robert Dahnke, William D. Hopkins, Chet C. Sherwood, Svenja Caspers, Simon B. Eickhoff, Felix Hoffstaedter, bioRxiv 2022.09.27.509685, doi: https://doi.org/10.1101/2022.09.27.509685

The Uniqueness of Human Vulnerability to Brain Aging in Great Ape Evolution

Sam Vickery[1,2], Kaustubh R. Patil[1,2], Robert Dahnke[3,4,5], William D. Hopkins[6], Chet C. Sherwood[7], Svenja Caspers[8,9,10], Simon B. Eickhoff[1,2], Felix Hoffstaedter[1,2]

[1] Institute of Systems Neuroscience, Medical Faculty & University Hospital Düsseldorf, Heinrich-Heine-University, Düsseldorf, Germany.

[2] Institute of Neuroscience and Medicine (INM-7) Research Centre Jülich, Jülich, Germany

[3] Structural Brain Mapping Group, Department of Neurology, Jena University Hospital, Jena, Germany

[4] Structural Brain Mapping Group, Department of Psychiatry and Psychotherapy, Jena University Hospital, Jena, Germany

[5] Center of Functionally Integrative Neuroscience, Department of Clinical Medicine, Aarhus University, Denmark

[6] Department of Comparative Medicine, Michale E Keeling Center for Comparative Medicine and Research, The University of Texas MD Anderson Cancer Center, Bastrop, Texas

[7] Department of Anthropology and Center for the Advanced Study of Human Paleobiology, The George Washington University, Washington, DC, USA.

[8] Institute of Neuroscience and Medicine (INM-1), Research Centre Jülich, Jülich, Germany

[9] Institute for Anatomy I, Medical Faculty & University Hospital Düsseldorf, Heinrich-Heine-University, Düsseldorf, Germany

[10] JARA-BRAIN, Jülich-Aachen Research Alliance, Jülich, Germany

Abstract

Aging is associated with stable decline in the brain's gray matter. This spatially specific, morphological change in humans has also recently been shown in chimpanzees. The correspondence between species-specific cortical expansion and the degree of brain structure deterioration in aging remains poorly understood. Here, we present a data-driven, cross-species comparative framework and apply it to explore the relationship between gray matter alterations with age and cross-species cerebral expansion in chimpanzees and humans. In humans, we found a positive relationship between cerebral aging and cortical expansion, whereas, in chimpanzees no such relationship was found between aging and cortical expansion. The greater aging and expansion effects in higher-order cognitive regions like the orbito-frontal cortex were observed to be unique to humans. This resembles the last-in, first out hypothesis for neurodevelopment on the evolutionary scale and may suggest a biological cost for recent evolutionary developments of human faculties.

Introduction

With age, pronounced alterations occur in morphology and organization of the human brain with a distinct spatial pattern resulting in part from cellular atrophy in later life[1,2]. These changes are part of the normal aging process, although they may be further accelerated in some people by age-mediated disorders such as Alzheimer's disease, Parkinson's disease, and other neurodegenerative conditions[3]. Furthering our understanding about specific neurobiological and possible evolutionary influences on these brain aging spatial patterns, may provide insight into the brain changes in healthy aging and possible diagnostic markers for clinical outcomes. Historically, comparative neuroscience has been an effective catalyst for important discoveries regarding principles of anatomy and functional specializations of the human brain[4]. With open and collaborative endeavors such as the National Chimpanzee Brain Resource (NCBR) and the PRIMatE Date Exchange (PRIME-DE)[5], along with improved methodologies and imaging technology, large scale comparative neuroanatomy has become more accessible to answer new questions[6].

Morphological gray matter (GM) changes during aging have recently been shown to be present in one of humans' closest extant primate relative, chimpanzees (*Pan troglodytes*)[7,8]. The age-related morphological changes observed in chimpanzees are similar but at a lower magnitude compared to humans[8]. For example, age-related volumetric reduction of overall hippocampus and frontal cortex size are not evident in chimpanzees, but occurs in humans that could be related to humans comparatively extended lifespan[9]. Cognitive decline is also present in chimpanzees, but appears not as prominent as in humans[10]. In this context, understanding GM alterations during brain aging in great ape evolution (e.g. which includes humans and chimpanzees, as well as bonobos, gorillas, and orangutans) may aid in explaining the spatial distribution of morphological changes due to healthy aging and disease.

The comparison of neuroanatomy and brain functions across primate species is commonly informed by analyzing homologous brain regions[6,11–13]. Classically, these regional homologies are defined by manually delineating brain partitions, based on macroanatomy, gene expression, connectivity, and/or cytoarchitectonic features. This approach rests on the assumption that similar anatomical features result in a common functional organization across species and thereby enable an informative and meaningful comparison. However, homologies can be debatable and therefore can be influenced by subjective biases which is minimizes through a data-driven approach. The homologous-centric approach has proven to be effective and informative, although utilizing a more data-driven approach could supplement these techniques by removing subjective biases while still capturing important cross-species differences and incorporating species-specific features in a data-centric manner.

Chimpanzees offer an ideal referential model to investigate evolutionary changes in the human lineage as they share a last common ancestor with humans approximately 6 - 8 million years ago[14]. Accordingly, chimpanzees and humans have many genomic similarities[15] as well as cerebral structural features in common[16–18]. Consequently, chimpanzees present a unique comparison to infer distinctive evolutionary adaptations of the human brain, keeping in mind that their neurobiology reflects their own species-specific evolutionary adaptations. The multitude of commonalities and recent evolutionary divergence allows a further understanding of changes associated with selection for human specific adaptations that occurred after the split from a common ancestor. Previous studies have shown that multimodal association cortices in humans are disproportionately larger than in non-human primates[11,19,20]. The higher expansion of certain areas through human evolution may relate to specific functions, important for modern human cognition. Specifically, the expanded human prefrontal cortex (PFC)[11] might be associated with self-control and executive functioning[21] and the larger precuneus[19] with visuospatial processing[22]. Furthermore, the vulnerability of frontal cortical areas to aging processes is hypothesized to be related to their late maturation[23]. This refers

to the "last in, first out hypothesis" and interestingly similarities have been shown between cortical development and cross-species expansion[24].

In this study, we directly compare age-mediated GM changes in chimpanzees and humans, which represent two species in the Hominidae family (i.e., great apes) and explore their relationship with cross-species cerebral expansion. For inter-species comparison, we developed a multivariate data-driven comparative framework that applies voxel-wise clustering based on GM variability within each species independently. The optimal low dimensional representation of brain morphology for each species is then employed in a cross-species investigation of aging and cortical expansion. Comparative data for calculating cross-species expansion was provided by relatively recent phylogenetic ancestors. Accordingly, humans were compared to chimpanzees and chimpanzees were compared to olive baboons (Papio anubis) and rhesus macaques (Macaca mulatta), two commonly researched cercopithecid monkey species. Therefore, we can ascertain whether such a relationship is unique to modern humans or instead might be a feature shared with chimpanzees that originated at the divergence of the great ape lineages from other primates.

To summarize, we present a novel technique for cross-species comparison of structural brain organization and demonstrate its utility by comparing the relationship between cerebral aging and cross-species expansion in humans and chimpanzees. Our data-driven approach uses both species-specific information in addition to cross-species similarity to create an interpretable low-dimensional brain parcellation for comparison. We show that the resulting parcellation aligns with known macroanatomical structures in humans and chimpanzees. Utilizing this comparative framework, we examine spatial differences in brain aging and cerebral expansion between the two great ape species. Finally, we present evidence for a relationship between local age-mediated GM changes and recent cortical expansion in humans that is not present in chimpanzees.

Results

Our cross-species comparative approach was based on structural magnetic resonance imaging (MRI) scans from 189 chimpanzees and 480 human brains (Fig. 1B). Orthogonal projective non-negative matrix factorization (OPNMF)[25,26] was applied to normalized GM maps within each species independently. The orthogonality and non-negativity constraints of OPNMF results in a spatially continuous, parts-based representation of the input data based on regional covariance of brain structure within each species[27]. OPNMF has been extensively used with human neuroimaging data yielding anatomically meaningful correspondence of clustering solutions[25,28–31].

The comparative framework utilizing OPNMF as well as the creation of the cross-species expansion maps is outlined in Figure 1A. The approach begins with separately segmenting and normalizing the individual chimpanzee and human images utilizing species-specific templates and pipelines[8,32]. The processed GM maps for each species are parcellated independently using OPNMF over a range of granularities (2-40) and bootstrapped to ensure stability of the solutions accuracy. The bootstrapped solution accuracy measure assessed using the reconstruction error (RE) is used in part, to select the optimal number of parcels for cross-species comparison. For direct cross-species comparison, the JunaChimp average chimpanzee T1-weighted (T1w) template[8] is applied to the human preprocessing pipeline to create a representative chimpanzee to human deformation field map. This represents the non-linear deformations required to map morphological macroanatomical

features of the JunaChimp[8] template brain to the standard ICBM 2009c Nonlinear Asymmetric human template[33]. The chimpanzee to human deformation map is used to non-linearly register the chimpanzee OPNMF solutions to the human template space for the analysis of parcel or factor similarity using the adjusted rand index (ARI). This cross-species parcel similarity of multivariate GM morphology are used for the selection of optimal parcellation granularity, together with species-specific OPNMF reconstruction error change (see *Comparative Brain Parcellations* for more information). To create cross-species expansion maps, average population templates from three non-human primate species were processed, chimpanzee[8], olive baboon[34], and rhesus macaque[35–37].

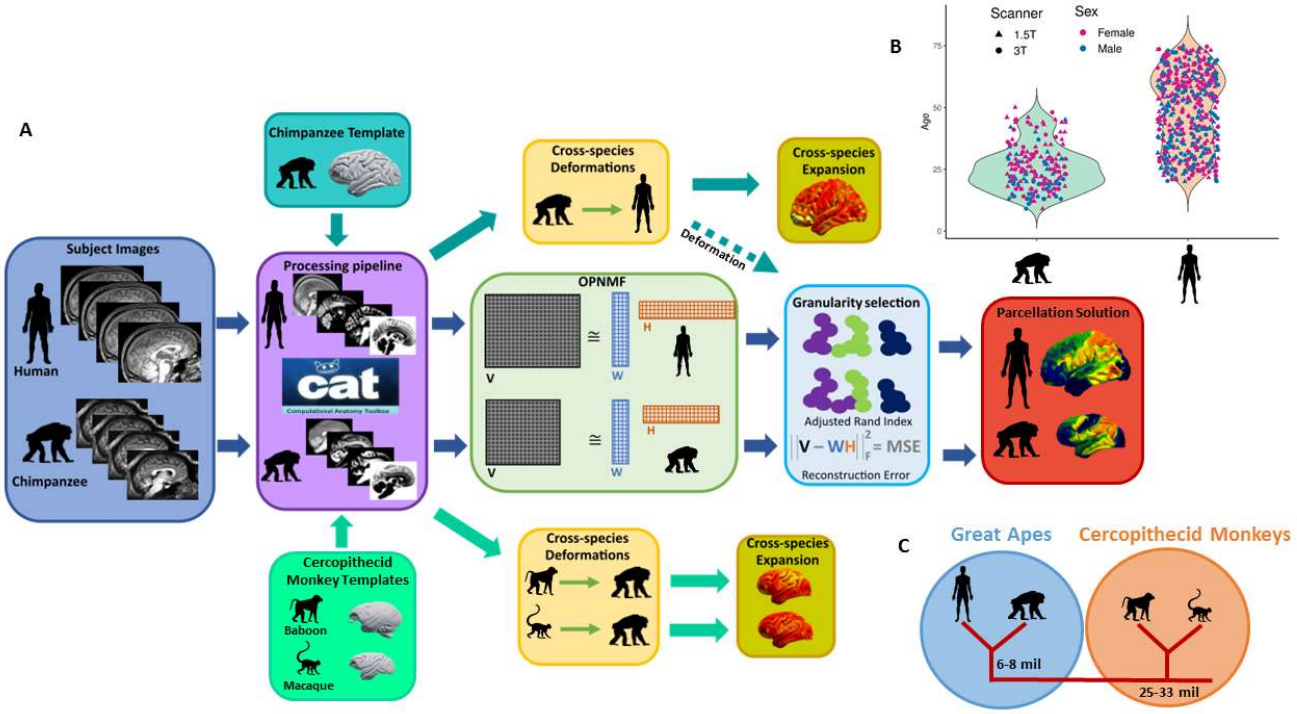

Figure 1. Overview of our comparative approach. A – Workflow outlining the steps taken in our comparative approach by utilizing OPNMF and creating cross-species expansion maps. B – The age, sex, and scanner field strength distribution of the chimpanzee (N=189) and human (N=480) samples used in creating the OPNMF solutions for cross-species comparison. C – Diagram showing the phylogenetic relationship of humans to the other three primate species investigated in this study.

Comparative Brain Parcellation

OPNMF takes the volumetric GM maps and creates parcels or clusters which contain voxels that co-vary with on another across the sample. This unsupervised technique behaves similar to clustering[38] and requires an a priori decision on the number of factors or parcels to represent the original data[25]. The decision for the most appropriate OPNMF granularity was determined via assessing cross-species spatial similarity and the development of OPNMF solutions accuracy at different granularities (Fig. 2A). Cross-species parcel similarity was determined using the cluster similarity measure ARI. Chimpanzee parcellations are transformed to the human template space using the chimpanzee to human deformation map. Quality control of the chimpanzee to human deformation map was conducted by visually inspecting the Davi130 chimpanzee macroanatomical labels[8] in the human template space (Supplementary Figure 1). The granularity with highest ARI

represents common cross-species organizational patterns of GM covariance[27]. The RE indicates how accurately the input data (GM maps) can be represented by the OPNMF factorization. By increasing the number of factors, or parcels, more information can be used to represent the GM data and RE naturally decreases. Although this development is non-linear and sample specific (Fig. 2A). A relative plateau means that increasing the granularity only marginally improves the parcellations representation of the GM data and therefore, will largely model noise. Consequently, the beginning of the plateau provides a good tradeoff between the solutions reconstruction accuracy and number of factors. Finally, to ensure the robustness of the RE development curve, a computationally intensive 100 bootstraps were computed for each OPNMF granularity in both species independently.

The highest cross-species spatial similarity was found for the 17-factor solution with an ARI of 0.23 (Fig. 2A). This is not a very high ARI, although it is along with 16 a clear local maximum and contains many parcels with relatively high ARI (> 0.4) (Fig. 2B). The robust RE development curve did not show a clear indication of a plateau for both species. Instead, a relevant number of parcels is present in the range of 15 – 21 in chimpanzees and 14 – 20 in humans. Therefore, the 17-factor solution met our criteria for both chimpanzees (Fig. 3A) and humans (Fig. 3B) to conduct our cross-species comparative investigation.

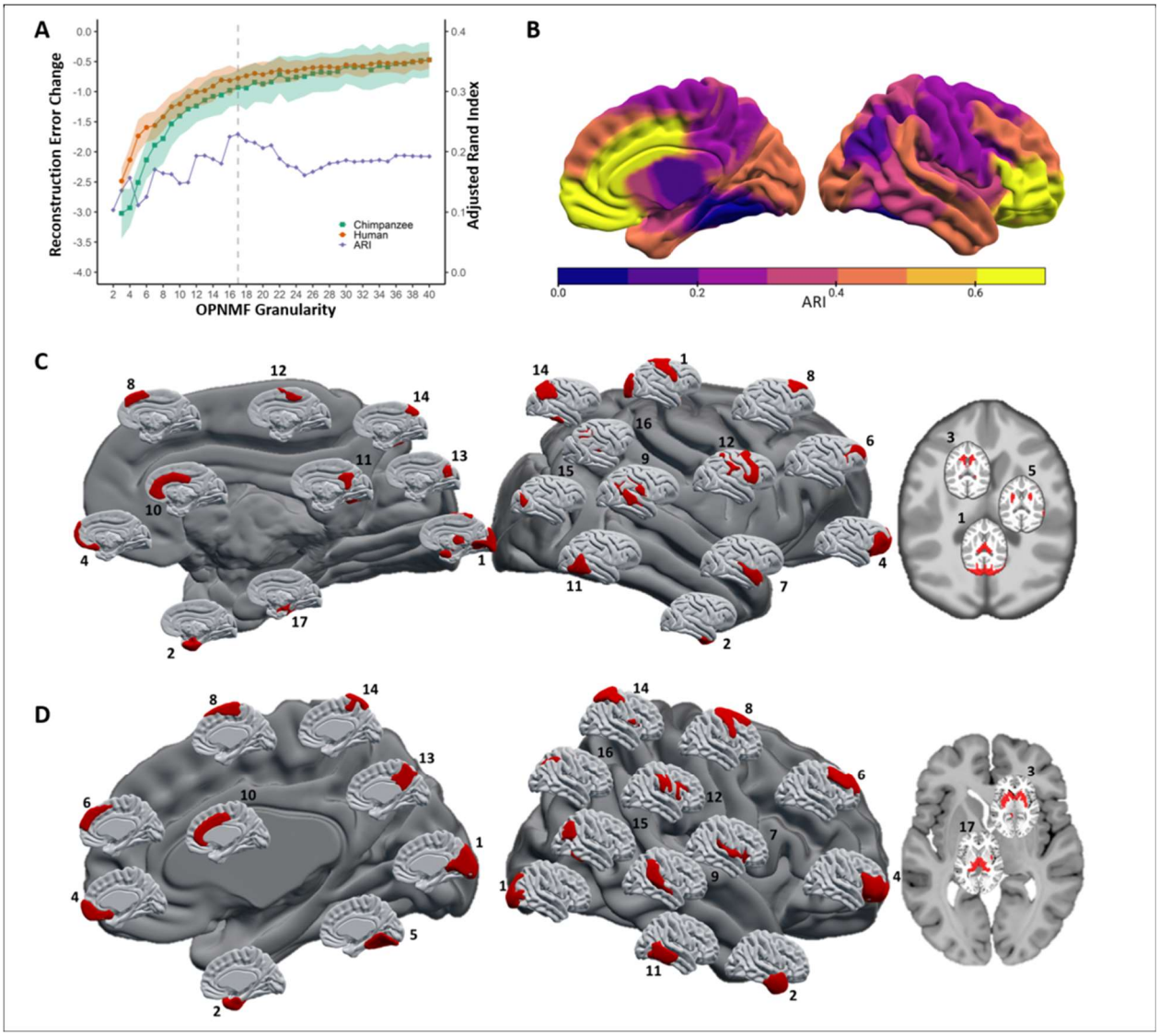

Figure 2 Selected OPNMF solution for cross-species comparison. A – OPNMF granularity selection utilizing ARI to assess cross-species similarity and change in reconstruction error (RE) over a granularity range of 2 – 40 factors and bootstrapped (k=100) to ensure stability. Cloud represents ±1 sd from the mean change in RE over 100 bootstraps and the gray dashed line represents the selected number of factors, 17. B – Presents the cross-species single factor ARI, whereby for each OPNMF factor the highest cross-species ARI is represented in human template space. C - Selected 17-factor OPNMF solution for chimpanzees. Macroanatomical labels are: 1 – occipital lobe, primary motor cortex, and thalamus, 2 – temporal pole, 3 – caudate nucleus, 4 – prefrontal and orbito-frontal cortex, 5 – putamen, 6 – middle frontal gyrus, 7 – superior temporal gyrus and anterior insula, 8 – posterior superior frontal gyrus, 9 – temporal parietal junction and supramarginal gyrus, 10 – anterior and middle cingulate cortex, 11 – posterior cingulate, precuneus, and peristriate cortex, 12 – supplementary and pre-motor areas, 13 – cuneus and medial occipital-parietal sulcus, 14 – superior and inferior parietal lobe and inferior temporal gyrus, 15 – lateral parietal-occipital sulcus, 16 – superior parietal sulcus and posterior insula, 17 – amygdala and hippocampus. D – Human selected 17-factor OPNMF solution. Macroanatomical labels are: 1 – occipital lobe, 2 – temporal pole, 3 – putamen, caudate nucleus, amygdala, and hippocampus, 4 – prefrontal and orbito-frontal cortex, 5 – lingual and fusiform gyrus, 6 – superior and middle frontal gyrus, 7 – insula, 8 – pre-central gyrus and pre-motor area, 9 – temporal parietal junction, 10 – anterior and middle cingulate cortex, 11 – posterior middle and inferior temporal gyri, 12 – supramarginal gyrus, inferior post-central gyrus, and inferior pre-central sulcus, 13 – precuneus, 14 – superior parietal lobe, 15 – angular and fusiform gyrus, 16 – superior parietal sulcus and parahippocampal cortex, 17 – thalamus.

The 17-factor OPNMF solutions in both chimpanzees (Fig. 2D) and humans (Fig. 2C) represents a data-driven parcellation of both species cerebral GM. These regions were established through a hard parcellation by assigning each voxel to the parcel with the highest weight, which is aided by the orthogonality constraint of OPNMF. Some resulting brain parcels closely align with known macroanatomical regions within both species. Both species 17-factor solutions contained parcels accurately representing the orbito-frontal cortex, middle frontal gyrus, anterior and middle cingulate cortex, and the temporal pole (Fig. 2C&D). In humans additionally parcels separated the insula, superior parietal lobule, precuneus, occipital lobe, and thalamus (Fig. 2D). On the other hand, chimpanzees additionally showed parcels that separated the pre-motor cortex, hippocampus, putamen, and caudate nucleus (Fig. 2C). The parcels representing the orbito-frontal cortex and the cingulate cortex show the highest cross-species similarity with an ARI of 0.66 and 0.64 respectively (Fig. 2B). This was assessed by calculating the highest single parcel-to-parcel cross-species similarity. A striking difference between the species can be seen in the parcellation of the sensory-motor cortices. In chimpanzees, two parcels represented major sensory-motor structures, one for the occipital lobe, pre- and post-central gyrus, and thalamus and another for the pre-motor cortex. In humans, separate parcels represented the thalamus and occipital lobe while the motor and pre-motor cortices are split between different parcels. Specifically in humans, multi-modal parietal regions like the precuneus, superior parietal lobule, angular gyrus, and temporal-parietal junction were more specifically parcellated compared to chimpanzees.

Comparison of Brain Aging and Relative Expansion between Chimpanzees and Humans

Age-mediated GM decline in chimpanzees and humans was assessed for the OPNMF 17-factor solution. The average GM density of each parcel was used as the dependent variable in a multiple linear regression model with age, sex, total intracranial volume (TIV), and scanner field strength as independent variables, as has been conducted previously[8]. To improve comparability, the human sample age range was matched to the chimpanzees by accounting for the interspecies differences in brain aging. The comparative aging difference of human years equal to 1.15 years in chimpanzees was used based on a comprehensive study using a combination of anatomic, genetic, and behavioral data[39]. Accordingly, as the oldest chimpanzees were 50 years old humans over 58

219 years old were removed to include 304 IXI subjects (150 females; mean age = 39.0±11.0) for the age
220 regression model. Of note, this represents a middle-aged human sample, including minimal
221 morphological changes due to age-related neurodegenerative or pre-clinical conditions such as mild
222 cognitive impairment. In both species, significant age effects were found in nearly all parcels
223 following correction for multiple comparisons across parcels at p≤0.05[40]. Humans showed aging
224 effects across all parcels, largest in the frontal cortex and in particular, the PFC. Chimpanzees
225 displayed overall aging effects in all parcels except for three, which represent the peristriate cortex,
226 posterior insula, cuneus, and superior parietal sulcus. Both species showed a relatively low aging
227 effect in occipital and motor areas. The largest aging effect in chimpanzees was found in the
228 striatum, in particular the caudate nucleus. Humans showed overall a much greater age effect
229 compared to chimpanzees. Additionally, a comparable aging effect and distribution was found when
230 employing the higher granularity macroanatomical Davi130 parcellation[8] in chimpanzees and
231 humans (Supplementary Figure 2).

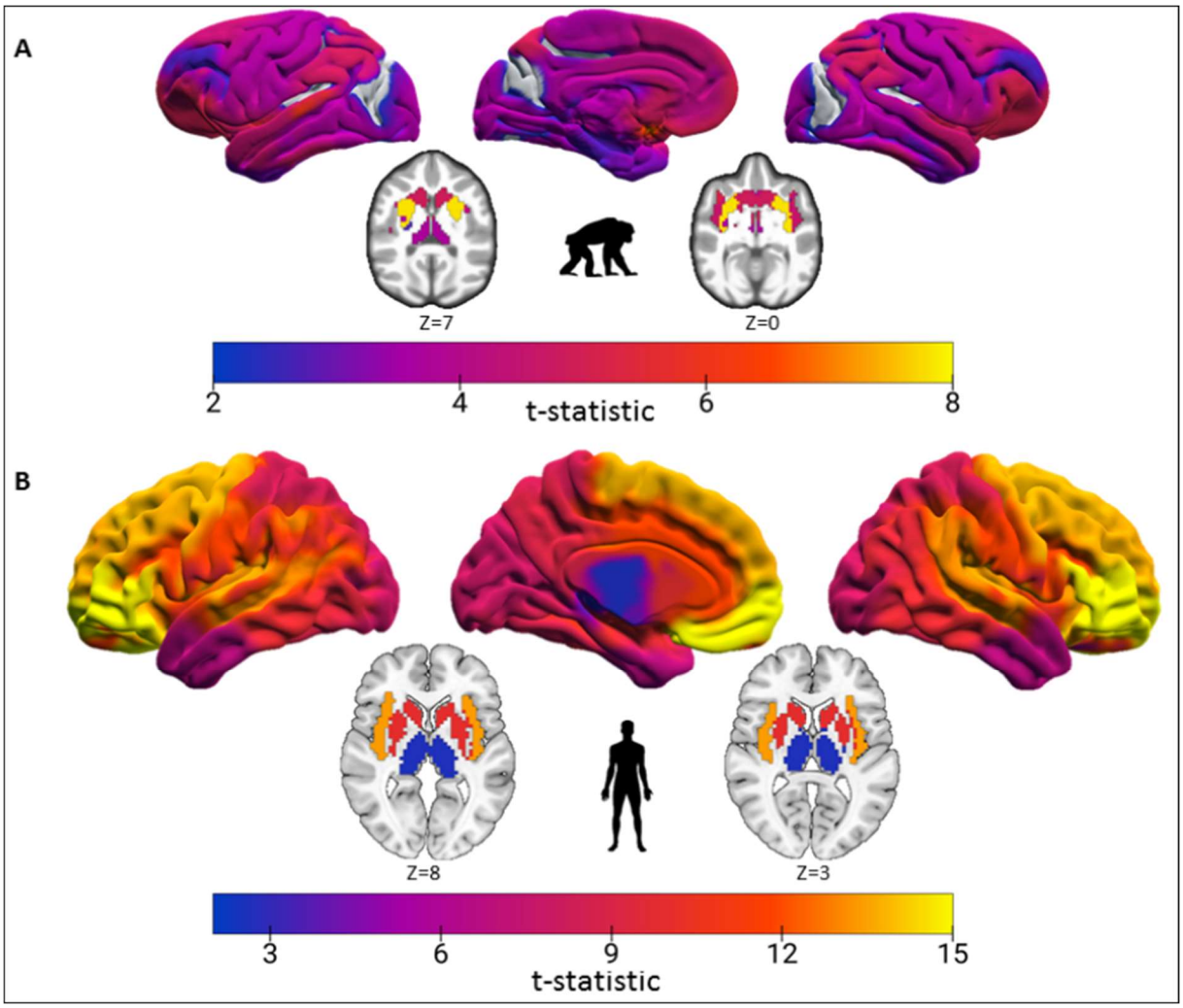

232

233 **Figure 3**. **Comparison of aging effect on GM volume**. OPNMF 17-factor solution age-mediated GM
234 changes presented as factor-wise regression model absolute t-statistics in A - chimpanzees and B – humans.
235 The t-statistic of significant parcels are plotted and determined by a FWE p≤0.05.

236

237 Utilizing the 17-factor solution, we compared the cross-species expansion based on
238 population representative T1w templates from humans[33], chimpanzees[8], olive baboons[34] and rhesus

macaques[35–37]. Using template images provides the added benefit of artificially improved tissue contrast in addition to being representative of an average brain within a particular species aiding generalizability. Cross-species non-linear registrations were computed to provide estimations for the expansion from chimpanzee to human, baboon to chimpanzee, and macaque to chimpanzee.

In chimpanzee to human expansion, the largest deformation was found in the orbito-frontal cortex, which additionally showed the greatest aging effect (Fig. 3B) and highest cross-species parcel similarity (Fig. 2B). High expansion was additionally found in other multimodal association cortical areas such as the middle and medial frontal cortex, superior parietal, precuneus, insula, and cingulate cortex (Fig. 5A). The large expansion in frontal and parietal regions are comparable to those shown using cortical surface measures to estimate the expansion from chimpanzee to human[20] as well as macaque to human [24]. Low chimpanzee to human expansion was found in temporal, occipital, motor, and subcortical areas (Fig. 5A). When comparing the chimpanzee to human (Fig. 5A) with the baboon (Fig. 5B) and macaque (Fig. 5C) to chimpanzee expansion maps, similar low expansion was found in the temporal lobe and subcortical regions as well as relatively large deformations in the frontal and superior parietal lobe. The general pattern of expansion from the two cercopithecid monkeys to chimpanzees is similar although some regional differences are present. In baboon to chimpanzee, the largest expansion occurred in the superior frontal gyrus/pre-motor area (Fig. 5B) while in macaque to chimpanzee, the sulcal fundi of the parietal lobe and posterior insula (Fig. 5C) featured the largest expansion. Furthermore, macaque to chimpanzee showed comparably more expansion in the occipital-parietal junction and lower expansion in the motor/pre-motor area, occipital cortex, and basal ganglia compared to baboon to chimpanzee expansion. To summarize, chimpanzee to human as well as cercopithecid monkeys to chimpanzee expansion maps all show relatively high expansion in frontal and parietal cortical regions. Chimpanzee to human features the greatest expansion in prefrontal areas while in cercopithecid monkeys to chimpanzee the largest expansion was seen in pre-motor/frontal and lateral parietal regions. Finally, notable differences between macaques and baboons relative to chimpanzees are seen in the degree of expansion within unimodal and sensory motors areas.

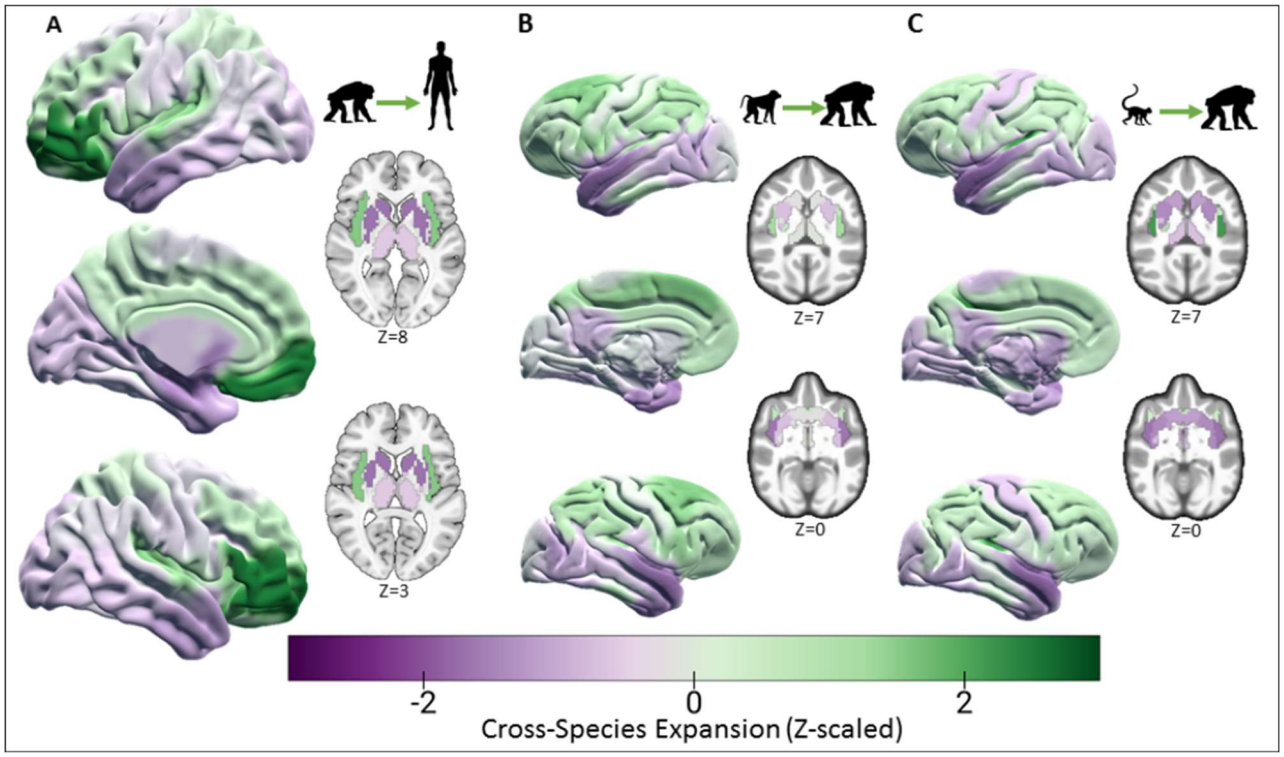

Figure 4. Cross-species expansion. OPNMF 17-factor solution volumetric Cross-species expansion in A - chimpanzee to human, B - baboon to chimpanzee, & C - macaque to chimpanzee. Expansion values have been z-scaled for easier comparison.

Correlation between Aging and Cross-species Expansion in Chimpanzees and Humans

We investigated the relationship between cross-species expansion (Fig. 4) and age-mediated GM changes (Fig. 3) in chimpanzees and humans. For humans, brain aging was compared with relative cortical expansion from chimpanzee to human (Fig. 5A) while for chimpanzees, aging effect was compared with both baboon and macaque (Fig. 5B). A strong positive correlation was found between cross-species expansion and the aging effect in humans (Fig. 5A), following permutation testing at $p \leq 0.05$ ($r = 0.59$; $p = 0.004$). This relationship is particularly evident in the orbito-frontal cortex and insula, which presents considerable expansion as well as an extensive aging effect. Relatively low aging effects and less cross-species expansion was found in the basal ganglia, occipital lobe, temporal pole, and medial temporal lobe. This general association was replicated in the lifespan eNKI (Enhanced Nathan Kline Institute; n = 765; $r = 0.51$; $p = 0.01$)[41] dataset using the same OPNMF parcellation to extract the aging effect (Supplementary Figure 4).

In chimpanzees, no significant relationship was seen between aging and baboon to chimpanzee cross-species expansion ($r = -0.005$, $p = 0.49$) although a marked negative correlation was found in macaque to chimpanzee expansion ($r = -0.53$, $p = 0.01$). Even though the macaque and baboon to chimpanzee expansion maps show a quite similar spatial distribution, there is an apparent trend that regions showing large chimpanzee age effect have low macaque to chimpanzee expansion and the opposite for regions with low aging effect. This is driven by the comparably lower macaque to chimpanzee expansion in the basal ganglia, which shows a large age effect in chimpanzees and the higher expansion in the peristriate cortex and the lateral parietal and posterior insula cortices that presents lower aging effects in chimpanzees.

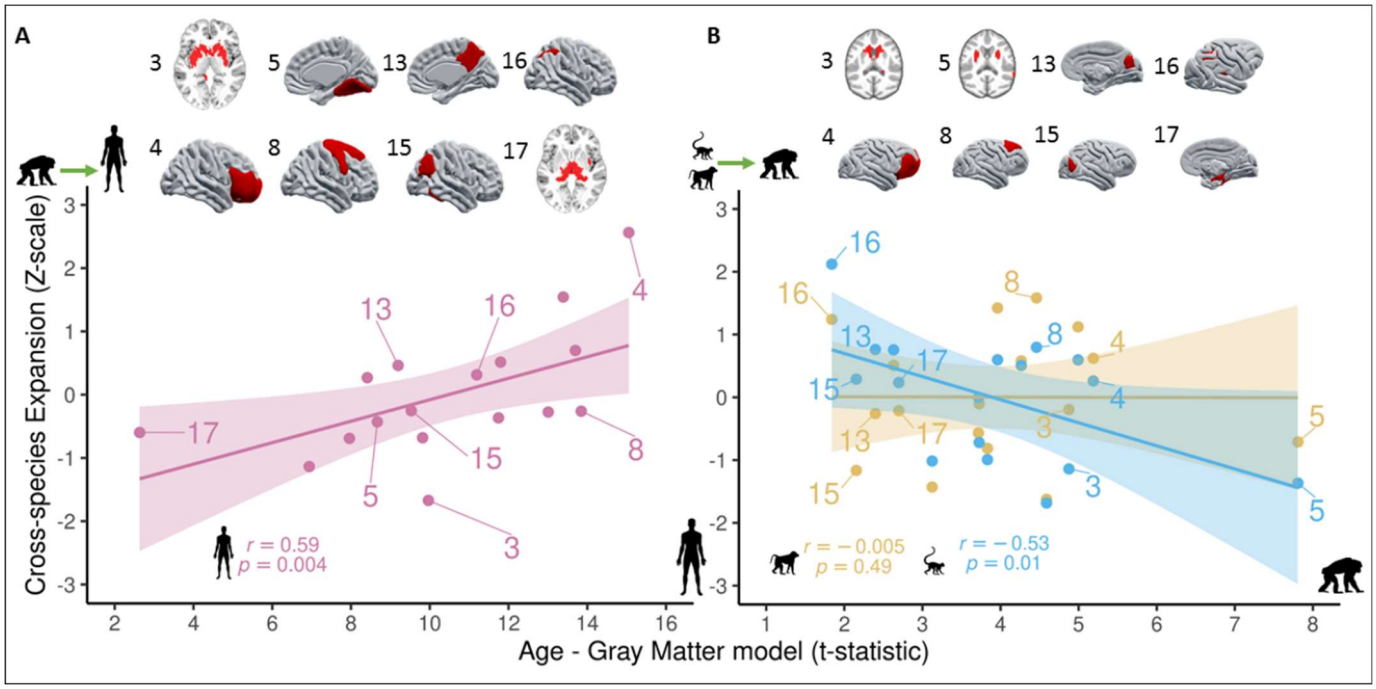

Figure 5. Aging – expansion comparison. Scatter plots showing of cross-species expansion and aging effect between A – chimpanzee to human expansion and human aging effect (Pink), B – macaque to chimpanzee

295 expansion and chimpanzee aging effect (Blue) and baboon to chimpanzee expansion and chimpanzee aging
296 effect (Yellow). A selection of single OPNMF factors in both species are presented. Significance (p) of
297 correlation (Person's r) for cross-species expansion and aging effect relationship is determined by permutation
298 testing (k = 100 000).

299

300 Discussion

301 Through our comparative framework, we found a human-specific positive relationship
302 between age-related GM decline and cortical expansion in comparison to chimpanzees. In
303 chimpanzees, on the other hand, there was no correlation between the spatial distribution of aging
304 effect and areas of cortical cross-species expansion relative to baboons and a positive correlation
305 with the expansion relative to macaques. These findings suggest that the extensive expansion of
306 higher-order cortical areas in human brain evolution, which is dominated by the PFC, and in
307 particular the orbito-frontal cortex, comes at the price of more pronounced age-related
308 deterioration.

309 We demonstrated OPNMFs ability to provide a low dimensional space matching
310 macroanatomy that serves as a basis for cross-species comparison of brain organization. Our
311 approach (Fig. 1A) is centered on OPNMF, which establishes a brain parcellation that contains
312 species-specific information that also identifies comparable organizational features between species.
313 The chimpanzee factorization solution (Fig. 2D) shows overall hemispheric symmetry, spatial
314 contiguity, and aligns with known macroanatomical structures[8] which were reported in previous
315 applications of OPNMF in humans[25,28–30,42]. The 17-factor solution that was selected based on cross-
316 species similarity and within-species reconstruction accuracy comprises a very similar granularity that
317 was selected in OPNMF for infants[42] and an adolescent human sample[30]. Along with the similar
318 granularity, some human (Fig. 2C) and chimpanzee (Fig. 2D) parcels show apparent spatial similarity
319 to previously reported OPNMF solutions[30,42]. Similarities include parcels representing the precuneus,
320 insula, and superior parietal lobe, in the human factorization while both the chimpanzee and human
321 solutions show similarities to previous findings in the PFC and temporal pole. Additionally, the
322 superior parietal lobe and PFC parcels show similarities to spatial clusters representing genetic
323 influence on cortical thickness[43].

324 The PFC plays an important role in higher-order cognitive functions, such as executive
325 control[21,44] and working memory[45]. The OPNMF 17-factor solution created independently in
326 chimpanzees (Fig. 2D) and humans (Fig. 2C) established a parcel representing the ventrolateral and
327 orbital parts of the PFC. This region showed the highest cross-species similarity as well being
328 expanded greatly in humans relative to chimpanzees. Therefore, the uniqueness of this region's GM
329 organization was conserved between humans and chimpanzees, even though there was considerable
330 cross-species expansion. Despite the PFC being proportionally larger in humans compared to
331 chimpanzees [11], which is due in part to allometric scaling[46,47]. Our multivariate data-driven analysis
332 suggests a possible similarity in the organization of the ventral and orbital sub-regions of the PFC.
333 Furthermore, this region showed an exceptionally large GM aging effect in humans as well as a high
334 degree of expansion in humans relative to chimpanzees. This suggests that the greater expansion of
335 PFC, which has been instrumental in evolutionary changes in primate cognition[48], comes with the
336 detriment of severe age-related GM decrease in humans. The much greater PFC expansion and aging
337 effect in humans compared to chimpanzees, provides an additional dimension to the "last in, first
338 out" hypothesis[23] of later developmental maturation and aging. With later evolutionary expansion
339 also related to early and strong age-mediated GM morphology decline, furthering previous research
340 showing similarities between macaque to human expansion and neurodevelopment[24].

The relationship between human GM volume decline and cortical expansion indicates an evolutionary link between functional development of these particular cortical areas in humans and increased vulnerability to neurodegenerative processes. Interestingly, such a relationship was not present in the expanded cortical regions of chimpanzee relative to baboons and macaques even though a significant GM decline was present in chimpanzees [8]. The main difference between humans and chimpanzees seems to be the more prominent expansion in sensorimotor regions in chimpanzees relative to the cercopithecid monkeys, whereas regions of human cortical expansion relative to chimpanzees is generally seen in more multimodal association regions. This could be related to chimpanzees improved abilities for tool use and spatial understanding as compared to cercopithecid monkeys although showing similar abilities in social-cognitive tasks[49].

In general, multimodal association cortex in humans show greater expansion as well as large aging effects on GM volume. Those multimodal cortical areas are characterized by lower neuronal cell density, as well as higher dendritic branching and spine numbers of pyramidal neurons[50,51]. Interestingly, compared to other great apes, the human brain has a large neuropil fraction in the frontal pole[52] and the anterior insula[53]. The neuropil fraction represents the space surrounding cell bodies occupied by dendritic and axonal interconnectedness through local intrinsic and extrinsic connections of a region. Both these areas (frontal pole and insula) show a combination of large expansion and aging effect on GM volume (Fig. 4A) in humans. With dendritic reduction and synapse loss being characteristics of normal aging processes[54], the relatively increased neuropil space of human association cortex may partly explain the aging – expansion relationship we observe.

Some possible neurobiological mechanisms could explain the large aging effect in regions that expanded most in humans relative to chimpanzees. The medial and orbito-frontal cortex as well as the insula that displayed large expansion and aging effects have been previously found to have high deterioration of glucose metabolism and large accumulation uptake of β-amyloid in human aging[55–57]. Additionally, the novel relationship we present may aid future research to better understand the neurobiological mechanism of why certain areas have expanded more than others.

Several considerations need to be considered when interpreting the results presented in this study. First, our voxel-based morphometry analysis was limited to structural information present in the T1w contrast and does not include structural connectivity or functional dynamics. Such complimentary information provided by additional modalities will help to establish a more comprehensive cross-species comparison. Second, our inferences of age-related GM volume decline are driven by cross-sectional normal aging data (age $\leq$ 58 y/o), although a longitudinal design can provide additional information on structural changes that occur to the brain throughout the lifespan. Third, to infer the unique relationship in human evolution between aging and regions of cortical expansion we only used templates of one great ape species (chimpanzee) and two different cercopithecid monkey species (macaque & baboon). Further research is required using additional primate species. A broader phylogenetic investigation will enable a better understanding at which evolutionary branches these aspects of the neurobiology of aging occur.

In conclusion, we demonstrate the applicability of a data-driven comparative framework in revealing organizational features of great ape brains. By establishing a species-specific parcellation containing both inter- and intra-species GM organizational features, we found a novel relationship of cortical expansion and age-related decline in great ape evolution. Our multivariate data-driven framework found regions with high expansion to show large age-mediated GM decline in humans, whereas this was not present in chimpanzees. These findings allude to a possible cost the human cortex pays, in the form of age-mediated GM decline, because of evolutionary expansion.

Methods

Sample Description

The chimpanzee T1w MRI scans were provided by the NCBR containing brain scans of 223 captive animals (137 females; 9 - 54 y/o; mean age 26.9 ± 10.2 years). The chimpanzees were housed at the National Center for Chimpanzee Care (NCC) at The University of Texas MD Cancer Center (N=147; 1.5 Tesla G.E echo-speed Horizon LX scanner) or the Yerkes National Primate Research Center (YNPRC; N=76; 3.0 Tesla Siemens Trio scanner). The MRI scanning procedures for chimpanzees at both the NCC and YNPRC were designed to minimize stress for the animals. Data were acquired with the approval of ethics committees at both sites and were obtained prior to the 2015 implementation of the U.S. Fish and Wildlife Service and National Institutes of Health regulations governing research with chimpanzees. Image quality control (QC) was conducted by assessing sample outliers in voxel-wise GM intensity correlations. 194 chimpanzees (130 females, 9 - 54 y/o, mean age = 26.2 ± 9.9) passed QC. To minimize the effect of extreme aging on the OPNMF solutions subjects over 50 years old were removed for a final sample of 189 chimpanzees (126 females, 9 - 50 y/o, mean age = 25.6 ± 9.1).

The human structural T1w MRI scans were provided from the IXI (Information eXtraction from Images) dataset. This open dataset was specifically chosen for comparison with the NCBR chimpanzees as it contains both 1.5 and 3 Tesla brain scans and has a comparable distribution of age and sex. IXI consists of 565 healthy subjects (314 females; 20 - 86 y/o; mean age 48.69 ± 16.46 years) without missing metadata. To further match the two NCBR scanners, subjects from the Hammersmith Hospital (HH; N=181; 3.0 Tesla Philips Medical Systems Intera scanner) and Guy's Hospital (GUYS; N=315; 1.5 Tesla Philips Medical Systems Gyroscan Intera scanner) were considered. These 496 subjects (270 females; 20 - 86 y/o; mean age 49.57 ± 16.28 years) all passed QC. To aid in comparability to the chimpanzee sample, the very old IXI subjects (>75 y/o) were removed for the construction of the OPNMF solutions for a final sample of 480 subjects (262 females, 20 - 74 y/o, mean age = 48.7 ± 16.5). We used the eNKI open neuroimaging dataset[41] to replicate the aging – expansion relationship in a larger lifespan sample. The eNKI scans were all acquired using a single 3T scanner (Siemens Magnetom TrioTim). T1w images were obtained using a MPRAGE sequence with 1mm isotropic voxels and TR = 1900 ms. The T1w images were preprocessed the same as IXI using CAT12. Following preprocessing, patient identified subjects were removed and QC was conducted by removing subjects that had CAT12 image quality ratings above two standard deviation from the mean. We then used 765 images from eNKI[41] (502 females; 6 – 85 y/o; mean age = 39.9 ± 22.2) for our replication analysis.

Image Processing

The chimpanzee (NCBR) and human (IXI, & eNKI) samples were preprocessed using the SPM12 (Statistical Parametric Mapping; https://www.fil.ion.ucl.ac.uk/spm/software/spm12/; v7487) toolbox, CAT12[58] (Computational Anatomy Toolbox; http://www.neuro.uni-jena.de/cat/; r1725). The NCBR sample was processed utilizing the newly established chimpanzee specific pipeline[8] while the IXI sample utilized the default human processing pipeline with high accuracy shooting regestration[59]. The general steps of preprocessing were, first, the single subject images are affine registered to template space and segmented into the three tissue types, gray matter, white matter, and cerebrospinal fluid, utilizing a tissue probability map (TPM). Next, each tissue map is nonlinearly

registered to five shooting templates with increasing registration accuracy[59] to bring all subjects' tissue maps into the same template space. Finally, the deformation fields required to register the subjects into template space are used to modulate the tissue maps to conserve original local volume. Following preprocessing the modulated GM maps for each species were down-sampled (2 mm & 3 mm resolution) and smoothed (4 mm & 6 mm full width half maximum) in the NCBR and IXI samples, respectively. Finally, a GM mask at 0.3 and 0.2 probability for the chimpanzee and human samples respectively was applied encompassing the cortex and basal ganglia.

Orthogonal Projective Non-negative Matrix Factorization (OPNMF) and Granularity Selection

To estimate the GM structural covariance parcellation the orthogonal variant of NMF[60], OPNMF was used[225,26]. OPNMF establishes a low dimensional representation of the voxel-wise GM data where non-negativity is enforced on all elements. The low dimensional space comprises a parcellation matrix with the factorization loadings for each voxel and a subject matrix containing the subject loadings for each component. By constraining the matrices to non-negative values provides a parts-based representation of the cerebral GM data by the way of spatially continuous and additive covariance parcels. A hard parcellation is created by appointing each voxel to the parcel with the highest weight. Selection of the most appropriate OPNMF granularity for cross-species comparison was assessed through analysis of the reconstruction error development over bootstraps (k = 100) in combination with cross-species OPNMF solution parcel similarity over the range of 2 – 40 parcels. Further details can be found in the Supplementary.

Template Processing and Expansion Maps

Employing CAT12 preprocessing we established cross-species deformation maps which represent an approximation of the cross-species expansion. Utilizing population average T1 maps of a species and the processing pipeline of the target species, we could create deformation maps that represent an estimation of cross-species expansion. Species templates were selected as they represent an average brain, improving interpretability of the expansion estimates as well as having high tissue contrasts aiding segmentation and registration. We used two species-specific processing pipeline, chimpanzee [8] and human, to create our expansion maps. The chimpanzee to human expansion map was created using the chimpanzee template in the human pipeline while the baboon and macaque to chimpanzee expansion maps were created using the chimpanzee pipeline[8] with the baboon[34] and macaque[35–37] templates respectively. We averaged the expansion map of three commonly used macaque templates to encompass inter-sample variation. Further information regarding the expansion map creation can be found in the Supplementary. QC was performed on all deformation and expansion maps by assessing the smoothness and feasibility of the macroanatomical structures. Additionally, for the chimpanzee to human map we visually inspected the spatial location of the Davi130[8] regions when registered to the human template space (Supplementary Figure 1).

Gray Matter Aging and Expansion Analyses

We assessed the relationship between age related GM decline and relative expansion in chimpanzees and humans, utilizing the data-driven low dimensional OPNMF solution. The aging effect on GM volume was assessed for the chimpanzee and human samples utilizing an OPNMF

parcel-wise linear regression model. The age-range of the IXI sample was matched to the chimpanzee to improve comparability, by accounting for the difference in aging processes (human ≈ 1.15x chimpanzee)[39]. Therefore, 304 IXI subjects (females = 150; 20 – 58 y/o; age = 39.0 ± 11.0) and 189 chimpanzees (126 females; 9 - 50 y/o; age = 25.6 ± 9.1) were used for the age regression model. Average GM density values for each OPNMF parcel from the chimpanzees and humans were entered into a regression model for each species, as the independent variable with age, sex, total intracranial volume (TIV), and scanner field strength as the dependent variables. Parcels showing a significant age effect was assessed at p≤0.05 following correction for multiple comparisons using FWE[40]. The parcel-wise age model t-statistics in the human sample were compared with the chimpanzee to human expansion while the chimpanzee age effect was compared with the baboon and macaque cross-species expansion. Cross-species expansion was estimated by taking the mean expansion from each component for the various cross-species expansion maps and z-scored to present the inter-regional inter-species expansion. Significance of Pearson's correlation and difference between correlations was determined through permutation testing (k=100 000) at p≤0.05. Finally, the human parcel-wise age effect was replicated in the eNKI[41] lifespan neuroimaging dataset and correlated with chimpanzee to human expansion to assess the robustness of our findings in humans.

Data and Code Availability

The chimpanzee (www.chimpanzeebrain.org) and two human neuroimaging datasets, IXI (http://brain-development.org/ixi-dataset/) and eNKI (http://fcon_1000.projects.nitrc.org/indi/enhanced/index.html) are openly available. The human (MNI) and chimpanzee (JunaChimp) reference templates are available as part of the CAT12 (v12.7+) toolbox or can be individually downloaded at http://www.bic.mni.mcgill.ca/ServicesAtlases/ICBM152NLin2009 and http://junachimp.inm7.de/ respectively. The cercopithecid monkey template are also openly available for download, baboon (Haiko89 - https://www.nitrc.org/projects/haiko89/) and macaques (D99 – https://afni.nimh.nih.gov/pub/dist/doc/htmldoc/nonhuman/macaque_tempatl/atlas_d99v2.html; INIA19 – https://www.nitrc.org/projects/inia19/; NMT - https://afni.nimh.nih.gov/pub/dist/doc/htmldoc/nonhuman/macaque_tempatl/template_nmtv2.html#download-symmetric-nmt-v2-datasets). The GM masks for chimpanzees and humans can be downloaded at https://zenodo.org/record/6463123#.YyljX_exVhG. The remaining data created for this manuscript can be downloaded at https://zenodo.org/record/7116203#.YzLvCfexWV4 and code for the analyses can be found at https://github.com/viko18/GreatApe_Aging.

References

1. Crivello, F., Tzourio-Mazoyer, N., Tzourio, C. & Mazoyer, B. Longitudinal assessment of global and regional rate of grey matter atrophy in 1,172 healthy older adults: Modulation by sex and age. *PLoS ONE* **9**, (2014).
2. Good, C. D. *et al.* A voxel-based morphometric study of ageing in 465 normal adult human brains. *Neuroimage* **14**, 21–36 (2001).
3. Minkova, L. *et al.* Gray matter asymmetries in aging and neurodegeneration: A review and meta-analysis. *Human Brain Mapping* **38**, 5890–5904 (2017).

4. Vogt, C. & Vogt, O. Die vergleichend-architektonische und die vergleichend-reizphysiologische Felderung der Großhirnrinde unter besonderer Berücksichtigung der menschlichen. *Naturwissenschaften* **14**, 1190–1194 (1926).
5. Milham, M. P. *et al.* An Open Resource for Non-human Primate Imaging. *Neuron* **100**, (2018).
6. Friedrich, P. *et al.* Imaging evolution of the primate brain: the next frontier? *Neuroimage* **228**, 117685 (2021).
7. Mulholland, M. M., Sherwood, C. C., Schapiro, S. J., Raghanti, M. A. & Hopkins, W. D. Age- and cognition-related differences in the gray matter volume of the chimpanzee brain (Pan troglodytes): A voxel-based morphometry and conjunction analysis. *American Journal of Primatology* **83**, e23264 (2021).
8. Vickery, S. *et al.* Chimpanzee brain morphometry utilizing standardized MRI preprocessing and macroanatomical annotations. *eLife* **9**, e60136 (2020).
9. Sherwood, C. C. *et al.* Aging of the cerebral cortex differs between humans and chimpanzees. *Proc Natl Acad Sci U S A* **108**, 13029–13034 (2011).
10. Hopkins, W. D. *et al.* Age-related changes in chimpanzee (Pan troglodytes) cognition: Cross-sectional and longitudinal analyses. *American Journal of Primatology* **83**, e23214 (2021).
11. Donahue, C. J., Glasser, M. F., Preuss, T. M., Rilling, J. K. & Van Essen, D. C. Quantitative assessment of prefrontal cortex in humans relative to nonhuman primates. *Proceedings of the National Academy of Sciences* (2018).
12. Hopkins, W. D. & Nir, T. M. Planum temporale surface area and grey matter asymmetries in chimpanzees (Pan troglodytes): The effect of handedness and comparison with findings in humans. *Behavioural Brain Research* **208**, 436–443 (2010).
13. Schenker, N. M. *et al.* Broca's Area Homologue in Chimpanzees (Pan troglodytes): Probabilistic Mapping, Asymmetry, and Comparison to Humans. *Cereb Cortex* **20**, 730–742 (2010).
14. Langergraber, K. E. *et al.* Generation times in wild chimpanzees and gorillas suggest earlier divergence times in great ape and human evolution. *Proceedings of the National Academy of Sciences of the United States of America* **109**, 15716–15721 (2012).
15. Waterson, R. H., Lander, E. S. & Wilson, R. K. Initial sequence of the chimpanzee genome and comparison with the human genome. *Nature* **437**, 69–87 (2005).

16. Hopkins, W. D., Li, X., Crow, T. & Roberts, N. Vertex- and atlas-based comparisons in measures of cortical thickness, gyrification and white matter volume between humans and chimpanzees. *Brain Struct Funct* **222**, 229–245 (2017).
17. Hopkins, W. D. *et al.* Evolution of the central sulcus morphology in primates. **84**, 19–30 (2014).
18. Rilling, J. K. & Insel, T. R. The primate neocortex in comparative perspective using magnetic resonance imaging. *J Hum Evol* **37**, 191–223 (1999).
19. Bruner, E., Preuss, T. M., Chen, X. & Rilling, J. K. Evidence for expansion of the precuneus in human evolution. *Brain Struct Funct* **222**, 1053–1060 (2017).
20. Wei, Y. *et al.* Genetic mapping and evolutionary analysis of human-expanded cognitive networks. *Nat Commun* **10**, 4839 (2019).
21. Miller, E. K. The prefontral cortex and cognitive control. *Nat Rev Neurosci* **1**, 59–65 (2000).
22. Cavanna, A. E. & Trimble, M. R. The precuneus: a review of its functional anatomy and behavioural correlates. *Brain* **129**, 564–583 (2006).
23. Fjell, A. M., McEvoy, L., Holland, D., Dale, A. M. & Walhovd, K. B. What is normal in normal aging? Effects of aging, amyloid and Alzheimer's disease on the cerebral cortex and the hippocampus. *Progress in Neurobiology* **117**, 20–40 (2014).
24. Hill, J. *et al.* Similar patterns of cortical expansion during human development and evolution. *PNAS* **107**, 13135–13140 (2010).
25. Sotiras, A., Resnick, S. M. & Davatzikos, C. Finding imaging patterns of structural covariance via Non-Negative Matrix Factorization. *Neuroimage* **108**, 1–16 (2015).
26. Yang, Z. & Oja, E. Linear and Nonlinear Projective Nonnegative Matrix Factorization. *IEEE Transactions on Neural Networks* **21**, 734–749 (2010).
27. Alexander-Bloch, A., Giedd, J. N. & Bullmore, E. Imaging structural co-variance between human brain regions. *Nat Rev Neurosci* **14**, 322–336 (2013).
28. Nassar, R. *et al.* Gestational Age is Dimensionally Associated with Structural Brain Network Abnormalities Across Development. *Cereb Cortex* **29**, 2102–2114 (2019).
29. Patel, R. *et al.* Investigating microstructural variation in the human hippocampus using non-negative matrix factorization. *NeuroImage* **207**, 116348–116348 (2020).

30. Sotiras, A. *et al.* Patterns of coordinated cortical remodeling during adolescence and their associations with functional specialization and evolutionary expansion. *Proc Natl Acad Sci U S A* **114**, 3527–3532 (2017).
31. Varikuti, D. P. *et al.* Evaluation of non-negative matrix factorization of grey matter in age prediction. *Neuroimage* **173**, 394–410 (2018).
32. Gaser, C. *et al.* CAT – A Computational Anatomy Toolbox for the Analysis of Structural MRI Data. 2022.06.11.495736 Preprint at https://doi.org/10.1101/2022.06.11.495736 (2022).
33. Fonov, V. *et al.* Unbiased average age-appropriate atlases for pediatric studies. *NeuroImage* **54**, 313–327 (2011).
34. Love, S. A. *et al.* The average baboon brain: MRI templates and tissue probability maps from 89 individuals. *NeuroImage* **132**, 526–533 (2016).
35. Reveley, C. *et al.* Three-dimensional digital template atlas of the macaque brain. *Cerebral Cortex* (2017) doi:10.1093/cercor/bhw248.
36. Rohlfing, T. *et al.* The INIA19 Template and NeuroMaps Atlas for Primate Brain Image Parcellation and Spatial Normalization. *Frontiers in Neuroinformatics* **6**, 27–27 (2012).
37. Seidlitz, J. *et al.* A population MRI brain template and analysis tools for the macaque. *NeuroImage* **170**, 121–131 (2018).
38. Ding, C., He, X. & Simon, H. D. On the Equivalence of Nonnegative Matrix Factorization and Spectral Clustering. in *Proceedings of the 2005 SIAM International Conference on Data Mining (SDM)* 606–610 (Society for Industrial and Applied Mathematics, 2005). doi:10.1137/1.9781611972757.70.
39. Charvet, C. J. Cutting across structural and transcriptomic scales translates time across the lifespan in humans and chimpanzees. *Proceedings of the Royal Society B: Biological Sciences* **288**, 20202987 (2021).
40. Holm, S. A Simple Sequentially Rejective Multiple Test Procedure. *Scandinavian Journal of Statistics* **6**, 65–70 (1979).
41. Nooner, K. B. *et al.* The NKI-Rockland Sample: A Model for Accelerating the Pace of Discovery Science in Psychiatry. *Front Neurosci* **6**, 152 (2012).

42. Wang, F. *et al.* Developmental topography of cortical thickness during infancy. *PNAS* **116**, 15855–15860 (2019).
43. Chen, C.-H. *et al.* Genetic topography of brain morphology. *PNAS* **110**, 17089–17094 (2013).
44. Friedman, N. P. & Robbins, T. W. The role of prefrontal cortex in cognitive control and executive function. *Neuropsychopharmacol.* **47**, 72–89 (2022).
45. Owen, A. M., McMillan, K. M., Laird, A. R. & Bullmore, E. N-back working memory paradigm: a meta-analysis of normative functional neuroimaging studies. *Hum Brain Mapp* **25**, 46–59 (2005).
46. Barton, R. A. & Venditti, C. Human frontal lobes are not relatively large. *Proc Natl Acad Sci U S A* **110**, 9001–9006 (2013).
47. Smaers, J. B., Gómez-Robles, A., Parks, A. N. & Sherwood, C. C. Exceptional Evolutionary Expansion of Prefrontal Cortex in Great Apes and Humans. *Current Biology* **27**, 1549 (2017).
48. Preuss, T. M. & Wise, S. P. Evolution of prefrontal cortex. *Neuropsychopharmacol.* **47**, 3–19 (2022).
49. Schmitt, V., Pankau, B. & Fischer, J. Old World Monkeys Compare to Apes in the Primate Cognition Test Battery. *PLOS ONE* **7**, e32024 (2012).
50. Jacobs, B. *et al.* Regional dendritic and spine variation in human cerebral cortex: a quantitative golgi study. *Cereb Cortex* **11**, 558–571 (2001).
51. Sherwood, C. C. *et al.* Invariant Synapse Density and Neuronal Connectivity Scaling in Primate Neocortical Evolution. *Cerebral Cortex* **30**, 5604–5615 (2020).
52. Semendeferi, K. *et al.* Spatial organization of neurons in the frontal pole sets humans apart from great apes. *Cereb Cortex* **21**, 1485–1497 (2011).
53. Spocter, M. A. *et al.* Neuropil distribution in the cerebral cortex differs between humans and chimpanzees. *J Comp Neurol* **520**, 2917–2929 (2012).
54. Morrison, J. H. & Hof, P. R. Life and Death of Neurons in The Aging Cerebral Cortex. in *International Review of Neurobiology* vol. 81 41–57 (Academic Press, 2007).
55. Carbonell, F., Zijdenbos, A. P. & Bedell, B. J. Spatially Distributed Amyloid-β Reduces Glucose Metabolism in Mild Cognitive Impairment. *J Alzheimers Dis* **73**, 543–557 (2020).
56. Kakimoto, A. *et al.* Age-Related Sex-Specific Changes in Brain Metabolism and Morphology. *Journal of Nuclear Medicine* **57**, 221–225 (2016).

57. Lowe, A. J. *et al.* Targeting age-related differences in brain and cognition with multimodal imaging and connectome topography profiling. *Human Brain Mapping* **40**, 5213–5230 (2019).

58. Gaser, C., Dahnke, R., Kurth, K., Luders, E., & Alzheimer's Disease Neuroimaging Initiative. A computational Anatomy Toolbox for the Analysis of Structural MRI Data. *Neuroimage* (2020).

59. Ashburner, J. & Friston, K. J. Diffeomorphic registration using geodesic shooting and Gauss-Newton optimisation. *Neuroimage* **55**, 954–967 (2011).

60. Lee, D. D. & Seung, H. S. Learning the parts of objects by non-negative matrix factorization. *Nature* **401**, 788–791 (1999).oi.org/10.1038/nrn3465

Supplementary

Orthogonal Projective Non-negative Matrix Factorization

To extract multivariate GM factors for cross-species comparison we employed an orthogonal modification of non-negative matrix factorization (NMF), orthogonal projective NMF (OPNMF)[1,2]. NMF factorizes a data matrix (X) with dimensions m x n (here GM density voxels x No. subjects) into a factor matrix W (m x k, voxels x factors) and a subject-specific factor weight matrix H (k x n, factors x subjects), whereby all three matrices contain elements of non-negative value. The construction of the factor (W) and weight (H) matrices is achieved by minimizing the reconstruction error between the original input matrix and its reconstruction by the multiplication of the two factorized matrices (W & H). NMF establishes a parts-based representation of the original input data through the created factors[3]. Therefore, the factors represent separate interpretable parts of the multivariate input data extracted from the underlying patterns of variance.

OPNMF factorizes the data matrix by solving the minimization problem $||X - WW^TX||$ which is subject to $W^TW = I$; $W \geq 0$ where, $||.||$ refers to the squared Frobenius norm and I denotes the identity matrix. To first initialize the W matrix for the factorization we employed non-negative double singular value decomposition (NNSVD)[4] which encourages sparsity of factors. Subsequently, W is iteratively updated (k=10 000) with the multiplicative update rule, $W_{ij}^{'} = W_{ij}$ until it reaches an optimal solution[2]. The final step is to project X onto W to calculate H.

We decided to employ OPNMF variation instead of the original NMF as it provides several advantages when representing structural T1w MRI data as a small number of structural covariance factors[1,5]. OPNMF is different from standard NMF in how it constructs the factor loading weights of the H matrix. In standard NMF, the matrix H is estimated separately while in OPNMF it is estimated by projecting the input matrix (X) onto the factor matrix (W) using $H = W^TX$. Therefore, in OPNMF all factors participate in the reconstruction of all data points while in NMF a subset of factors is involved in reconstructing a subset of data points leading to greatly less overlap of factors and more sparsity in OPNMF as compared to NMF. This leads to the creation of structural covariance factors that are spatially continuous with minimal overlap providing a low dimensional representation of the underlying GM data that is easier to interpret. Such features in OPNMF enable each voxel to be assigned a factor in the brain by employing a winner takes all approach when back projecting the factors back onto the brain to create the final cluster solution.

Selected OPNMF Parcellation Solution

To determine an informative low dimensional structural covariance representation of GM tissue utilizing OPNMF we employed a data-driven approach accounting for accuracy, stability, and inter-species cluster spatial similarity. As the reconstruction error is a depiction of how well the factorization solution estimates the original input matrix, we assessed its change (decrease) as the number of factors increased to determine factor solutions that accurately represent the input data. This allows us to determine the improvement of the factorizations estimation of the original data when increasing the granularity or factor number. Therefore, a plateau in this improvement represents factor solutions where increasing the granularity has minimal improvements in the estimation of the original data. Consequently, some intrinsic and informative dimension of the data

has been reached and the data modeled by further factors is more difficult to discern whether they represent signal or noise. Accordingly, we averaged the change in reconstruction error over 100 bootstrapped implementations of OPNMF across a range of factor numbers (2 – 40 steps of 1) to provide a stable indication of the accuracy change for each species separately. Additionally, to improve the inter-species comparability we selected the factor solution with the highest inter-species spatial similarity measured using adjusted rand index (ARI). The ARI was calculated following the deformation of the chimpanzee OPNMF solutions to the human MNI space. It determines the factors spatial similarity above chance with a value between zero and one. Through this approach, the 17-factor solution was selected for both chimpanzees and humans.

Quality Control

Quality control (QC) was conducted by checking the sample inhomogeneity utilizing CAT12 (Computational Anatomy Toolbox). The modulated GM maps with a mean correlation below two standard deviations were flagged for visual inspection. The flagged images were then removed if they contained tissue misclassification, artifacts, irregular deformations, or very high intensity values. This process was repeated a second time with the passed images in the chimpanzee sample only as no images were removed in the IXI sample. Following the second iteration in the chimpanzee sample no more images were flagged. Following QC, 194 (130 females; 9–54 y/o; mean age = 26.2 ± 9.9) chimpanzees and 496 (270 females; 20 - 86 y/o; mean age 49.57 ± 16.28 years) human T1-weighted images qualified for further investigation.

To ascertain the feasibility and usability of the cross-species, chimpanzee to human, deformation maps visual QC was conducted. The chimpanzee Davi130 macroanatomical parcellation[6] was deformed to the human MNI space and visually inspected for large systematic misalignment with the expected macroanatomical structures (Supp. Fig. 1). There are some slight misalignment of gyri and the superior cerebellum and posterior part of the superior frontal gyrus have moved too far superiorly. As the OPNMF factors used in cross-species comparison are quite large and additional gray matter (GM) masking was conducted, these small differences will not greatly affect our analysis. Therefore, it shows the cross-species deformation map is able to approximate chimpanzee macroanatomical features onto a human template brain. Additionally, we visually inspected the deformed chimpanzee OPNMF factor solutions in MNI space for any large artifacts.

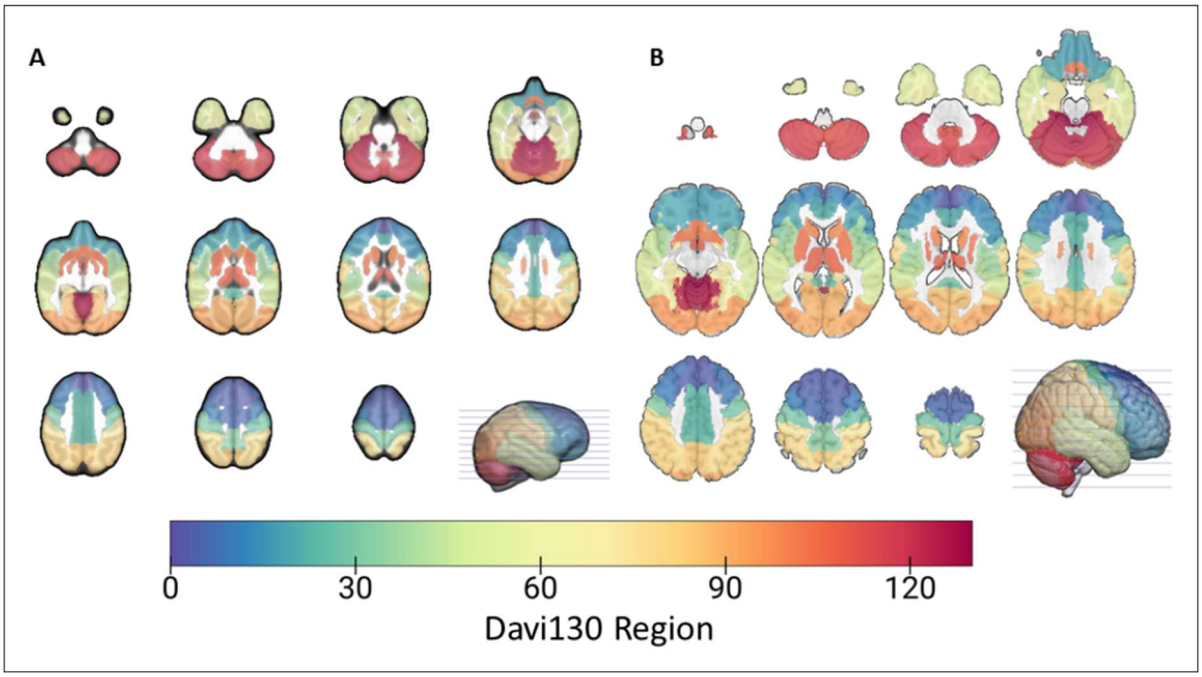

Supplementary Figure 1. Deformation map quality control. Davi130 chimpanzee parcellation in chimpanzee (A) and human (B) template space used for visual quality control of chimpanzee to human deformation map.

Davi130 Aging Effect on Gray Matter

We assessed the age related changes to GM volume in chimpanzees and humans at a higher granularity than the 17-factor OPNMF solution, by using the chimpanzee macroanatomical Davi130 parcellation[6]. The chimpanzee parcellation was projected to human template space utilizing the chimpanzee to human deformation map. To be comparable with the OPNMF factor solution aging results the Davi130 cerebellum regions were not analyzed which left 110 cortical and sub-cortical regions. The same chimpanzee (n=189; 126 females; 9 – 50 y/o; mean age = 25.6 ± 9.1) and human (n=304; 150 females; 20 – 58 y/o; mean age = 39.0±11.0) samples were used as for the OPNMF factor aging analysis. The aging effect on GM volume was determined with a multiple linear regression model over all regions. Average GM for each region was used as the dependent variable with age, sex, total intracranial volume (TIV), and scanner field strength as independent variables. Significant age effect was determined at $p \leq 0.05$ following correction for multiple comparisons using family wise error (FWE)[7]. The Davi130 aging effect (Supp. Fig. 2) shows a similar spatial pattern as the OPNMF 17-factor solution results in both species. In the chimpanzee, significant aging effect was found in the basal ganglia, cingulate cortex, lateral temporal lobe, frontal cortex, and precuneus. This is considerably less than the OPNMF result due to the higher threshold for significance following multiple comparison correction with the higher amount of regions. The largest aging effect was found in the caudate nucleus and the lowest in the motor cortex and occipital lobe comparable to the OPNMF aging result. In the human sample the Davi130 aging result showed similar large aging effect in the frontal and lateral temporal cortex and low effect in the basal ganglia, in particular the thalamus.

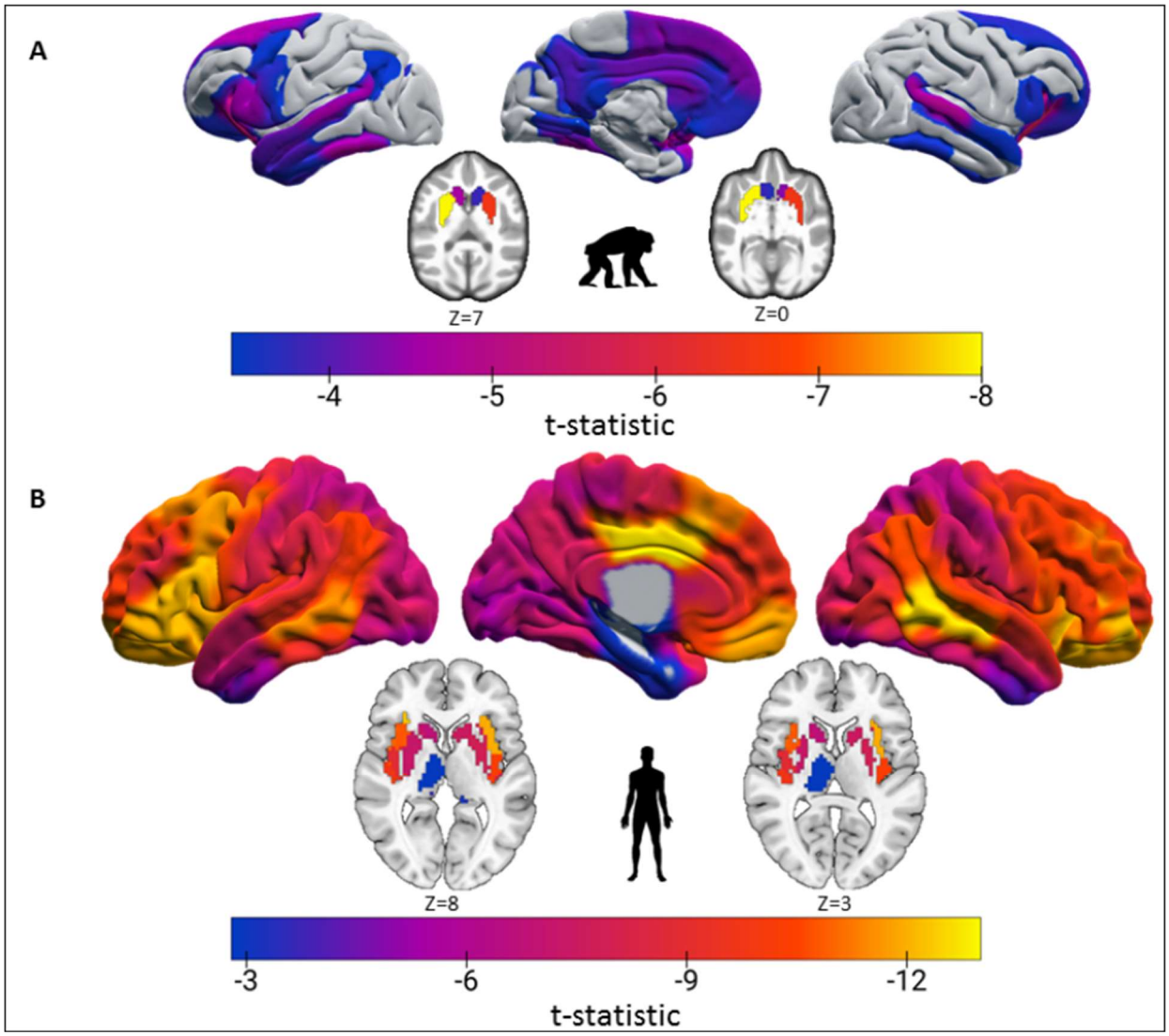

Supplementary Figure 2. Comparison of aging effect on GM volume. Aging effect on GM volume across all cortical and sub-cortical Davi130 regions in chimpanzees (A) and human (B) samples. Significant regions at p≤0.05 are presented following correcting for multiple comparisons using FWE.

Expansion map creation

We imported a species average T1 map (e.g. chimpanzee – JunaChimp[6]) into the pipeline for the other species (e.g. human – MNI[8]) to create maps of the non-linear registration across species. Following processing the JunaChimp[6] chimpanzee template using the standard the CAT12 human pipeline the deformation field map was used to register the chimpanzee OPNMF parcellations to MNI space to conduct similarity analysis for granularity selection. To create the relative expansion maps, we used the modulated Jacobians from processing and conducted post-hoc manipulation by masking (brain mask) and converting the Jacobian values into cross-species expansion approximations. The expansion maps were created by dividing the jacobians by a scaling factor, which was the inverse of the relative difference in brain size between species. Therefore, as the human brain is approximately 3.5x larger than the chimpanzee a scaling factor of 0.286 (1/3.5) was applied. The chimpanzee brain is approximately 2.5x larger than the baboon and 4.5x the macaque so a factor of 0.4 and 0.22 were applied respectively.

Brain Aging and Cross-species Expansion Comparison Replication

Davi130 Parcellation

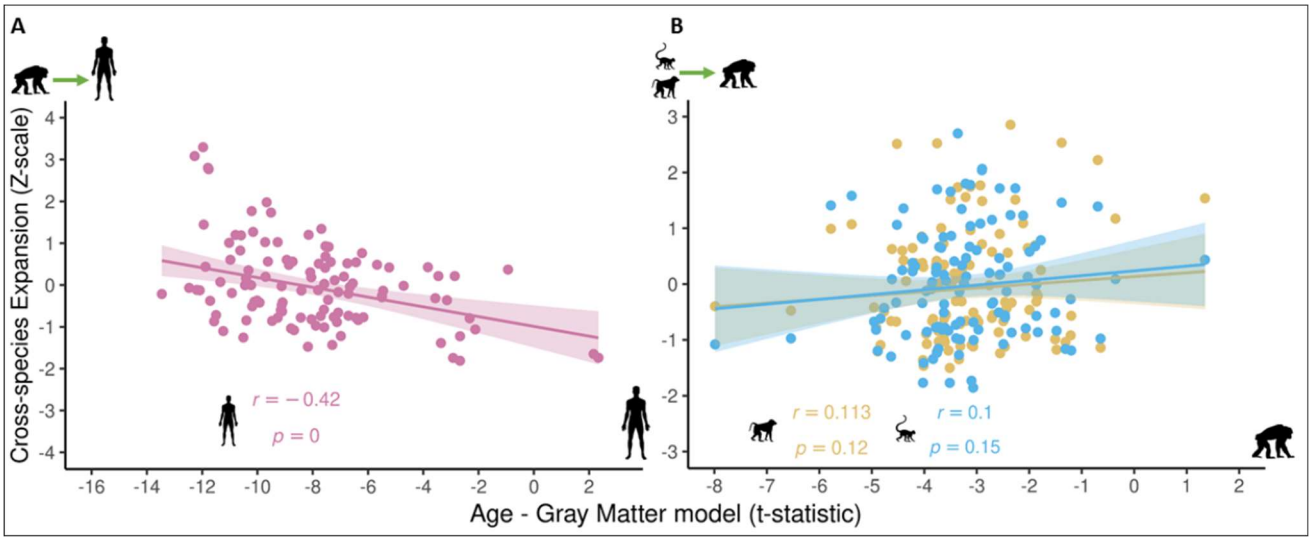

Supplementary Figure 3. Aging – expansion comparison (Davi130). Scatter plots showing of cross-species expansion and aging effect between A – chimpanzee to human expansion and human aging effect (Pink), B – macaque to chimpanzee expansion and chimpanzee aging effect (Blue) and baboon to chimpanzee expansion and chimpanzee aging effect (Yellow). Significance (p) of correlation (Person's r) for cross-species expansion and aging effect relationship is determined by permutation testing (k = 100 000).

eNKI Human Lifespan Sample

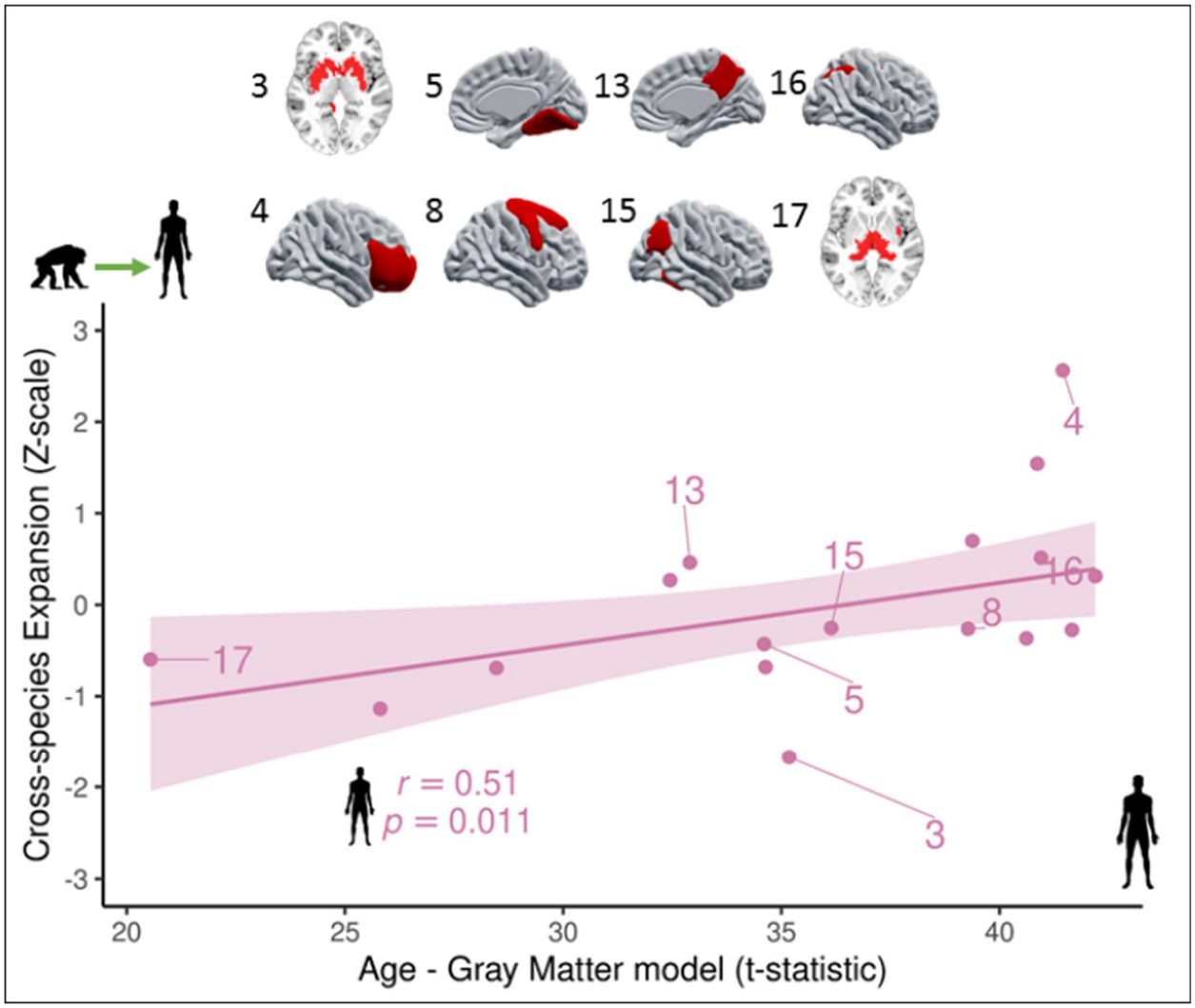

Supplementary Figure 4. Aging – expansion comparison (eNKI). Scatter plots showing of cross-species expansion and aging effect using the IXI sample OPNMF 17-factor solution to extract aging effect for each factor using the eNKI sample (n=765). A selection of OPNMF factors are projected onto volume slice or rendering of the MNI human template. Significance (p) of correlation (Person's r) for cross-species expansion and aging effect relationship is determined by permutation testing (k = 100 000).

References

1. Sotiras, A., Resnick, S. M. & Davatzikos, C. Finding imaging patterns of structural covariance via Non-Negative Matrix Factorization. *Neuroimage* **108**, 1–16 (2015).
2. Yang, Z. & Oja, E. Linear and Nonlinear Projective Nonnegative Matrix Factorization. *IEEE Trans. Neural Netw.* **21**, 734–749 (2010).
3. Lee, D. D. & Seung, H. S. Learning the parts of objects by non-negative matrix factorization. *Nature* **401**, 788–791 (1999).

4. Boutsidis, C. & Gallopoulos, E. SVD based initialization: A head start for nonnegative matrix factorization. *Pattern Recogn* **41**, 1350–1362 (2008).
5. Varikuti, D. P. *et al.* Evaluation of non-negative matrix factorization of grey matter in age prediction. *Neuroimage* **173**, 394–410 (2018).
6. Vickery, S. *et al.* Chimpanzee brain morphometry utilizing standardized MRI preprocessing and macroanatomical annotations. *eLife* **9**, e60136 (2020).
7. Holm, S. A Simple Sequentially Rejective Multiple Test Procedure. *Scand. J. Stat.* **6**, 65–70 (1979).
8. Fonov, V. *et al.* Unbiased average age-appropriate atlases for pediatric studies. *NeuroImage* **54**, 313–327 (2011).

6. Discussion

Modern MRI techniques in combination large open datasets, novel methodologies, and improved computational possibilities has led to a renaissance in primate comparative neuroscience. This dissertation is concentrated on macroanatomical GM organisation in humans and chimpanzees with a particular focus on how aging effects such organisation. Additionally, an overview is provided over some novel primate neuroimaging findings and possibilities as well as a spotlight on the IPL connectivity and asymmetry. In study 1 a chimpanzee specific VBM processing pipeline is established containing associated registration and segmentation templates in addition to a population T1w template and hand-drawn macroanatomical parcellation. Furthermore, this processing workflow and parcellation were implemented to show significant aging effect on GM volume as well as regional hemispheric asymmetry. The second study provides an outline on the state of the art in primate neuroimaging regarding asymmetry, gyrification, function, connectivity, sulcal anatomy, and novel comparative techniques. Along these lines a further exploration into the study of connectivity asymmetry in the IPL of humans, chimpanzees, and macaques. This showed a similar pattern of subregional IPL lateralization in chimpanzees and humans. Although the connectivity of the IPL subregions in humans were more leftward lateralized, with more plentiful connections to motor and frontal regions possibly associated with the evolution of language and tool-use. Study 3 presents a data-driven cross-species comparative workflow, which provides a macroanatomically informed low dimensional space for inter-species comparison. Utilizing this comparative framework, a novel relationship between age-mediated GM volume decline and brain volumetric expansion was present in humans and no such relationship was seen in chimpanzees.

5.1 Gray Matter Volume Comparative Techniques

Considering the plentiful benefits of chimpanzees as a comparative animal model, such as sharing the closest common ancestor, a similar genome, and comparable brain organizational features. Methods facilitating brain analysis on a large scale have been found somewhat lacking. Therefore, two approaches (study 1 and 3) are provided and implemented within this dissertation. The chimpanzee-specific preprocessing pipeline (study 1) not only provides an accurate means to segment and spatially normalize T1w brain scans, but it also additionally establishes a common reference space for chimpanzee brain analysis. The chimpanzee population template space, in which the additional processing template are also situated, enables chimpanzee to have a reference space similar to the other commonly used

primate species (Love et al., 2016; Reveley et al., 2017; Rohlfing et al., 2012; Seidlitz et al., 2018). The common template space facilitates the accurate and reproducible presentation of results from chimpanzee studies. It also acts as a space to register brains from other species as well as present results of a different species that have been registered or transferred into chimpanzee space. Consequently, the chimpanzee template space was used in both these aspects in study 3. By using non-linear spatial registration an estimate of brain expansion between chimpanzees and humans was determined and deformation maps both from chimpanzee to human and the inverse. These openly provided maps (https://zenodo.org/record/7116203#.YzLvCfexWV4) allow researchers to deform parcellation maps or ROI's between chimpanzee and human volumetric template space automatically. Furthermore, the chimpanzee template space also enables the cross-species registration and in term expansion maps from smaller monkey species. Such expansion maps from baboon and macaque to chimpanzee are provided in study 3 and represent the first examples of cercopithecid monkey to great ape brain expansion maps.

The second novel approach presented in this dissertation, is a data-driven method for the investigating inter-species macroanatomical brain organisation. The method creates a macroanatomically informed low dimensional parcellation using GM volume in both species independently. As the parcellation granularity for comparison is informed by using within species reconstruction accuracy and cross-species similarity, both species-specific and cross-species organizational features are provided. OPNMF effectively showed that it can be used to create GM brain parcellation to be employed as a data-driven low-dimensional space for cross-species comparison. The selected 17-factor OPNMF solution for cross-species comparison contains a similar granularity to previously report OPNMF solutions in human children (Sotiras et al., 2017; Wang et al., 2019). The comparative solution selected for both species also contained the same parcellation features of general hemispheric symmetry, spatial contiguity, and alignment to known macroanatomical structures as have been previously reported in OPNMF in humans (Nassar et al., 2019; Sotiras et al., 2017, 2015; Varikuti et al., 2018). This is particularly promising for the chimpanzee factorization solution (Study 3 Fig. 2C) as this is, to our knowledge, the first instance of OPNMF GM parcellation conducted in non-human primates.

5.2 Gray matter volume decline during aging in humans and chimpanzees

Utilizing multiple techniques to extract GM volume data and model its decline during aging, this dissertation provides clear evidence for widespread significant GM decline mediated by aging in chimpanzees. Global whole brain age regression models were

employed on total GM volume and across all voxels using VBM. ROI models were conducted using the Davi130 macroanatomical parcellation and the OPNMF data-driven comparative parcellation. The GM decline seen in chimpanzees (Study 1 Fig. 3A, 4, 5, & Study 3 Fig. 3A) was less prominent than that shown in humans (Study 1 Fig. 3D & Study 3 Fig. 3B). Whereby, humans in an age, sex, and scanner matched sample presented a greater negative correlation between aging and total GM volume then chimpanzees, R^2=0.55 compared to R^2=0.12 (Study 1 Fig. 3B & D). Additionally, using the 17-factor solution humans showed an overall greater age -related GM decline over cortical parcels compared to chimpanzees (Study 3 Fig. 3B), although chimpanzees presented a relatively greater effect in the basal ganglia, in particular the striatum (Study 3 Fig. 3A). In both species higher age-mediated GM volume decline was present in frontal, parietal, and lateral temporal areas while occipital and primary motor regions showed less decline. The multiple brain regions showing significant GM decline during aging, in chimpanzees, have also been shown in human healthy aging (Crivello et al., 2014; Good et al., 2001; Kennedy et al., 2009; Minkova et al., 2017).

Along with the studies presented in this dissertation, a growing body of research further suggests that the age-related GM decline is present in chimpanzees. The increase of stress hormone levels with age as well as accumulation of Alzheimer's neuropathology molecules, neurofibrillary and β-amyloid plaques, in elderly chimpanzees (Edler et al., 2017; Emery Thompson et al., 2020). Both these processes are known to cause neuronal loss in humans (Jagust, 2016; Llado et al., 2018). This provides possibly biological mechanisms for the GM atrophy presented here. Additionally, recent studies have shown GM volume and cognitive decline in aging chimpanzees (Hopkins et al., 2021; Mulholland et al., 2021). These findings in different studies using the same sample strengthen the robustness of the aging results shown.

5.3 Relationship Between Aging and Cross-species Expansion in Great Apes

The cross-species expansion maps provide an indication of possible structural changes between species that may relate to evolutionary development. The volumetric chimpanzee to human expansion map presented here (Study 3 Fig. 4A), show some similarities to previously reported cortical expansion between chimpanzees (Donahue et al., 2018; Wei et al., 2019) and macaques (Hill et al., 2010; Xu et al., 2020) to humans. The high expansion in the prefrontal cortex and precuneus shown here is comparable to previous studies (Donahue et al., 2018; Wei et al., 2019). Although, previous research has shown high expansion in the IPL and lateral temporal lobe in macaques (Hill et al., 2010; Xu et al., 2020)

and to a lesser extent in chimpanzee (Wei et al., 2019) to humans. That is not shown in the chimpanzee to human expansion maps presented in study 3. Additionally, previously report expansion maps contained less expansion in the medial and orbital frontal cortex as compared to in here. Moderate expansion is seen in the lateral temporal lobe in both cercopithecid monkeys to chimpanzees (Study 3 Fig. 4B & C), therefore, it would be expected that the chimpanzee to human expansion in the lateral temporal lobe is less than that form macaques to humans as shown here and previously (Wei et al., 2019). The higher chimpanzee to human expansion shown previously in the lateral temporal lobe (Wei et al., 2019), may be related to the different granularity of parcellation used for extracting the expansion values as well as being based on cortical surface reconstruction measures instead of volume. Moreover, the low expansion in the IPL in study 3 compared to the high expansion previously reported in macaque to human cortical surface expansion maps (Hill et al., 2010; Xu et al., 2020) may also be due to the difference in structural measures employed. Even though the IPL showed comparably less cross-species expansion the temporal-parietal junction presented greater expansion in the left hemisphere (Study 3 Fig. 4A), which corresponds to previous comparative structural connectivity findings between chimpanzees and humans in relation to the development of modern complex language (Eichert et al., 2020).

The PFC presented a combination of exceptionally high age-mediated GM decline and cross-species expansion in humans. Interestingly, the chimpanzee OPNMF 17-factor solution presented a PFC factor with the highest cross-species similarity to humans independently. Even though the PFC plays an important role in prominent human cognitive facilities, like executive control, the GM organizational features of this regions seem to be partly conserved between chimpanzees and humans. The frontal pole has shown a greater neuropil fraction in humans compared to other great apes (Semendeferi et al., 2001). Such a comparatively greater fraction in humans has additionally been shown in the insula (Spocter et al., 2012) that also showed high age-related GM decline and expansion. A greater neuropil fraction refers to more space containing dendrites and axons as well as their interconnections. This increase in the interconnectivity requirements of the PFC could be a possibly factor for the large amount of expansion. Then as dendritic loss is a characteristic of the human brain atrophy process during aging, the neuropil fraction differences between chimpanzees an humans may partly explain the human specific relationship. Additionally, the human-specific PFC aging-expansion relationship furthers the “last in, first out” hypothesis of the developmental maturation relationship with aging (Hill et al., 2010), here relating to possible later evolutionary development. Even though both chimpanzees and humans present a highly developed PFC, evidence suggest that the human PFC seems to be larger compared to other primates

(Donahue et al., 2018). This exceptional growth in recent human evolution may have enabled a greater vulnerability to aging earlier in life. Moreover, the PFC in chimpanzees was able to be delineated independently using OPNMF and showed significant age-related GM decline but did not present high expansion compared to cercopithecid monkeys.

5.4 Conclusions

Chimpanzees showed substantial GM atrophy with age, however, not as widespread, and not at the same magnitude as seen in aging humans. A new chimpanzee specific CAT12 preprocessing pipeline was presented and applied to determine that significant GM atrophy occurs during aging in chimpanzees. The chimpanzee pipeline is provided with a population reference, segmentation, and registration templates along with the Davi130 macroanatomical parcellation. The chimpanzee pipeline, templates, and hand-drawn parcellation are publicly available to the neuroimaging community. Additionally, hemispheric asymmetry was examined using the newly created processing pipeline that showed chimpanzees to contain a general rightward lateralization of greater GM volume.

Primate neuroimaging enables a multi-dimensional probe into the various organizational, functional, and developmental aspects of the primate brain. Modeling the wealth of information available from imaging our primate ancestors enables a deeper understanding of the commonalities and divergences between species. As well as a better overall comprehension of primate brain organization, if such a generalization Is even possible. For the comparison of brains within and across species common spaces are beneficial. Such spaces can be in the form of templates, homologous structures, or modeled organizational features. The methodological developments along with the increase depth of primate imaging data provide the possibility to understand the brain adaptations constrained by the factors of evolution. Furthermore, in more a concentrated spotlight on the comparison of brain organization over multiple primate species. The asymmetrical WM connections of the IPL in humans are predominantly left lateralized and more plentiful than chimpanzees and macaques. With increased asymmetrical connections to frontal, motor, and temporal areas that may have contributed to the evolution of tool-use, language, and handedness.

The data-driven comparative framework utilizing OPNMF was demonstrated as a feasible approach to reveal organizational features of great ape brains. The technique establishes a species-specific brain parcellations containing a combination of within and

across species GM macroanatomically informed features. The multivariate comparative framework found a novel relationship in humans between local brain expansion and age-related GM decline, which was not seem in chimpanzees. Whereby, the regions in humans that showed high expansion between chimpanzees and humans additionally presented large age-mediated GM decline, whereas no such a relationship was seen in chimpanzees compared to cercopithecid monkeys. Consequently, there may exist a penalty of large vulnerability to age-mediated GM decline from the high regional evolutionary expansion occurring since the last common ancestor of humans and chimpanzees.

Looking forward, the growing body of non-human primate neuroimaging data enable many possibilities for interesting and important multiple species investigations. The methods presented within this dissertation supplement established primate comparative techniques. The chimpanzee-specific processing workflow enables accurate, reproducible, and automatic registration and segmentation of chimpanzee T1w brain scans. Making possible additional structural morphometry investigations both univariate or multivariate using not only GM but also WM and CSF tissue segments. Furthermore, the proposed data-driven comparative framework can be extended to additional species further along the phylogenetic tree. This creates a more general understanding of primate brain organization by utilizing a comparative space consisting of both inter- and intra-species organizational features. Possibly leading to novel findings of the evolution of the primate brain.

6. References

Alexander-Bloch, A., Giedd, J.N., Bullmore, E., 2013. Imaging structural co-variance between human brain regions. Nat Rev Neurosci 14, 322–336. https://doi.org/10.1038/nrn3465

Amunts, K., Zilles, K., 2015. Architectonic Mapping of the Human Brain beyond Brodmann. Neuron 88, 1086–1107. https://doi.org/10.1016/j.neuron.2015.12.001

Ashburner, J.& K.J.Friston., 2000. voxel based morphometry-The methods. Neuroimage.

Autrey, M.M., Reamer, L.A., Mareno, M.C., Sherwood, C.C., Herndon, J.G., Preuss, T., Schapiro, S.J., Hopkins, W.D., 2014. Age-related effects in the neocortical organization of chimpanzees: gray and white matter volume, cortical thickness, and gyrification. Neuroimage 101, 59–67. https://doi.org/10.1016/j.neuroimage.2014.06.053

Bogart, S.L., Mangin, J.F., Schapiro, S.J., Reamer, L., Bennett, A.J., Pierre, P.J., Hopkins, W.D., 2012. Cortical sulci asymmetries in chimpanzees and macaques: A new look at an old idea. NeuroImage 61, 533–541. https://doi.org/10.1016/j.neuroimage.2012.03.082

Brodmann, K., 1909. Vergleichende Lokalisationslehre der Grosshirnrinde in ihren Prinzipien dargestellt auf Grund des Zellenbaues. Barth, Leipzig.

Bruner, E., Preuss, T.M., Chen, X., Rilling, J.K., 2017. Evidence for expansion of the precuneus in human evolution. Brain Struct Funct 222, 1053–1060. https://doi.org/10.1007/s00429-015-1172-y

Cantalupo, C., Hopkins, W.D., 2001. Asymmetric broca's area in great apes: A region of the ape brain is uncannily similar to one linked with speech in humans. Nature 414, 505–505. https://doi.org/10.1038/35107134

Cavanna, A.E., Trimble, M.R., 2006. The precuneus: a review of its functional anatomy and behavioural correlates. Brain J. Neurol. 129, 564–583. https://doi.org/10.1093/brain/awl004

Chen, X., Errangi, B., Li, L., Glasser, M.F., Westlye, L.T., Fjell, A.M., Walhovd, K.B., Hu, X., Herndon, J.G., Preuss, T.M., Rilling, J.K., 2013. Brain aging in humans, chimpanzees (Pan troglodytes), and rhesus macaques (Macaca mulatta): magnetic resonance imaging studies of macro- and microstructural changes. Neurobiol Aging 34, 2248–2260. https://doi.org/10.1016/j.neurobiolaging.2013.03.028

Cheng, L., Zhang, Y., Li, G., Wang, J., Sherwood, C., Gong, G., Fan, L., Jiang, T., 2021. Connectional asymmetry of the inferior parietal lobule shapes hemispheric specialization in humans, chimpanzees, and rhesus macaques. eLife 10, e67600. https://doi.org/10.7554/eLife.67600

Crivello, F., Tzourio-Mazoyer, N., Tzourio, C., Mazoyer, B., 2014. Longitudinal assessment of global and regional rate of grey matter atrophy in 1,172 healthy older adults: Modulation by sex and age. PLoS ONE 9. https://doi.org/10.1371/journal.pone.0114478

Donahue, C.J., Glasser, M.F., Preuss, T.M., Rilling, J.K., Van Essen, D.C., 2018. Quantitative assessment of prefrontal cortex in humans relative to nonhuman primates. Proc. Natl. Acad. Sci.

Economo, C.F. von, Koskinas, G.N., 1925. Die Cytoarchitektonik der Hirnrinde des erwachsenen Menschen. J. Springer.

Edler, M.K., Sherwood, C.C., Meindl, R.S., Hopkins, W.D., Ely, J.J., Erwin, J.M., Mufson, E.J., Hof, P.R., Raghanti, M.A., 2017. Aged chimpanzees exhibit pathologic hallmarks of Alzheimer's disease. Neurobiol Aging 59, 107–120. https://doi.org/10.1016/j.neurobiolaging.2017.07.006

Eichert, N., Robinson, E.C., Bryant, K.L., Jbabdi, S., Jenkinson, M., Li, L., Krug, K., Watkins, K.E., Mars, R.B., 2020. Cross-species cortical alignment identifies different types of anatomical reorganization in the primate temporal lobe. eLife 9, e53232. https://doi.org/10.7554/eLife.53232

Eickhoff, S.B., Yeo, B.T.T., Genon, S., 2018. Imaging-based parcellations of the human brain. Nat. Rev. Neurosci. 19, 672–686. https://doi.org/10.1038/s41583-018-0071-7

Emery Thompson, M., Fox, S.A., Berghänel, A., Sabbi, K.H., Phillips-Garcia, S., Enigk, D.K., Otali, E., Machanda, Z.P., Wrangham, R.W., Muller, M.N., 2020. Wild chimpanzees exhibit humanlike aging of glucocorticoid regulation. Proc. Natl. Acad. Sci. 201920593–201920593. https://doi.org/10.1073/pnas.1920593117

Friedrich, P., Forkel, S.J., Amiez, C., Balsters, J.H., Coulon, O., Fan, L., Goulas, A., Hadj-Bouziane, F., Hecht, E.E., Heuer, K., Jiang, T., Latzman, R.D., Liu, X., Loh, K.K., Patil, K.R., Lopez-Persem, A., Procyk, E., Sallet, J., Toro, R., Vickery, S., Weis, S., Wilson, C.R.E., Xu, T., Zerbi, V., Eickoff, S.B., Margulies, D.S., Mars, R.B., Thiebaut de Schotten, M., 2021. Imaging evolution of the primate brain: the next frontier? NeuroImage 228, 117685. https://doi.org/10.1016/j.neuroimage.2020.117685

Gannon, P.J., Holloway, R.L., Broadfield, D.C., Braun, A.R., 1998. Asymmetry of chimpanzee planum temporale: Humanlike pattern of Wernicke's brain language area homolog. Science 279, 220–222. https://doi.org/10.1126/science.279.5348.220

Glasser, M.F., Coalson, T.S., Robinson, E.C., Hacker, C.D., Harwell, J., Yacoub, E., Ugurbil, K., Andersson, J., Beckmann, C.F., Jenkinson, M., Smith, S.M., Van Essen, D.C., 2016. A multi-modal parcellation of human cerebral cortex. Nature 536. https://doi.org/10.1038/nature18933

Good, C.D., Johnsrude, I.S., Ashburner, J., Henson, R.N., Friston, K.J., Frackowiak, R.S., 2001. A voxel-based morphometric study of ageing in 465 normal adult human brains. Neuroimage 14, 21–36. https://doi.org/10.1006/nimg.2001.0786
Gupta, C.N., Turner, J.A., Calhoun, V.D., 2018. Source-Based Morphometry: Data-Driven Multivariate Analysis of Structural Brain Imaging Data, in: Spalletta, G., Piras, F., Gili, T. (Eds.), Brain Morphometry, Neuromethods. Springer, New York, NY, pp. 105–120. https://doi.org/10.1007/978-1-4939-7647-8_7
Hecht, E.E., Mahovetz, L.M., Preuss, T.M., Hopkins, W.D., 2017. A neuroanatomical predictor of mirror self-recognition in chimpanzees 12, 37–48. https://doi.org/10.1093/scan/nsw159
Herndon, J.G., Tigges, J., Anderson, D.C., Klumpp, S.A., McClure, H.M., 1999. Brain weight throughout the life span of the chimpanzee. J. Comp. Neurol. 409, 567–72.
Hill, J., Inder, T., Neil, J., Dierker, D., Harwell, J., Essen, D.V., 2010. Similar patterns of cortical expansion during human development and evolution. Proc. Natl. Acad. Sci. 107, 13135–13140. https://doi.org/10.1073/pnas.1001229107
Hopkins, W.D., Mareno, M.C., Neal Webb, S.J., Schapiro, S.J., Raghanti, M.A., Sherwood, C.C., 2021. Age-related changes in chimpanzee (Pan troglodytes) cognition: Cross-sectional and longitudinal analyses. Am. J. Primatol. 83, e23214. https://doi.org/10.1002/ajp.23214
Hopkins, W.D., Meguerditchian, A., Coulon, O., Bogart, S., Mangin, J.F., Sherwood, C.C., Grabowski, M.W., Bennett, A.J., Pierre, P.J., Fears, S., Woods, R., Hof, P.R., Vauclair, J., 2014. Evolution of the central sulcus morphology in primates 84, 19–30. https://doi.org/10.1159/000362431
Hopkins, W.D., Meguerditchian, A., Coulon, O., Misiura, M., Pope, S., Mareno, M.C., Schapiro, S.J., 2017. Motor skill for tool-use is associated with asymmetries in Broca's area and the motor hand area of the precentral gyrus in chimpanzees (Pan troglodytes). Behav Brain Res 318, 71–81. https://doi.org/10.1016/j.bbr.2016.10.048
Jagust, W., 2016. Is amyloid-β harmful to the brain? Insights from human imaging studies. Brain 139, 23–30. https://doi.org/10.1093/brain/awv326
Kennedy, K.M., Erickson, K.I., Rodrigue, K.M., Voss, M.W., Colcombe, S.J., Kramer, A.F., Acker, J.D., Raz, N., 2009. Age-related differences in regional brain volumes: A comparison of optimized voxel-based morphometry to manual volumetry. Neurobiol. Aging 30, 1657–1676. https://doi.org/10.1016/j.neurobiolaging.2007.12.020
Langergraber, K.E., Prüfer, K., Rowney, C., Boesch, C., Crockford, C., Fawcett, K., Inoue, E., Inoue-Muruyama, M., Mitani, J.C., Muller, M.N., Robbins, M.M., Schubert, G., Stoinski, T.S., Viola, B., Watts, D., Wittig, R.M., Wrangham, R.W., Zuberbuḧler, K., Pääbo, S., Vigilant, L., 2012. Generation times in wild chimpanzees and gorillas suggest earlier divergence times in great ape and human evolution. Proc. Natl. Acad. Sci. U. S. A. 109, 15716–15721. https://doi.org/10.1073/pnas.1211740109
Lee, D.D., Seung, H.S., 1999. Learning the parts of objects by non-negative matrix factorization. Nature 401, 788–791. https://doi.org/10.1038/44565
Llado, A., Tort-Merino, A., Sanchez-Valle, R., Falgas, N., Balasa, M., Bosch, B., Castellvi, M., Olives, J., Antonell, A., Hornberger, M., 2018. The hippocampal longitudinal axis-relevance for underlying tau and TDP-43 pathology. Neurobiol Aging 70, 1–9. https://doi.org/10.1016/j.neurobiolaging.2018.05.035
Love, S.A., Marie, D., Roth, M., Lacoste, R., Nazarian, B., Bertello, A., Coulon, O., Anton, J.-L., Meguerditchian, A., 2016. The average baboon brain: MRI templates and tissue probability maps from 89 individuals. NeuroImage 132, 526–533. https://doi.org/10.1016/j.neuroimage.2016.03.018
Messinger, A., Sirmpilatze, N., Heuer, K., Loh, K.K., Mars, R.B., Sein, J., Xu, T., Glen, D., Jung, B., Seidlitz, J., Taylor, P., Toro, R., Garza-Villarreal, E.A., Sponheim, C., Wang, X., Benn, R.A., Cagna, B., Dadarwal, R., Evrard, H.C., Garcia-Saldivar, P., Giavasis, S., Hartig, R., Lepage, C., Liu, C., Majka, P., Merchant, H., Milham, M.P., Rosa, M.G.P., Tasserie, J., Uhrig, L., Margulies, D.S., Klink, P.C., 2021. A

collaborative resource platform for non-human primate neuroimaging. NeuroImage 226, 117519. https://doi.org/10.1016/j.neuroimage.2020.117519
Milham, M.P., Ai, L., Koo, B., Xu, T., Amiez, C., Balezeau, F., Baxter, M.G., Blezer, E.L.A., Brochier, T., Chen, A., Croxson, P.L., Damatac, C.G., Dehaene, S., Everling, S., Fair, D.A., Fleysher, L., Freiwald, W., Froudist-Walsh, S., Griffiths, T.D., Guedj, C., Hadj-Bouziane, F., Ben Hamed, S., Harel, N., Hiba, B., Jarraya, B., Jung, B., Kastner, S., Klink, P.C., Kwok, S.C., Laland, K.N., Leopold, D.A., Lindenfors, P., Mars, R.B., Menon, R.S., Messinger, A., Meunier, M., Mok, K., Morrison, J.H., Nacef, J., Nagy, J., Rios, M.O., Petkov, C.I., Pinsk, M., Poirier, C., Procyk, E., Rajimehr, R., Reader, S.M., Roelfsema, P.R., Rudko, D.A., Rushworth, M.F.S., Russ, B.E., Sallet, J., Schmid, M.C., Schwiedrzik, C.M., Seidlitz, J., Sein, J., Shmuel, A., Sullivan, E.L., Ungerleider, L., Thiele, A., Todorov, O.S., Tsao, D., Wang, Z., Wilson, C.R.E., Yacoub, E., Ye, F.Q., Zarco, W., Zhou, Y. di, Margulies, D.S., Schroeder, C.E., 2018. An Open Resource for Non-human Primate Imaging. Neuron 100. https://doi.org/10.1016/j.neuron.2018.08.039
Miller, E.K., 2000. The prefontral cortex and cognitive control. Nat. Rev. Neurosci. 1, 59–65. https://doi.org/10.1038/35036228
Minkova, L., Habich, A., Peter, J., Kaller, C.P., Eickhoff, S.B., Klöppel, S., 2017. Gray matter asymmetries in aging and neurodegeneration: A review and meta-analysis. Hum. Brain Mapp. 38, 5890–5904. https://doi.org/10.1002/hbm.23772
Mulholland, M.M., Sherwood, C.C., Schapiro, S.J., Raghanti, M.A., Hopkins, W.D., 2021. Age- and cognition-related differences in the gray matter volume of the chimpanzee brain (Pan troglodytes): A voxel-based morphometry and conjunction analysis. Am. J. Primatol. 83, e23264. https://doi.org/10.1002/ajp.23264
Nassar, R., Kaczkurkin, A.N., Xia, C.H., Sotiras, A., Pehlivanova, M., Moore, T.M., Garcia de La Garza, A., Roalf, D.R., Rosen, A.F.G., Lorch, S.A., Ruparel, K., Shinohara, R.T., Davatzikos, C., Gur, R.C., Gur, R.E., Satterthwaite, T.D., 2019. Gestational Age is Dimensionally Associated with Structural Brain Network Abnormalities Across Development. Cereb. Cortex N. Y. NY 29, 2102–2114. https://doi.org/10.1093/cercor/bhy091
Palomero-Gallagher, N., Zilles, K., 2019. Differences in cytoarchitecture of Broca's region between human, ape and macaque brains. Cortex, The Evolution of the Mind and the Brain 118, 132–153. https://doi.org/10.1016/j.cortex.2018.09.008
Reveley, C., Gruslys, A., Ye, F.Q., Glen, D., Samaha, J., Russ, B.E., Saad, Z., Seth, A.K., Leopold, D.A., Saleem, K.S., 2017. Three-dimensional digital template atlas of the macaque brain. Cereb. Cortex. https://doi.org/10.1093/cercor/bhw248
Rilling, J.K., Insel, T.R., 1999. The primate neocortex in comparative perspective using magnetic resonance imaging. J Hum Evol 37, 191–223. https://doi.org/10.1006/jhev.1999.0313
Rohlfing, T., Kroenke, C.D., Sullivan, E.V., Dubach, M.F., Bowden, D.M., Grant, K.A., Pfefferbaum, A., 2012. The INIA19 Template and NeuroMaps Atlas for Primate Brain Image Parcellation and Spatial Normalization. Front. Neuroinformatics 6, 27–27. https://doi.org/10.3389/fninf.2012.00027
Savage-Rumbaugh, E.S., 1986. Ape language : from conditioned response to symbol. Oxford University Press.
Seidlitz, J., Sponheim, C., Glen, D., Ye, F.Q., Saleem, K.S., Leopold, D.A., Ungerleider, L., Messinger, A., 2018. A population MRI brain template and analysis tools for the macaque. NeuroImage 170, 121–131. https://doi.org/10.1016/j.neuroimage.2017.04.063
Semendeferi, K., Armstrong, E., Schleicher, A., Zilles, K., Van Hoesen, G.W., 2001. Prefrontal cortex in humans and apes: a comparative study of area 10. Am J Phys Anthr. 114, 224–241. https://doi.org/10.1002/1096-8644(200103)114:3<224::aid-ajpa1022>3.0.co;2-i

Sherwood, C.C., Gordon, A.D., Allen, J.S., Phillips, K.A., Erwin, J.M., Hof, P.R., Hopkins, W.D., 2011. Aging of the cerebral cortex differs between humans and chimpanzees. Proc Natl Acad Sci U A 108, 13029–13034. https://doi.org/10.1073/pnas.1016709108
Shumaker, R.W., Walkup, K.R., Beck, B.B., 2011. Animal tool behavior : the use and manufacture of tools by animals. Johns Hopkins University Press.
Sotiras, A., Resnick, S.M., Davatzikos, C., 2015. Finding imaging patterns of structural covariance via Non-Negative Matrix Factorization. Neuroimage 108, 1–16. https://doi.org/10.1016/j.neuroimage.2014.11.045
Sotiras, A., Toledo, J.B., Gur, R.E., Gur, R.C., Satterthwaite, T.D., Davatzikos, C., 2017. Patterns of coordinated cortical remodeling during adolescence and their associations with functional specialization and evolutionary expansion. Proc Natl Acad Sci U A 114, 3527–3532. https://doi.org/10.1073/pnas.1620928114
Spocter, M.A., Hopkins, W.D., Barks, S.K., Bianchi, S., Hehmeyer, A.E., Anderson, S.M., Stimpson, C.D., Fobbs, A.J., Hof, P.R., Sherwood, C.C., 2012. Neuropil distribution in the cerebral cortex differs between humans and chimpanzees. J. Comp. Neurol. 520, 2917–2929. https://doi.org/10.1002/cne.23074
Tomasello, M., Call, J., 1997. Primate Cognition.
Varikuti, D.P., Genon, S., Sotiras, A., Schwender, H., Hoffstaedter, F., Patil, K.R., Jockwitz, C., Caspers, S., Moebus, S., Amunts, K., Davatzikos, C., Eickhoff, S.B., 2018. Evaluation of non-negative matrix factorization of grey matter in age prediction. Neuroimage 173, 394–410. https://doi.org/10.1016/j.neuroimage.2018.03.007
Vickery, S., Eickhoff, S.B., Friedrich, P., 2022. Hemispheric Specialization of the Primate Inferior Parietal Lobule. Neurosci. Bull. 38, 334–336. https://doi.org/10.1007/s12264-021-00807-4
Vickery, S., Hopkins, W.D., Sherwood, C.C., Schapiro, S.J., Latzman, R.D., Caspers, S., Gaser, C., Eickhoff, S.B., Dahnke, R., Hoffstaedter, F., 2020. Chimpanzee brain morphometry utilizing standardized MRI preprocessing and macroanatomical annotations. eLife 9, e60136. https://doi.org/10.7554/eLife.60136
Vogt, C., Vogt, O., 1926. Die vergleichend-architektonische und die vergleichend-reizphysiologische Felderung der Großhirnrinde unter besonderer Berücksichtigung der menschlichen. Naturwissenschaften 14, 1190–1194. https://doi.org/10.1007/BF01451766
Vogt, C., Vogt, O., 1919. Allgemeine Ergebnisse unserer Hirnforschung. J.A. Barth.
Waal, F.B.M. de (Frans B.M.), 1996. Good natured : the origins of right and wrong in humans and other animals. Harvard University Press.
Wang, F., Lian, C., Wu, Z., Zhang, H., Li, T., Meng, Y., Wang, L., Lin, W., Shen, D., Li, G., 2019. Developmental topography of cortical thickness during infancy. Proc. Natl. Acad. Sci. 116, 15855–15860. https://doi.org/10.1073/pnas.1821523116
Waterson, R.H., Lander, E.S., Wilson, R.K., 2005. Initial sequence of the chimpanzee genome and comparison with the human genome. Nature 437, 69–87. https://doi.org/10.1038/nature04072
Wei, Y., de Lange, S.C., Scholtens, L.H., Watanabe, K., Ardesch, D.J., Jansen, P.R., Savage, J.E., Li, L., Preuss, T.M., Rilling, J.K., Posthuma, D., van den Heuvel, M.P., 2019. Genetic mapping and evolutionary analysis of human-expanded cognitive networks. Nat. Commun. 10, 4839. https://doi.org/10.1038/s41467-019-12764-8
Xu, T., Nenning, K.-H., Schwartz, E., Hong, S.-J., Vogelstein, J.T., Goulas, A., Fair, D.A., Schroeder, C.E., Margulies, D.S., Smallwood, J., Milham, M.P., Langs, G., 2020. Cross-species functional alignment reveals evolutionary hierarchy within the connectome. NeuroImage 223, 117346. https://doi.org/10.1016/j.neuroimage.2020.117346
Yeo, T.BT., Krienen, F.M., Sepulcre, J., Sabuncu, M.R., Lashkari, D., Hollinshead, M., Roffman, J.L., Smoller, J.W., Zöllei, L., Polimeni, J.R., Fisch, B., Liu, H., Buckner, R.L., 2011. The organization of the human cerebral cortex estimated by intrinsic functional connectivity. J. Neurophysiol. 106, 1125–1165. https://doi.org/10.1152/jn.00338.2011

Zilles, K., Armstrong, E., Moser, K.H., Schleicher, A., Stephan, H., 1989. Gyrification in the cerebral cortex of primates 34, 143–150. https://doi.org/10.1159/000116500

Acknowledgments

I would first like to thank Professor Simon Eickhoff for the opportunity to study in his institute, first as a master student and then for my PhD. I'm greatly appreciative of the support, guidance, and motivation throughout my studies. I would also like to thank Professor Svenja Caspers for her guidance and assistance as my secondary supervisor during my PhD project. A particular thanks goes to Felix Hoffstaedter for assisting me in all aspects of my PhD and masters projects and for the countless enlightening scientific discussion about my work. Your supervision has helped me to become an independent researcher and prepared me for my future career in science. An additional thanks goes to all my colleagues from INM-7 who have always been very kind and made my PhD more enjoyable. Particularly my Dussledorf office colleagues, Kaustubh, Jean-Phillip, Sami, Jürgen, Leo, Tobias, and Georgios for the interesting lunch time discussions.

A special thanks goes to my lovely wife Meike. The birth of our two beautiful girls during my PhD made our life wonderfully more challenging and without your unwavering support and encouragement I could not have finished my studies. I will be forever grateful for everything you have done for me and our family. Finally, I would like to thank my parents for their continued support throughout my life.